Volume 7 No 2, November, 2023

SCIENCE & DEVELOPMENT

(Online)
ISSN 2821-9007
9 772821 900005

CBAS
College of Basic and Applied Sciences
University of Ghana

A Journal of College of Basic and Applied Sciecence (CBAS), University of Ghana.

Water consumption changes during and after COVID-19 in Ghana

Peace Korshiwor Amoatey[1*], Godwin King-Nyamador[2], Micheal Martey[3], Maxwell Kusi-Akosah[4], Cynthia Naa Adoley Acquaye[5], and Wonder Nutsugah[6]

[1]Department of Agricultural Engineering, University of Ghana, Legon
[2]Institute for Environment and Sanitation Studies (IESS), University of Ghana, Legon
[3]Ghana Institute of Management and Public Administration, GIMPA, Achimota.
[4]Ghana Water Company Limited, Accra
[5]Department of Built Environment, University of Environment and Sustainable Development (UESD), Somanya, Ghana
[6]Department of Public Administration, UGBS, University of Ghana, Legon

***Corresponding Author:** pkamoatey@ug.edu.gh

ABSTRACT

Maintenance of good hygiene practices are encouraged in the outbreak of infectious diseases like COVID-19 and therefore, water consumption is expected to increase. There is evidence that across the globe, water consumption increased as a result of hygiene practices as people stayed at home during the pandemic, blending work, study and other daily activities. To adequately tackle the infection rate, the government of Ghana announced "free water" for all policy. This study seeks to investigate whether the pandemic and subsequent policy in 2020 has influenced water consumption over the last 2 years. The study employed descriptive statistics and Interrupted Time Series Analysis (ITSA) on monthly water consumption data from 2018 to 2022. 60 data points consisting of 27 pre and 33 post-interruption data points were used to allow the model to measure the trend before the intervention (policy) and the immediate impact of the intervention. On the average, consumption in terms of volumes increased by about 30%, and ITSA showed a significant immediate impact and increasing trend on monthly water use. The findings of the study have implications on further research, engineering practice, policy and its implementation to help in preparation for future pandemics.

Keywords: Covid-19, Interrupted Time Series Analysis (ITSA), Intervention, lockdown, water consumption

1.0 BACKGROUND

With the outbreak of any viral respiratory disease, the World Health Organisation (WHO) usually announces and encourages the washing of hands as a preventive measure. Brauer, Zhao, Bennitt and Stanaway (2020) indicated that systematic reviews have shown the effectiveness of handwashing in reducing the transmission of respiratory disease-causing viruses. For example, evidence suggests that a handwashing session with 0.2 litres is sufficient to keep one safe from being exposed to viral infection

(Mattioli et al., 2014). It has been observed that in the event of epidemics and pandemics such as Cholera, Ebola among others, water consumption generally increases. This is because an important way of preserving human lives during infectious disease outbreaks includes supply of safe drinking water, good hygiene and adequate sanitation practices (Kalra et al., 2014; WHO, 2015, 2020). This explains the reason for the all-time high increase in water consumption during the total and partial lockdown that resulted from the deadly Severe Acute Respiratory Syndrome Coronavirus 2 (SARS-CoV2) pandemic. Children were out of school and most workers were working from home leading to an increase in domestic water demand. Activities such as the drinking of water and flushing of toilets significantly increased in homes and diminished at the various places of work, and in schools.

Drinking lots of water and washing hands under running water became a mantra for both the young and old. Behavioural changes in personal hygiene were confirmed with increased frequency in handwashing and showering upon their return, after they had gone shopping for groceries or attended to anything outside their homes. Activities such as the washing of clothes and disinfection of surfaces such as tables, may have also contributed to increased daily water volumes consumed at home. With the lockdowns, time spent doing housework increased, leisure increased and the amount of gardening might have increased as well (Campos et al., 2021; Del Boca et al., 2020; Kalbusch et al., 2020; Nemati, 2020). On the other hand, some industries had to shut down or reduce production as a result, thus, industrial and institutional consumption was expected to decrease. Significant changes in the global consumption of water influenced continuity of water supply in terms of quantity and quality of services to customers (International Water Association, 2020). The World Health Organisation (WHO, 2020) and Kalbusch et al. (2020) reported that the pandemic caused a surge in the quantities of water consumed in health facilities due to continuous cleaning of equipment and facilities as well as in the treatment of patients. Therefore, hospitals were most likely the only non-residential use with increased consumption. With these developments, the International Water Association (IWA, 2020) reported that changes in consumption patterns had increased during the day as people worked from their homes. A general decrease in pre-pandemic weekday morning peaks was observed in many countries. Morning peaks were reported to have been delayed by one to two hours and were also observed during weekdays (Abu-Bakar et al., 2021; Balacco et al., 2020; Lüdtke et al., 2021). Aquatech (2020) confirmed that the city of Karlsruhe, Germany observed water consumption changes over a period.

Kalbusch et al. (2020) reported a similar situation in Joinville, Southern Brazil; the study revealed that there was an 11% increase in the water consumption in the residential category whereas there was a significant decrease in the quantity of water consumed in the public. Lüdtke et al. (2021) reported

a 14.3% increase in consumption in northern Germany during the first wave of the pandemic while an 18% increase was observed in Rovigo, Italy (Alvisi et al., 2021). In England and Wales, a 35% increase in peak daily consumption was observed in certain regions during the lockdown (Abu-Bakar et al., 2021; Alda-Vidal et al., 2020; Marshallsay, 2020). Similarly in Portsmouth in England, there was a 15% increase in water demands (Portsmouth Water, 2020) while Eastman et al. (2020) reported a 14% increase in a water utility in Arizona, USA. Likewise, residential demand in San Francisco, California increased by 10% (Cooley et al., 2020). Birişçi and Öz (2021) reported a 20% increase in residential consumption in Bursa, Turkey. Almulhim and Aina, (2022) reported a whopping 50% increase in water use in the Dammam Metropolitan Area, Saudi Arabia. Sayeed et al. (2021) reported water usage in Bangladesh to have been 1.7 L in excess of the norm due to handwashing practices. Although not much statistics is documented for African countries, Niasse and Varis (2020) confirmed that COVID-19 has led to an increase in domestic water demand in African countries like Nigeria and Rwanda who are already suffering from water insecurity. There have been a number of studies that sought to examine how COVID-19 spreads, its effect on human activities and possible ways of mitigating it.

Other studies have equally assessed the impact of lockdown and its possible effect on the quality of water as well as the quality of air (Mahato et al., 2020; Muhammad et al., 2020; Yunus et al., 2020). Furthermore, other studies have focussed on the spatio-temporal changes of daily routines (Alda-Vidal et al., 2020). Abu-Bakar et al. (2021) measured households' unique water consumption patterns in England and Cooley et al. (2020) assessed the financial implications for customers and utilities, as well as impacts on water and wastewater operational conditions. These studies have been useful in making predictions in preparation against future pandemics. It is in this light that this study seeks to assess what the situation in Ghana was during and after the pandemic. In Ghana, every citizen was supplied water for free from April 2020 till March 2021 (Dapaah, 2020; Government of Ghana, 2020; Graphic Online, 2020) which led to changes in consumer behaviour as communities which did not have piped water pre-COVID were equally served with water in tankers. Also, when the government withdrew the waiver, a section of the populace pleaded that the government reconsider a further extension of non-payment for water. This led to the government making consumption free for those whose monthly consumption was less than 5 m3 from January to March 2021 (Government of Ghana, 2021; Nyavi, 2021). For forecasting and planning purposes, it is essential to understand the dynamics and adaptations the pandemic has brought on, as well as the factors influencing these dynamics or patterns, hence the need for this study.

It is uncertain how the changes in water consumption have continued 2 years on. Cooley et al. (2020) has emphatically stated for example that, as people

continue to work from home, COVID-related impacts on water demand may be short-lived when people return to work. Lüdtke et al. (2021) also posits that the change in practices that might have caused the increase in the observed water consumption may or may not persist into the future. Additionally, Nemati (2020) reports that analysing changes in water use is valuable for water agencies, water managers, and policymakers. The changes affect the operational conditions, revenue, finances and wastewater generated as far as water agencies are concerned. The fact that water was distributed or shared for free might impact residential/domestic consumption as pricing is known to control per-capita water consumption (Amoah, 2020). A direct consequence of such a social intervention during emergencies such as COVID-19, as what happened in Ghana, impacts customers willingness to pay for water, which causes a reduction in revenues for the water utility company and thus creates a vicious circle (Cooper, 2020). This study seeks to investigate whether bulk water consumption changed in Ghana, potential reasons for the change in water use, the dynamics and peculiarities of the change specific to different regions and whether COVID-19 and the "free water" policy significantly influenced these changes.

2.0 METHOD

2.1 General overview of water supply in Ghana

The Ghana Water Company Limited (GWCL) is a fully owned state utility company mandated to supply potable water to all urban communities in Ghana. The average daily production is around 882,000 m3. The current water consumption is predicted to be around 1,100,000 m3 per day making water supply coverage to be about 77% (GWCL, 2023). GWCL has a customer size of about 800,000 of which 86% are metered. The water supply administration in Ghana is organised under 13 regions with Greater Accra and Ashanti Regions having 3 and 2 respectively due to the level of population (customer size) in these regions. There are 90 water treatment plants supplying water to the entire country. Bulk water production volumes, customer size, billing records and revenue collection among others were collected from these 90 plants of the various regions. Bulk monthly water consumption and customer strength records from 2018 to 2022 were obtained from the GWCL for this study. The essence is to understand the situation prior to and during COVID-19. Interrupted Time Series Analysis (ITSA) was conducted taking April 2020 as the start of the intervention since the lockdown and the "free water" policy all took place at the end of March. This imply that the full effect of the interruption will be felt in April. A total of 60 data points, 27 data points pre-interruption and 33 data points post-interruption were used for the ITSA. The purpose of the ITS analysis is to determine whether the water consumption data patttern observed after

the outbreak (interruption) varies compared to that observed before the interruption.

2.2 Statistical Analysis: ITSA

One way of assessing whether water consumption behaviour has changed during the outbreak of the recent Coronavirus (COVID-19) pandemic in Ghana is to use the ITSA design to evaluate if there has been an immediate impact and/or decrease or increase in the trend of water use. This was done using the "itsa addon" in stata (Linden, 2015). It is an increasingly popular quasi-experimental design involving the analysis of time series data, like an outcome measured over a time period of a defined population (Hudson et al., 2019). Basically, it refers to a set of measurements taken at equal intervals over a period of time that are interrupted by an intervention. The itsa is a wrapper program that uses the Newey-West method (Newey and West 1987) by default and produces Newey-West standard errors for coefficients estimated by ordinary least-squares regression (Linden, 2015). The standard errors are robust and adjusted for autocorrelation and heteroscedasticity (Dorward et al., 2021; Linden, 2018; Turner et al., 2021). It is very useful in solving complex situations, which is why this study employs the model to evaluate and compare the pre- and post-intervention water used during the COVID-19 pandemic. The method also allows the researcher to specify the number of lags to include in the model. The lag determines the extent to which previous information is relevant in predicting current happenings. The Cumby-Huizinga test for auto-correlation was employed to test for the maximum number of lags. The "itsa" accepts an outcome variable, a time variable for the pre-and post-intervention times, and a dummy variable for pre- and post-intervention and interaction term. The model time variable measures the trend before the intervention, the intervention variable measures the immediate impact of the intervention while the interaction term estimates the difference between the pre-intervention and post-intervention trend (Dorward et al., 2021; Linden, 2015). The model is specified as follows:

$$V_t = \beta_0 + \beta_1 T_t + \beta_2 X_t + \beta_3 T_t X_t + \varepsilon_t$$

where:

V_t is the monthly volume of water used

T_t is the time variable measuring the period from the start of the study

X_t is the interruption variable which is a dummy variable with 1 of interruption period and 0 otherwise

β_0 is the base level

β_1 is the trend before the intervention

β_2 is the immediate impact of the interruption

β_3 is the difference between the pre- and post-interruption trend

ε_t is the error term.

According to Penfold and Zhang (2013), a researcher may use a single time series to describe only the intervention or compare the changes by the intervention at one time point to another time point where there are no interventions introduced, usually referred to as the control.

3.0 RESULTS AND DISCUSSION

A comparison of the monthly bulk consumption data for 2018 - 2022 indicated that there was notable increase in the volume of water per region in 2020 in relation to the previous year 2019 when the pandemic had not occurred. This general increase in consumption in each region for the year 2020 can be observed in Figure 1. In 2021, nearly all regions still recorded a relatively higher consumption than pre-pandemic volumes, though lower than that of 2020, which suggests that people continued to observe the hygiene practices despite returning to their workplaces. However, it can also be seen that in 2022, some regions, except Ashanti South, Western and Central, recorded significantly higher consumption compared to 2021 but lower than 2020.

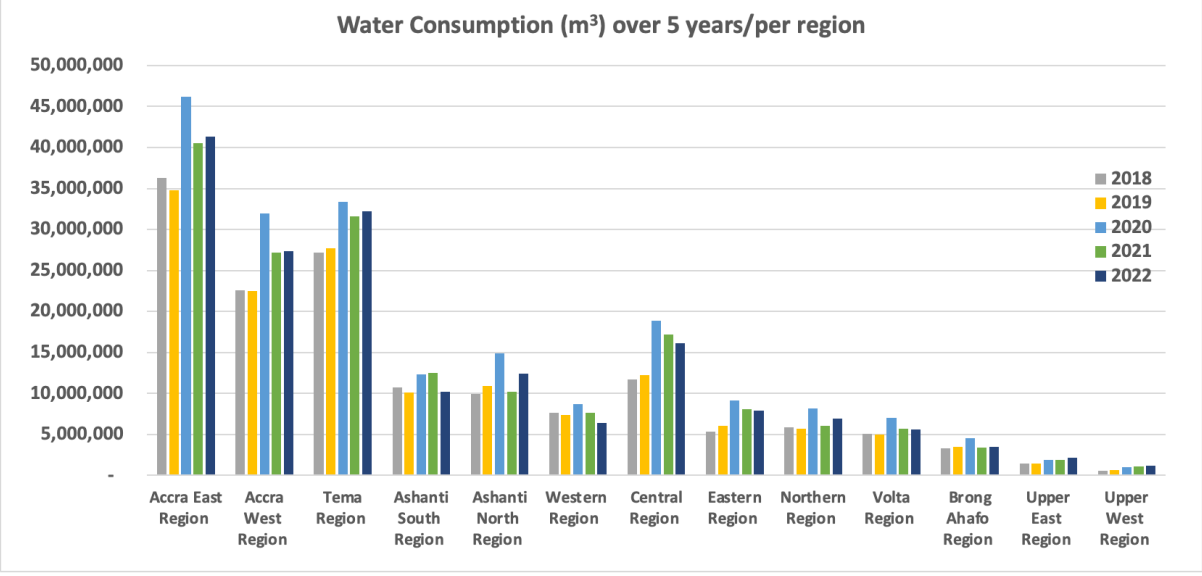

Figure 1: Water consumption per region over 5 years

It can also be seen from Figure 1 that; Accra East recorded the highest increase in water consumption compared to previous years (2018 - 2019). Overall, in 2020, the average national increase in consumption was 34% even though some regions recorded as low as 18% (Western region) and others as high as 67% (Upper West region) as shown in Table 1.

Table 1: Comparing percentage increase in consumption in the regions over the years

Region	2018 & 2019 (%)	2019 & 2020 (%)	2020 & 2021 (%)	2021 & 2022 (%)
Accra East	-4	33	-12	-23
Accra West	0	42	-15	-24
Ashanti North	10	36	-32	-26
Ashanti South	-5	22	1	-25
Brong Ahafo	6	30	-25	-22
Central	5	55	-9	-28
Eastern	13	51	-12	-24
Northern	-3	43	-26	-12
Tema	2	21	-5	-23
Upper East	1	32	-1	-12
Upper West	10	67	5	-36
Volta	-1	40	-19	-26
Western	-4	18	-12	-40
Average	**0**	**34**	**-13**	**-25**

It must be noted that the vast difference in overall water consumption over the years between Accra East, and Upper West Region (which has the lowest consumption) is due to the differences in the number of customers and water supply infrastructure coverage. Accra and Tema are mostly densely populated urban areas with high coverage of the water network, compared to the Upper West regions where the situation is the exact opposite in terms of network coverage and population density which influence customer strength. Table 2 shows the percent increase in customer strength for each region over the years. The average percentage increase in customer strength per annum prior to COVID-19 was 7%. In 2020 compared to 2019, there was an average increase of 10% while the years after the pandemic recorded an average increase of 9% and 8% respectively for 2021 and 2022. Some regions recorded significant increases in customer strength as high as 37% (Upper West), 14 % (Tema), 11% (Brong Ahafo) and 10% (Volta and Eastern). It must be indicated that, Upper West region consistently recorded an increase in customer strength due to its new water infrastructure and GWCL's general campaign to connect new customers to the network. In the main Cape Coast network, there is no expected increase in customer strength since it is the oldest urban network, densely populated and customers are already connected. It is therefore likely that, the 7% increase recorded may be due to relatively newer networks such as the Ekumfi, Baifikrom, Twifo Praso and Winneba networks in the Central region. Other reasons for the increase in water consumption were due to changes in hygiene practices, the lockdown which shifted consumptive uses and announcement of "free water" policy in addition to the expected natural increase due to population growth (Aquatech, 2020; Lüdtke et al., 2021).

The heightened campaign on hygiene practices such as hand washing, regular bathing and cleaning of surfaces contributed to an increase in water consumption in 2020. Due to the lockdown, institutional and industrial water uses shifted to domestic consumption (Aquatech, 2020; Cooley et al., 2020). As people stayed and worked from home, there were changes in lifestyle and adoption of new hobbies such as backyard gardening. In order to encourage the maintenance of hygiene practices, the government's announcement of "free water for all" policy led to access to water services 24/7 to Ghanaians irrespective of their status as customers of GWCL. This led to increase in customer strength due to reconnection of previously disconnected metres and reactivation of inactive accounts. Also, urban areas without pipe borne water or hitherto suffered intermittent supply were served with water in tankers (Abubakari et al., 2023). In some networks, where there is heavy reliance on public standpipes, commercial operators were mandated to allow people to fetch water freely. Furthermore, there is an expected natural increase in consumption due to population growth, however, it is not clear whether the 2022 consumption differences are purely due to

Table 2: Percentage increase in customer strength for each region over the years

Regions	2019 - 2018 (%)	2020 - 2019 (%)	2021 - 2020 (%)	2022-2021 (%)
Accra East	7	7	7	6
Accra West	6	8	8	6
Ashanti North	4	7	8	6
Ashanti South	2	4	4	4
Brong Ahafo	8	11	6	6
Central	11	7	12	8
Eastern	7	10	9	8
Northern	11	8	6	6
Tema	9	14	10	9
Upper East	5	8	15	23
Upper West	16	37	25	17
Volta	7	10	7	6
Western	4	5	6	4
Average	**7**	**10**	**9**	**8**

to natural increase or hygiene practices which have remained with people.

3.1 Effects of "free water" policy on water consumption

Before the actual model was estimated, the Cumby Huizinga test was conducted to determine the maximum number of lags to be included. Lag (1) was tested against a null of Lag (0). The results show that, the errors of the outcome variable are not serially correlated (p-value of 0.088). ITSA was therefore

carried out at level. Table 3 shows the coefficients and Newey-West standard errors of the ITSA carried out. From the table, the base volume of water before the start of the interruption was estimated as 12,200,000 cubic metres. The coefficient for the time variable was 23,420 which means that there was a positive natural trend in monthly water consumption over time, before the intervention of the "free water" policy was announced. This trend was however not significant at 10% alpha level. In the first month of the interruption, there appeared to be a significant increase in volume of water used by 4,048,293 cubic metres at a significant level of 1%. This indicates that the announcement of "free water" policy led to a huge jump in bulk water consumption suggesting that, the pandemic had a major impact due to increased awareness of hygiene practices such as hand washing, regular bathing and cleaning of surfaces.

Table 3: Impact of Covid-19 on Water Consumption

Variable	Coefficient (Newey-West Standard Errors)
Time (β_1)	23420.61 (22590.8)
Intervention (β_2)	4048293*** (675659.4)
Time*Intervention (β_3)	-127563.5*** (32382.5)
Constant (β_0)	12,200,000 *** (278942.9)
Treated	-104142.9 (23201)

Note: *** significant at 1%; ** significant at 5% and * significant at 10

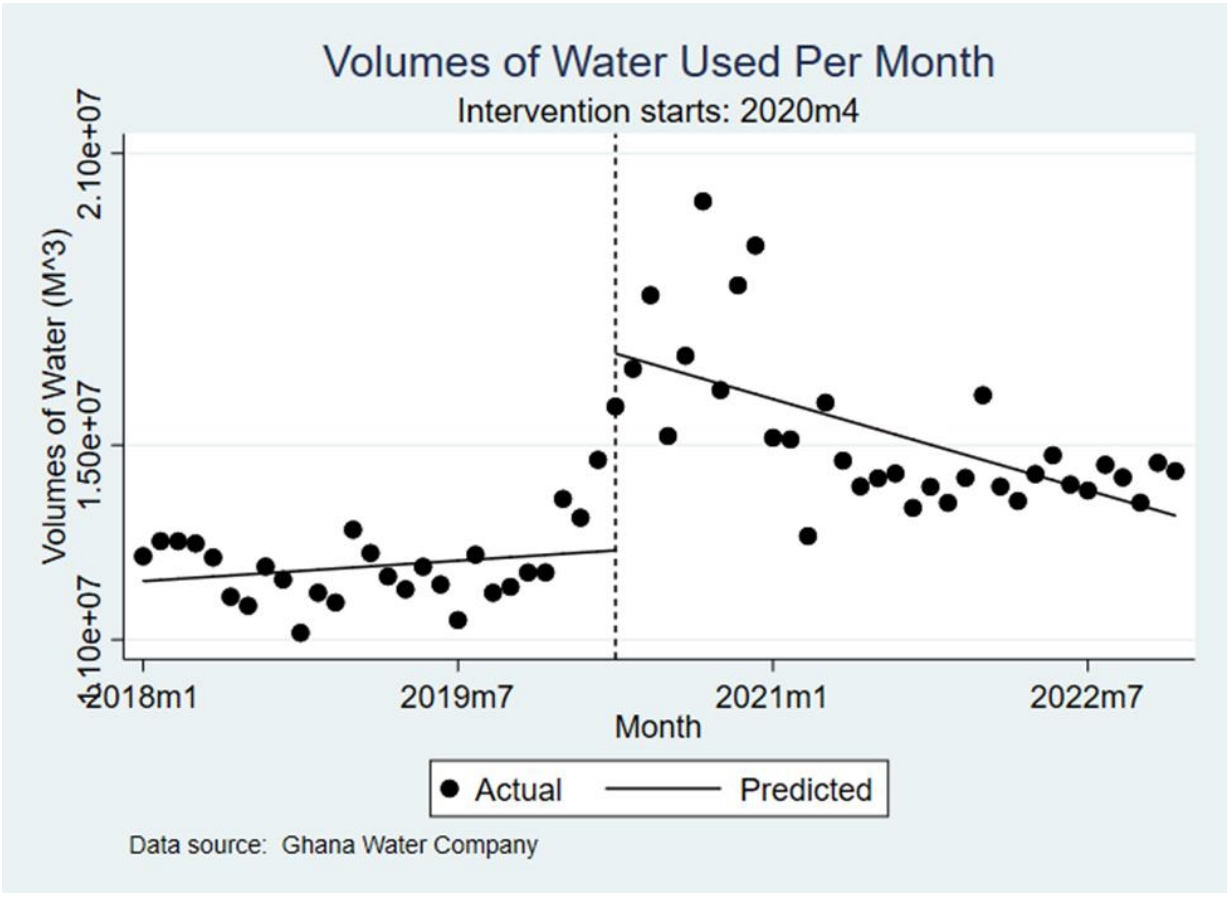

Figure 1: Single group ITSA with Newey–West standard errors and zero lag

There is a significant difference in the monthly trend before and after the interruption. However, there is a decrease in monthly bulk consumption post interruption, which is evident in the coefficient of -127,564 significant level of 1%. This suggests that the withdrawal of the "free water" policy had an effect on water consumption over time as payment for water services started in February 2021 and people needed to adjust their consumptive uses in order to avoid paying more for water. It must also be indicated that, the decreasing trend may have been sustained due to the recent hikes in tariffs. There was a 22% increase in water tariffs in September 2022 and a further increase of 8% in February 2023 (Ntow, 2023; PURC, 2022). Therefore, a further decrease is expected to bring consumption close to the pre-pandemic levels. The overall average increase in consumption due to the pandemic as indicated earlier was 34%. However, this study is unable to differentiate the changes in domestic, institutional and industrial consumption. Also, because monthly consumption volumes are used, the changes in typical daily patterns such as delayed morning peak and higher morning peaks as in Aquatech (2020) were not discussed.

The findings of this study concludes that the hygiene requirements of the Covid era, along with the "free water" policy from the government of Ghana led to increased water consumption.

4.0 CONCLUSION

The outbreak of the pandemic brought about the need to enhance hygiene practices as an important measure to control the spread of SARS - CoV2 (COVID-19) disease. The study sought to investigate the effects of the enhanced hygiene practices and measures such as the "free water" policy, on water consumption in Ghana, during and after COVID-19 pandemic. From the study, it can be concluded that there was a significant change in bulk water consumption during the COVID-19 pandemic. The study revealed an average increase in water consumption of 34%. This increase is attributed to changes in consumer behaviour (increased use of water for hygienic purposes), a more consistent supply of water to consumers (through activities such as reconnection of disconnected consumers by GWCL, and water provision through tanker services) and a 10% increase in customer size. The subsequent announcement of the "free water" policy also contributed significantly to an increase in consumption volumes across the nation. Moreover, this impact changed over time, which suggests that the free water supply policy may have had a varying effect on the different regions of the Ghanaian population. Such policies have implications on service delivery as was seen in the challenges such as abruptness of the intervention, poor communication and little or no consultation as stated in Abubakari et al. (2023).

This work has implications on further research, policy indications and engineering practice. For forecasting, planning and allocation of funds for investment purposes, a detailed study should be conducted to investigate the reasons that accounted for the increases in each region. There is the need to empirically analyse the behavioural changes in people's daily lives with respect to water use and its implications for water supply in Ghana. In preparation for future pandemics, the quantity of water required to meet the demands commensurate to fight the disease burden should be established. Also, understanding of the challenges that fraught the implementation of the "free water" policy should be documented. A future study would explore more than one intervention, for example, the "free water" policy and the first increase in tariff (in September 2022) after the policy was withdrawn. Furthermore, the influence of water tariffs on consumption in Ghana needs to be investigated.

REFERENCES

Abu-Bakar, H., Williams, L., & Hallett, S. H. (2021). Quantifying the impact of the COVID-19 lockdown on household water consumption patterns in England. Npj Clean Water, 4(1). https://doi.org/10.1038/s41545-021-00103-8

Abubakari, M., Agyemang, F. Y., & Tei, F. (2023). The limits and impact of communication and context in implementing social interventions in a pandemic: Ghana's free water policy revisited. Social Sciences & Humanities Open, 7(1), 100483.

Alda-Vidal, C., Smith, R., Lawson, R., & Browne, A. (2020). Understanding changes in domestic water consumption associated with COVID-19 in England and Wales. In Artesia Consulting and University of Manchester. https://shorturl.at/cEHKQ

Almulhim, A. I., & Aina, Y. A. (2022). Understanding Household Water-Use Behavior and Consumption Patterns during COVID-19 Lockdown in Saudi Arabia. Water (Switzerland), 14(3). https://doi.org/10.3390/w14030314

Alvisi, S., Franchini, M., Luciani, C., Marzola, I., & Mazzoni, F. (2021). Effects of the COVID-19 Lockdown on Water Consumptions: Northern Italy Case Study. Journal of Water Resources Planning and Management, 147(11), 5021021. https://doi.org/10.1061/(ASCE)WR.1943-5452.0001481

Amoah, A. (2020). Estimating averting expenditure in domestic water use: evidence from Ghana. Journal of Water, Sanitation and Hygiene for Development, 10(4), 894–904. https://doi.org/10.2166/washdev.2020.197

Aquatech. (2020). How Covid-19 impacts water consumption. https://www.aquatechtrade.com/news/utilities/covid-19-lockdowns-impact-water-consumption/

Balacco, G., Totaro, V., Iacobellis, V., Manni, A., Spagnoletta, M., & Piccinni, A. F. (2020). Influence of COVID-19 spread on water drinking demand: The case of Puglia Region (Southern Italy). Sustainability (Switzerland), 12(15). https://doi.org/10.3390/SU12155919

Birişçi, E., & Öz, R. (2021). Household water consumption behavior during the COVID-19 pandemic and its relationship with COVID-19 cases. Environmental Research and Technology, 4(4), 391–397. https://doi.org/10.35208/ert.953879

Brauer, M., Zhao, J. T., Bennitt, F. B., & Stanaway, J. D. (2020). Global Access to Handwashing: Implications for COVID-19 Control in Low-Income Countries. Environmental Health Perspectives, 128(5), 057005. https://doi.org/10.1289/EHP7200

Campos, M. A. S., Carvalho, S. L., Melo, S. K., Gonçalves, G. B. F. R., dos Santos, J. R., Barros, R. L., Morgado, U. T. M. A., da Silva Lopes, E., & Reis, R. P. A. (2021). Impact of the COVID-19 pandemic on water consumption behaviour. Water Supply, 21(8), 4058–4067. https://doi.org/10.2166/ws.2021.160

Cooley, H., Gleick, P. H., Abraham, S., & Cai, W. (2020). Water and the COVID-19 Pandemic Impacts on Municipal Water Demand. Pacific Institute. pacinst.org

Cooper, R. (2020). Water security beyond Covid-19 (Issue April).

Dapaah, E. (2020, April 5). Akufo-Addo announces free water for Ghanaians as government intensifies COVID-19 fight. Citinewsroom. https://citinewsroom.com/2020/04/akufo-addo-announces-free-water-for-ghanaians-as-government-intensifies-covid-19-fight/

Del Boca, D., Oggero, N., Profeta, P., & Rossi, M. (2020). Women's and men's work, housework and childcare, before and during COVID-19. Review of Economics of the Household, 18(4), 1001–1017. https://doi.org/10.1007/s11150-020-09502-1

Dorward, J., Khubone, T., Gate, K., Ngobese, H., Sookrajh, Y., Mkhize, S., Jeewa, A., Bottomley, C., Lewis, L., & Baisley, K. (2021). The impact of the COVID-19 lockdown on HIV care in 65 South African primary care clinics: an interrupted time series analysis. The Lancet HIV, 8(3), e158–e165.

Eastman, L., Smull, E., Patterson, L., & Doyle, M. (2020). COVID-19 Impacts on Water Utility Consumption and Revenues Through June 2020. Raftelis, June, 1–5. https://nicholasinstitute.duke.edu/sites/default/files/publications/COVID-19-Resources-Im- pacts-on-Water-Utility-Consumption-and-Reve- nues.pdf

Government of Ghana. (2020). Address To The Nation By President Akufo-Addo On Updates To Ghana's Enhanced Response To The Coronavirus Pandemic. Speeches. https://presidency.gov.gh/index.php/briefing-room/speeches/1555-address-to-the-nation-by-president-akufo-addo-on-updates-to-ghana-s-enhanced-response-to-the-coronavirus-pandemic

Government of Ghana. (2021, January 3). Update No 21: Measures Taken To Combat Spread Of Coronavirus - The Presidency, Republic of Ghana. Speeches. https://presidency.gov.gh/index.php/briefing-room/speeches/1848-update-no-21-measures-taken-to-combat-spread-of-coronavirus

Graphic Online. (2020). Gov't extends free water package to December 31. General News. https://www.graphic.com.gh/news/general-news/ghana-news-gov-t-extends-free-water-package-to-december-31.html

GWCL. (2023). Company Profile – GWCL - Welcome. https://www.gwcl.com.gh/company-profile/

Hudson, J., Fielding, S., & Ramsay, C. R. (2019). Methodology and reporting characteristics of studies using interrupted time series design in healthcare. BMC Medical Research Methodology, 19(1), 1–7. https://doi.org/10.1186/s12874-019-0777-x

IWA. (2020). Managing Water Loss During Lockdown. Water Loss. https://iwa-connect.org/group/water-loss/timeline

Kalbusch, A., Henning, E., Brikalski, M. P., Luca, F. V. de, & Konrath, A. C. (2020). Impact of coronavirus (COVID-19) spread-prevention actions on urban water consumption. Resources, Conservation and Recycling, 163(August). https://doi.org/10.1016/j.resconrec.2020.105098

Kalra, S., Kelkar, D., Galwankar, S. C., Papadimos, T. J., Stawicki, S. P., Arquilla, B., Hoey, B. A., Sharpe, R. P., Sabol, D., & Jahre, J. A. (2014). The emergence of Ebola as a global health security threat: From "lessons learned" to coordinated multilateral containment efforts. Journal of Global Infectious Diseases, 6(4), 164–177. https://doi.org/10.4103/0974-777X.145247

Linden, A. (2015). Conducting interrupted time-series analysis for single-and multiple-group comparisons. The Stata Journal, 15(2), 480–500.

Linden, A. (2018). Combining synthetic controls and interrupted time series analysis to improve causal inference in program evaluation. Journal of Evaluation in Clinical Practice, 24(2), 447–453.

Lüdtke, D. U., Luetkemeier, R., Schneemann, M., & Liehr, S. (2021). Increase in Daily Household Water Demand during the First Wave of the Covid-19 Pandemic in Germany. Water (Switzerland), 13(3). https://doi.org/10.3390/w13030260

Mahato, S., Pal, S., & Ghosh, K. G. (2020). Effect of lockdown amid COVID-19 pandemic on air quality of the megacity Delhi, India. Science of the Total Environment, 730(January). https://doi.org/10.1016/j.scitotenv.2020.139086

Marshallsay, D. (2020, June 30). New Waterwise article! The effect of the coronavirus lockdown on water use. https://www.artesia-consulting.co.uk/blog/New Waterwise article! The effect of the coronavirus lockdown on water use

Mattioli, M. C., Boehm, A. B., Davis, J., Harris, A. R., Mrisho, M., & Pickering, A. J. (2014). Enteric pathogens in stored drinking water and on caregiver's hands in Tanzanian households with and without reported cases of child diarrhea. PLoS ONE, 9(1). https://doi.org/10.1371/journal.pone.0084939

Muhammad, S., Long, X., & Salman, M. (2020). COVID-19 pandemic and environmental pollution: A blessing in disguise? Science of the Total Environment, 728, 138820. https://doi.org/10.1016/j.scitotenv.2020.138820

Nemati, M. (2020). COVID-19 and Urban Water Consumption. In ARE Update (Vol. 24, Issue 1, pp. 9–11). University of California Giannini Foundation of Agricultural Economics.

Niasse, M., & Varis, O. (2020). Quenching the thirst of rapidly growing and water-insecure cities in sub-Saharan Africa. International Journal of Water Resources Development, 36(2–3), 505–527. https://doi.org/10.1080/07900627.2019.1707073

Ntow, F. (2023, January 17). Electricity and water tariffs up by 29% and 8% for Q1 of 2023. Ghana News Agency. https://gna.org.gh/2023/01/electricity-and-water-tariffs-up-by-29-and-8-for-q1-of-2023/

Nyavi, G. A. (2021, January 3). Gov't extends free electricity, water initiative to March - Graphic Online. General News. https://www.graphic.com.gh/news/general-news/ghana-news-gov-t-extends-free-electricity-water-initiative-till-march.html

Penfold, R. B., & Zhang, F. (2013). Use of interrupted time series analysis in evaluating health care quality improvements. Academic Pediatrics, 13(6), S38–S44.

Portsmouth Water. (2020). Annual Performance Report. In Hilos Tensados (Vol. 1, Issue). https://www.portsmouthwater.co.uk/wp-content/uploads/2020/07/2020-APR-Portsmouth-Water.pdf

PURC. (2022). Publication of tariffs: September 2022. September. https://www.purc.com.gh

Sayeed, A., Rahman, M. H., Bundschuh, J., Herath, I., Ahmed, F., Bhattacharya, P., Tariq, M. R., Rahman, F., Joy, M. T. I., Abid, M. T., Saha, N., & Hasan, M. T. (2021). Handwashing with soap: A concern for overuse of water amidst the COVID-19 pandemic in Bangladesh. Groundwater for Sustainable Development, 13. https://doi.org/10.1016/j.gsd.2021.100561

Turner, S. L., Karahalios, A., Forbes, A. B., Taljaard, M., Grimshaw, J. M., & McKenzie, J. E. (2021). Comparison of six statistical methods for interrupted time series studies: empirical evaluation of 190 published series. BMC Medical Research Methodology, 21(1), 1–19.

WHO. (2015). Water sanitation and hygiene (WASH) package and WASH safety plans Training of trainers. https://www.who.int/csr/disease/ebola/wash-training-2015/en/

WHO. (2020). Water, sanitation, hygiene, and waste management for SARS-CoV-2, the virus that causes COVID-19: Interim Guidance (WHO/2019-nCoV/IPC_WASH/2020.4; Issue July). https://www.who.int/publications/i/item/WHO/2019-nCoV/IPC_WASH/2020.4

Yunus, A. P., Masago, Y., & Hijioka, Y. (2020). COVID-19 and surface water quality: Improved Lake water quality during the lockdown. Science of the Total Environment, 731, 139012. https://doi.org/10.1016/j.scitotenv.2020.139012

AUTHORS CONTRIBUTION

Peace Korshiwor Amoatey: Conceptualisation, background, literature review and Data Analysis (Descriptive statistics)

Godwin King-Nyamador: Literature review, data analysis theory, verification of references Micheal Martey: Data Analysis (Inferential Statistics)

Maxwell Akosah-Kusi: Data collection, organisation and preliminary analysis

A first-principles study of the Mechanical Stability and Electronic Properties of Lead-free Halide Inorganic Double Perovskites Cs_2InAgX_6 (X =F, Br, Cl, I)

Atarah, S. A.[1*], Gebreyesus, H. G.[1], and Egblewogbe, M. N. H[1]

[1]Department of Physics, University of Ghana, Legon, Ghana

***Corresponding author:** saatarah@ug.edu.gh

ABSTRACT

Lead-free double perovskites (DPs), Cs_2InAgX_6, specifically, were studied as candidate materials for photo voltaic cells (PVC). The density functional theory (DFT) methods as implemented in the Quantum Espresso suite was applied for the study. Equilibrium lattice parameters for the DP which are all face-centered cubic crystals, were determined as follows: a = 9.13 Å for X=F, a = 10.38 Å for X= Cl, a = 11.07 Å for X = Br and a = 11.39 Å for X = I. These findings align well with reported values. Additionally, elastic constants were calculated and found to be in fair agreement with reported values as well. Using the calculated elastic constants, all DPs were found to be ductile. The values of energy band gaps, Eg, calculated were Eg = 1.7 eV for X = F, Eg = 1.5 eV for X = Cl, Eg =0.9 for X = Br and Eg = 0.7 eV. It is noteworthy that, various studies, the experimentally reported Eg value for X = Cl, (in the range of 3.23-3.3 eV) significantly exceed the calculated Eg values in this work. The experimental Eg value for X = Cl as reported by several works is 3.23 - 3.3 eV, much higher than this and all calculated Eg values reported in this work. In summary, $Cs_2InAgCl_6$ emerges as a robust candidate material for PVCs, showcasing favorable mechanical stability and band gap characteristics. On the other hand, $Cs_2InAgBr_6$ would require band gap engineering to be a suitable material.

Keywords: Pb-free, halide double perovskite, photovoltaic cells, mechanical properties, first principles study

1.0 INTRODUCTION

Solar cell technology for harvesting energy is seen as a major source of energy for the future because it is eco-friendly and sustainable. The efficiency of solar cells has improved steadily over time as well (Nayak, P. K., Mahesh, S., Snaith, H. J., Cahen, 2019). It is also clear from the literature that Si based photovoltaic cells (PVCs) are by far the most successful technology for harvesting photovoltaic energy. However, power conversion efficiency (PCE) of Si based PVCs are rather low. Research for material alternatives to Si in solar cell and related technology is active and Perovskite materials are strong candidates for future PVC material due to their high laboratory PCE being reported. Perovskite materials have a general formula ABX_3, where A = monovalent cation, B = divalent, X is an anion, with

with commonly B = Pb. Pb-based halide perovskites have been studied extensively and are reported to hold promise for LED applications and for PVCs. They have been demonstrated to achieve power conversion efficiencies above 22%, and surpassing polycrystalline and thin-film silicon based PVCs (NREL, 2022). The features of perovskite material that lead to the high PCE are low carrier recombination, suitable absorption and extinction coefficients in the visible electromagnetic spectrum, high carrier mobility and direct energy band gap values (Mathew et al., 2019).

Optical, electronic and structural properties of various perovskite materials have been examined by many research groups both theoretically (D. Shi, V. Adinolfi, R. Comin, M. Yuan, E. Alarousu, A. Buin, Y. Chen & A. Rothenberger, 2015; J. H. Noh, S. H Im, J. H Heo, T. N Mandal, 2013; Meyer et al., 2018; Q. Dong, Y. Fang, Y. Shao, P. Mulligan, J. Qiu, L. Cao, 2015; S.D. Stranks, G.E. Eperon, G. Grancini, C. Menelaou, M.J. Alcocer, T. Leijtens & M. Herz, 2013; T.J. Jacobsson, M. Pazoki, A. Hagfeldt, 2015), and experimentally (Volonakis et al., 2017; W. Khan, S. Azam, M.B. Kanoun, 2016). Pb-based perovskite materials have been reported for their high PCE but Pb is toxic (Green et al., 2014), and environmentally hazardous when exposed to moisture which inevitably results from high humidity in the atmosphere (P.K. Kung, M.H. Li, P.Y. Lin, J.Y. Jhang, M. Pantaler, D.C. Lupascu, G. Grancini, 2020). Efforts are directed at minimizing or replacing Pb in PVCs. Therefore, the stability of Pb-free perovskites are being studied. An early attempt at realizing a Pb-free material was to replace Pb^{2+} with Sn^{2+} in the structure $APbX_3$ (X= Br, I, Cl). However such products were found to be unstable (Zhen Li, Mengjin Yang, Ji-Sang Park, Su-Huai Wei, Joseph J. Berry, 2016). Double perovskites are emerging as alternatives to the existing lead halide perovskites. The general formula for double perovskites is A_2BX_6 or $A_2BB'X_6$, where A and B are respectively inorganic cations and tetravalent ions with X a halide. Initial studies on double perovskites have reported mixed results. Combinations of Ag and Cu on one hand with Bi, In and Sn on the other in place of Pb^{2+} have been tried. Such products as Cs_2CuBiX_6 or $CsAgSnX_6$ were found to yield either indirect band gaps or energy band gaps larger than 2 eV(T.J. Jacobsson, M. Pazoki, A. Hagfeldt, 2015),(Volonakis et al., 2017)(Slavney, A. H.; Hu, T.; Lindenberg, A. M.; Karunadasa, 2016). Cs_2BiAgX_6 (X = Cl, Br) have been synthesized and found to exhibit band gaps in the visible range (Filip, M. R.; Hillman, S.; Haghighirad, A. A.; Snaith, H. J.; Giustino, 2016).

However, the band gaps of these compounds are indirect which is not ideal for applications in thin film photovoltaics. The study on $Cs_2AgBiBr_6$, by Savory et al reported an efficiency of less than 8% (Christopher N. Savory, Aron Walsh, 2016). W. Mukhtar et al (Waqas Mukhtar et al., 2021) using first principle studies reported that the double perov skites Rb_2NaInI_6 and Cs_2NaInI_6 are direct energy bandgaps of values 1.121 eV and 1.111 eV respectively.

Maughan et al (A.E. Maughan, A.M. Ganose, M.A. Almaker, D.O. Scanlon, 2018) and others (A. Kaltzoglou, D. Perganti, M. Antoniadou, A.G. Kontos, 2016) independently studied the Cs2SnI6 and reported an energy bandgap of nearly 1.2 eV) and carrier mobility of 509 cm2/V/ s. These reported band gap energies in the range of 1.0 eV are suitable for PVCs. Other promising double perovskites that are recommendable for use as active layers in PVCs are $Cs_2InSbCl_6$, $Cs_2AgInBr_6$, $Rb_2AgInBr_6$, and $Rb_2CuInCl_6$. Initial studies show that in addition to having desirable energy bandgaps, these have higher PCE compared to ABX_3 material (J. Zhou, J. Luo, X. Rong, P. Wei, M.S. Molokeev, Y. Huang, J. Zhao & X. Zhang, J. Tang, 2019; Michael M. Lee, Joël Teuschertsutomu, 2012; Xin-Gang Zhao, Dongwen Yang, Yuanhui Sun, Tianshu Li†, Lijun Zhang, Liping Yu, 2017). Although organic-inorganic compound combinations in perovskites have been used to implement optoelectronic devices, instability arising from long term expose to sunlight and humidity is reported as a factor to consider in adopting perovskites for PVC application (H.-S. Kim, C.-R. Lee, J.-H. Im, K.-B. Lee, T. Moehl, A. Marchioro & R. Humphry-Baker, J.-H. Yum, 2012), (Nam Joong Jeon, Jun Hong Noh, Woon Seok Yang, Young Chan Kim, Seungchan Ryu, 2015). The stability of perovskites is therefore a threat to their development as PVCs. Nishita et al (Mathew et al., 2019) presented preliminary results on the electronic and structural properties of Cs2InAgCl6 but the stability of the material was not reported. In this study, the mechanical stability of some lead–free double perovskite material (Cs_2InAgX_6; X= F, Cl, Br, I) was studied using DFT. Except $Cs_2InAgCl_6$, experimental data on which is being reported (Volonakis et al., 2017), the compounds with X = F, Br, and I are hypothetical but potentially represent an important class of promising PVC material. This study also discusses the electronic properties of the selected material.

2.0 METHODOLOGY AND COMPUTATIONAL DETAILS

For the current work, the Quantum Espresso (P Giannozzi, S Baroni, 2017) computational suite was used and the calculations were carried out using the plane wave DFT approach. The Perdew-Burke-Ernzerhof (PBE) Generalized Gradient Approximation (PBE-GGA) was applied. The electron exchange energy correlation functionals which were taken within the PBE formulation and ultrasoft pseudopotentials for solids (PBE-sol) were used to describe the atomic potentials. Indium 4d 5s orbitals were included for core correction whiles in general 4p 5s orbital were included for halides. For all calculations, the Hubbard +U correction was applied on Ag 3d orbital. The calculations did not include spin-orbital coupling effects as these have all The k-point meshes for all structures were generated according to Monkhorst-Pack scheme for the Brillouin zones. Sampling of Brillouin zone integration with k-point mesh 10×10×10 was set,

while denser k-mesh of 12×12×12 was used for DOS calculations. The kinetic energy cut-off for electrons was determined by the minimum required for the element with the highest energy cut-off requirement and ranged between 60 Ry for Cs_2InAgI_6 and 90 Ry for $Cs_2InAgCl_6$. Stringent convergence requirements were set for each compound with interatomic force thresholds typically 10^{-7} Ry/Å. In all calculations the electron convergence threshold was 10^{-12} Ry. The equilibrium lattice parameters of crystals were computed by self consistently calculating the minimum total energy per unit cell of each compound for a range of values of lattice constants. A plot of energy vs volume was then fitted by the Birch-Murnaghan equation of state and the equilibrium lattice parameters (corresponding to minimum energy) obtained for each compound. Elastic constants were obtained directly from self consistent thermal computations. In order to predict the formation of stable perovskite the Goldschmidt test was used. As all the unit cells of the compounds were face centered cubic crystals, the bulk modulus, B, was obtained from the elastic constants C_{11}, C_{12} and C_{44} at zero pressure as:

$$B = \frac{C_{11} + 2C_{12}}{3} \quad (1)$$

The shear modulus G is taken as an average of the Voight (G_V) (Lv et al., 2016), Reuss (G_R) (Li et al., 2017) and Hill (Erum & Iqbal, 2016) approximations as

$$G = \frac{G_V + G_R}{2} (2)$$

where

$$G_R = \frac{5C_{44}(C_{11} - C_{12})}{4C_{44} + 3(C_{11} - C_{12})} (3)$$

and $$G_V = \frac{C_{11} - C_{12} + 3C_{44}}{5} (4)$$

The possibility of the selected atoms forming perovskite crystals stably was assessed by use of the Goldschmidt (Volonakis et al., 2017) tolerance (*t)* and octahedral (μfactors defined as

$$\mu = \frac{R_B}{R_X} (5)$$

$$t = \frac{R_{Cs} + R_X}{\sqrt{2}(R_B + R_X)} (6)$$

$$R_B = 0.5(R| \quad |+R_{Ag}) (7)$$

where R_{Cs}, R_X are the Shannon ionic radii of the Cs cation and the X anion respectively. R_B was estimated as the average of In and Ag ionic radii as shown in (7).

3.0 RESULTS

3.1 Structural properties and mechanical stability

Table 1 shows the calculated lattice and bulk constants, the octahedral and tolerance factors and the Pugh ratios for the material. Also included in the table are values from references. The calculated bulk moduli were reproduced by fitting to the energy-volume plot using the Birch-Murnaghan equation of state.

Table 1: Lattice constants, bulk and shear moduli and relate ratios of the perovskites

Anion X	**F**	**Cl**	**Br**	**I**
a (Å) This work	9.015	10.3897	10.8989	11.5385
a (Å) (References)	9.138 (M. Tariq, Malak Azmat Ali, A. Laref, 2020)	10.467 (Z. Zhou, M.S. Xia, X. Molokeev, D. Peng Zhang, 2017), 10.65 (Enamul Haque, 2019), 10.47 (expt. (Volonakis et al., 2017))	10.74 (Volonakis et al., 2017)	11.52(Hang Yin, Yeming Xian, Yongli Zhang, Wenzhe Li, 2019)
B (Gpa)	47.028	38.270, 29.12 (M. Tariq, Malak Azmat Ali, A. Laref, 2020), 46.8 (Enamul Haque, 2019)	23.465 23.46 (M. Tariq, Malak Azmat Ali, A. Laref, 2020)	109.970

G (Gpa)	13.77	14.828	23.465	364.669
Pugh ratio (= B / G)	3.415	2.580	3.103	0.290
octahedral factor, *t*	0.733	0.538	0.497	0.443
Tolerance, μ	0.985	0.937	0.925	0.909
Poisson ratio	1.347	0.328	0.352	0.3800

Table 2: Elastic constant and test of stability using elastic constants

Anion X	**F**	**Cl**	**Br**	**I**
C_{11} (GPa)	66.941	64.575, 93.03 (Enamul Haque, 2019)	131.205	204.390
C_{12} (GPa)	37.072	25.119, 23.69 (M. Tariq, Malak Azmat Ali, A. Laref, 2020)	43.632	62.764
C_{44} (GPa)	-13.045	12.231	15.038	20.542
$C_{11} > \|C_{12}\|$	Yes	Yes	Yes	Yes
$C_{44} > 0$	No	Yes	Yes	Yes
$C_{11} + C_{12} > 0$	Yes	Yes	Yes	Yes

Elastic constants hold information on the mechanical stability, the bonding, stiffness and other related properties of materials subjected to externally applied stress (Amal Moussali, Mahdad Benzardjab Amina, Benattou Fassi, Ibrahim Ameri, Mohammed Ameri, 2020). Table 2 shows the calculated elastic constants and the stability test results, whereas the calculated energy band gaps are shown in Table 3.

Table 3: Calculated energy band gaps (in eV) for the double perovskite material studied

Anion X	**F**	**Cl**	**Br**	**I**
This work	1.7	1.5	0.4	0.7
Other work (Theoretical)	3.44 (M. Tariq, Malak Azmat Ali, A. Laref, 2020)	1.5 (Volonakis et al., 2017), 1.35 (N.K. Noel, S.D. Stranks, A. Abate, C. Wehrenfennig, S. Guarnera & Petrozza, 2014),	0.58 (Z. Zhang, J. Su, J. Hou, Z. Lin, Z. Hu, J. Chang, J. Zhang, 2019), 1.33 (G. Volonakis, 2018), 1.5 (Xin-Gang Zhao, Dongwen Yang, Yuanhui Sun, Tianshu Li†, Lijun Zhang, Liping Yu, 2017)	0.76 (M. Tariq, Malak Azmat Ali, A. Laref, 2020)
Other work Experiment	-	3.3 (Volonakis et al., 2017), 3.23 (Slavney, A. H.; Hu, T.; Lindenberg, A. M.; Karunadasa, 2016)	-	-

The energy band structure displays fundamental electronic characteristics of a material. Figure 1 shows the energy band diagrams and the density of states (DoS) plot for the halide-based double perovskites studied whilst the projected density of states are shown in Figure 2.

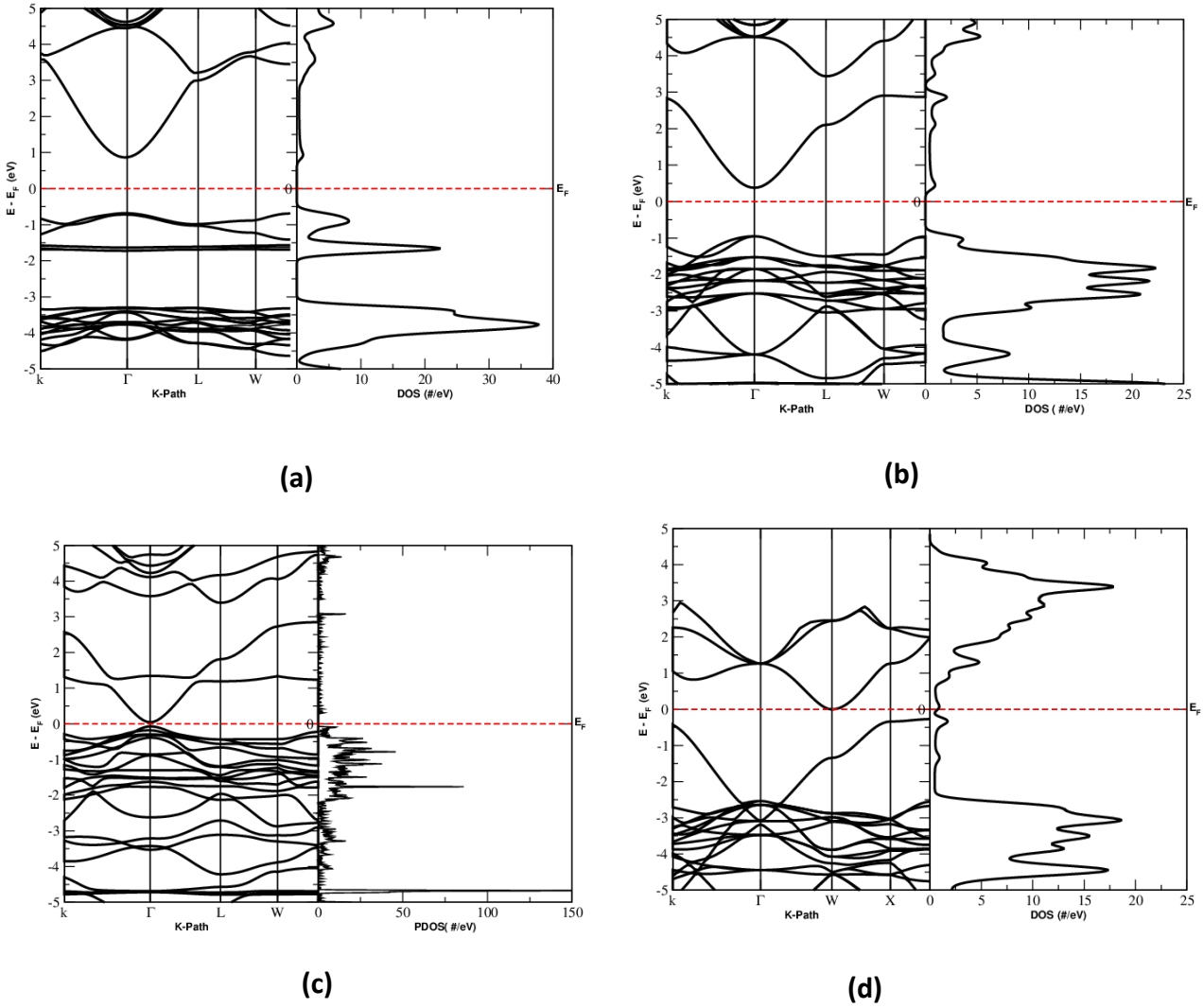

Figure 1: Energy band structures with DoS for all studied perovskites. (a) X = F, (b) X= Cl, (c) X=Br and (d) X = I

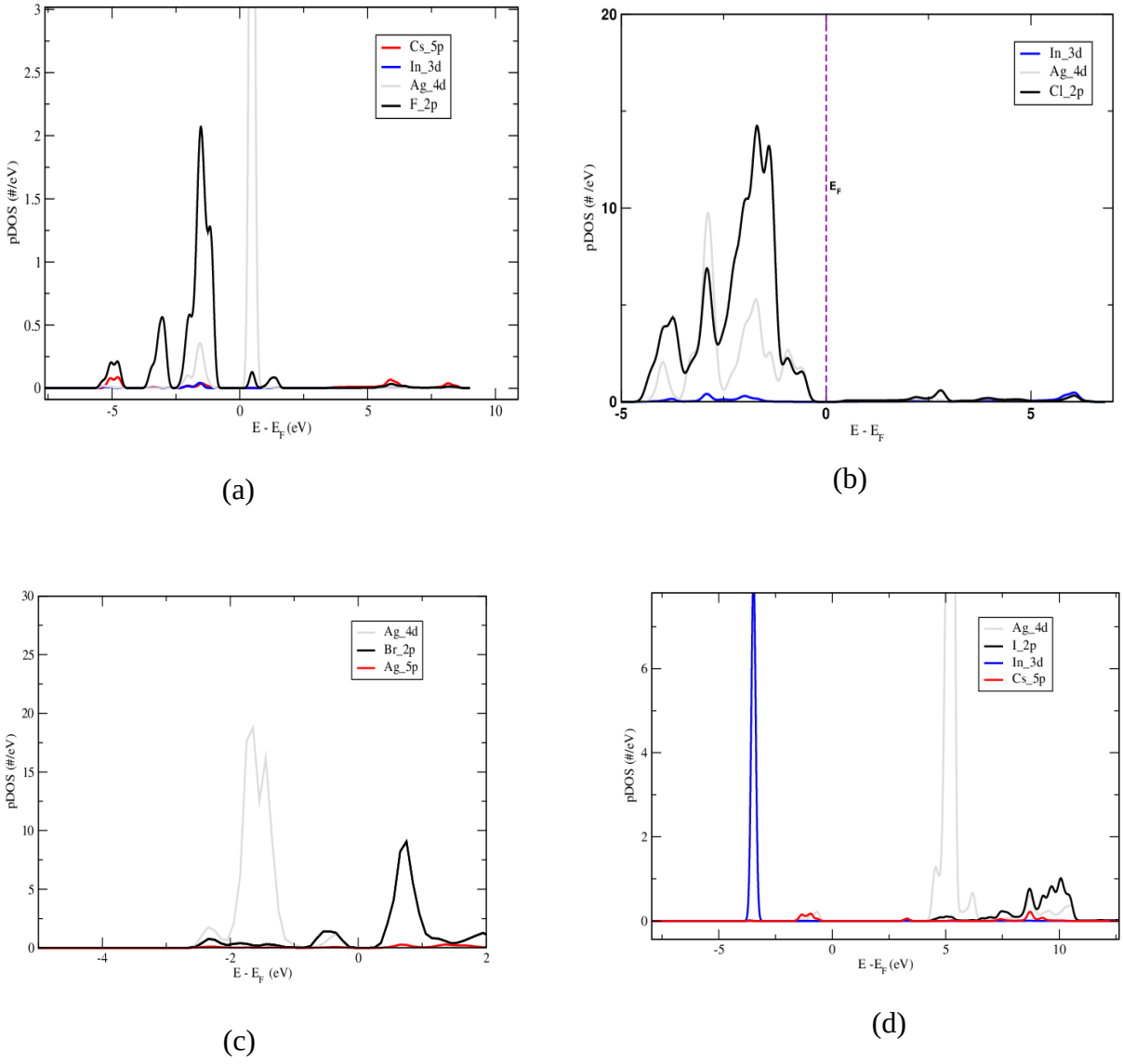

Figure 2: Projected DOS plots for (a) Cs_2InAgF_6, (b) $Cs_2InAgCl_6$, (c) $Cs_2InAgBr_6$ (d) Cs_2InAgI_6

4.0 DISCUSSION

All crystals were first relaxed to determine their equilibrium lattice parameters. It can be seen from Table 1 that compared to the lattice constants of the respective material reported by the indicated references, the calculated values can be said to be in fair agreement, deviating only in a narrow range

of +0.16% to +1.7%. As expected, it can be seen from the table that the calculated cell sizes increase as the halide atom changes from Fluorine to Iodine (i.e. down the periodic table). The bulk moduli of the perovskite material were also calculated in order to understand their mechanical properties. Bulk modulus measures the ease or resistance to volume changes (brittleness) whilst the ease of change in shape is measured by the shear modulus. The ratio of the bulk to the shear modulus, called the Pugh ratio is a measure of the ductile nature of the material. A Material is classified as ductile if its Pugh ratio is greater than 1.75 whilst the Poisson ratio should be greater than 0.26 (Waqas Mukhtar et al., 2021). Poisson's ratio is the ratio of the change in the width per unit width of a material, to the change in its length per unit length, as a result of strain.

The values of bulk moduli shown in Table 1 are similar to those obtained by Tariq *et al* (see Table 1 of (M. Tariq, Malak Azmat Ali, A. Laref, 2020). In particular for X = F, the values of bulk modulus was a match to earlier reported values (see Table 1 of (Sandeep et al., 2017)) giving confidence to our results. Except for X= I, all Pugh ratios are greater than 1.75 and would therefore be ductile in nature implying they would have a fair degree of flexibility which is suitable for solid state and flexible electronic applications. A Material is expected to form stable double perovskite if its tolerance value is in the range $0.8 \leq t \leq 1$ and its octahedral factor is greater 0.41 (Volonakis et al., 2017) or more precisely in the range $0.4 < t \leq 0.9$ (Meyer et al., 2018). The tolerance values and octahedral factors for the material, included in Table 1, are within the stability ranges. From these values it appears that all the materials studied would form stably as double perovskite crystals although the octahedral factor decreases as the ion X gets larger. The observation suggests that larger anions would least form as double perovskites.

The mechanical stability of the perovskite material was further assessed by determining whether they met the following conditions (for stability)(Bouafia et al., 2015): $|C_{44}| > 0$, $C_{11} - |C_{12}| > 0$ and $C_{11} + |C_{12}| > 0$. The results of the comparisons for all the compounds as displayed in Table 2 indicates that by this criterion alone all but for X = F are mechanically stable under reasonable stress.

The apparent conflict in the observation that all the studied material would form double perovskites yet Table 2 shows that for X = F, $C_{44} < 0$, can only be resolved by making a distinction between formation as double perovskite crystals and existing stably as such. For X=F, a hypothetical double perovskite may form but is not expected to exhibit stable mechanical properties.

4.1 Electronic properties

The electronic properties of the material is summarized in Figure 1 by the band structure and distribution of density of states. The band gap values derived from calculations are shown in Table 3. Values from other works are also indicated for comparison. Except for Cs_2InAgI_6, (which by the band structure, appears to be an indirect band gap material) the conduction band minima (CBM) and the valence band maxima (VBM) for all the compounds occur at the $\Gamma -$ point of the Brillouin zone, making them direct bandgap crystals. The indirect bandgap of Cs_2InAgI_6 indicates that it is not a good candidate perovskite for PVCs. Particularly noticeable is the very small energy band gap value for $Cs_2InAgBr_6$ which is consistent with the value reported earlier (Z. Zhang, J. Su, J. Hou, Z. Lin, Z. Hu, J. Chang, J. Zhang, 2019). This band gap value would make $Cs_2InAgBr_6$ electronically unsuitable particularly for solar energy harvesting. For X =Br, the double perovskite material may thus be considered for bandgap engineering. Of the three direct bandgap perovskites studied, $Cs_2InAgCl_6$ appears to offer the most promising electronic property with an energy bandgap of 1.5 eV.

Although an experimental band gap value of 3.3 eV has been reported, our value of 1.5 eV is consistent with several other calculations. (Z. Zhou, M.S. Xia, X. Molokeev, D. Peng Zhang, 2017) (Wonseok Lee, Seunghwa Hong, 2019). Projected partial densities of state, pDOS, plots show that across all the materials studied, the *2p* orbitals of the X anions dominate near their Fermi levels with the *4d* orbitals of the Ag cation (see Fig. 2) being the other most significant contributor of electrons to similar that energy band which is important to semiconducting properties. For clarity, other orbitals were left out of the plot as they were too small to be shown on the scale.

5.0 CONCLUSION

The mechanical stability of Pb-free double perovskites Cs_2InAgX_6 (X = halides F, Cl, Br, I) were studied along with their suitability, electronically, for photovoltaic cells. The results suggests that except for X = I, all perovskites in the series are direct bandgap semiconductors, but the bandgap for X = Br is so small that it is not good for PVC applications. Except for X = I, all material studied were found to be malleable. Results from the study shows that $Cs_2InAgCl_6$ would have the desired bandgap for PVC candidate material, and would be the most mechanically stable candidate among the series of halide double perovskites studied.

REFERENCES

A. Kaltzoglou, D. Perganti, M. Antoniadou, A.G. Kontos, P. F. (2016). Stress tests on Hole-transporting, dye-sensitized solar cells with the Cs2SnI6 defect perovskite as material. , *Energy Procedia*, *102*, 49–55.

A.E. Maughan, A.M. Ganose, M.A. Almaker, D.O. Scanlon, J. R. N. (2018). Tolerance factor and cooperative tilting effects in vacancy-ordered double perovskite halides. *Chem. Mater.*, *30*, 3909–3919.

Amal Moussali, Mahdad Benzardjab Amina, Benattou Fassi, Ibrahim Ameri, Mohammed Ameri, Y. A.-D. (2020). First-principles calculations to investigate structural and thermodynamic properties of Ni2LaZ (Z = As, Sb and Bi) Heusler alloys. *Indian Journal of Physics*, *94*, 1733–1747.

Bouafia, H., Sahli, B., Hiadsi, S., Abidri, B., Rached, D., Akriche, A., & Mesli, M. N. (2015). Theoretical investigation of structural, elastic, electronic, and thermal properties of KCaF3, K0.5Na0.5CaF3 and NaCaF3 Perovskites. *Superlattices and Microstructures*, *82*, 525–537. https://doi.org/10.1016/j.spmi.2015.03.004

Christopher N. Savory, Aron Walsh, and D. O. S. (2016). Can Pb-Free Halide Double Perovskites Support High-Efficiency Solar Cells? *ACS Energy Lett.*, *1*, 949–955.

D. Shi, V. Adinolfi, R. Comin, M. Yuan, E. Alarousu, A. Buin, Y. Chen, S. H., & A. Rothenberger, K. K. (2015). Low trap-state density and long carrier diffusion in organolead trihalide perovskite single crystals. *Science*, *347*, 519–522.

Enamul Haque, M. A. H. (2019). Electronic, phonon transport and thermoelectric properties of Cs2InAgCl6 from first-principles study. *Computational Condensed Matter*, *16*(e00374).

Erum, N., & Iqbal, M. A. (2016). First Principles Investigation of Fluorine Based Strontium Series of Perovskites. *Communications in Theoretical Physics*, *66*(5), 571–578. https://doi.org/10.1088/0253-6102/66/5/571

Filip, M. R.; Hillman, S.; Haghighirad, A. A.; Snaith, H. J.; Giustino, F. (2016). Band Gaps of Lead-Free Halide double perovskites Cs2BiAgCl6 and Cs2BiAgBr6 from theory and experiment. *J. Phys. Chem. Lett.*, *7*, 2579–2585.

G. Volonakis, F. G. (2018). No Title. *Appl. Phys. Lett.*, *112*, 243901.

Green, M. A., Ho-Baillie, A., & Snaith, H. J. (2014). The emergence of perovskite solar cells. *Nature Photonics*, *8*(7), 506–514. https://doi.org/10.1038/nphoton.2014.134

H.-S. Kim, C.-R. Lee, J.-H. Im, K.-B. Lee, T. Moehl, A. Marchioro, S.-J. M., & R. Humphry-Baker, J.-H. Yum, J. E. (2012). Lead Iodide Perovskite Sensitized All-Solid-State Submicron Thin Film Mesoscopic Solar Cell with Efficiency Exceeding 9%. . . *Moser, Sci. Rep*, *2*, 1–7.

Hang Yin, Yeming Xian, Yongli Zhang, Wenzhe Li, J. F. (2019). Structurally Stabilizing and Environment Friendly Triggers: Double-Metallic Lead-Free Perovskites. *Solar RRL*, *3*(9). https://doi.org/https://doi.org/10.1002/solr.201900148

J. H. Noh, S. H Im, J. H Heo, T. N Mandal, S. I. S. (2013). Chemical management for colorful, efficient, and stable inorganic–organic hybrid nanostructured solar cells. *Nano Letters*, *13*.

J. Zhou, J. Luo, X. Rong, P. Wei, M.S. Molokeev, Y. Huang, J. Zhao, Q. L., & X. Zhang, J. Tang, Z. X. (2019). Lead-free perovskite derivative Cs2SnCl6-xBrx single crystals for narrowband Photodetectors. *Adv. Optical Mater.*, *1*, 1900139.

Li, L., Wang, Y. J., Liu, D. X., Ma, C. G., Brik, M. G., Suchocki, A., Piasecki, M., & Reshak, A. H. (2017). Comparative first-principles calculations of the electronic, optical, elastic and thermodynamic properties of XCaF3 (X = K, Rb, Cs) cubic perovskites. *Materials Chemistry and Physics*, *188*, 39–48. https://doi.org/10.1016/j.matchemphys.2016.12.033

Lv, Z. L., Cui, H. L., Wang, H., Li, X. H., & Ji, G. F. (2016). Electronic and elastic properties of BaLiF3 with pressure effects: First-principles study. *Physica Status Solidi (B) Basic Research*, *253*(9), 1788–1794. https://doi.org/10.1002/pssb.201600094

M. Tariq, Malak Azmat Ali, A. Laref, G. M. (2020). Anion replacement effect on the physical properties of metal halide double perovskites Cs2AgInX6 (X¼F, Cl, Br, I). *Solid State Communications*, *113929*, 314–315.

Mathew, N. P., Kumar, N. R., & Radhakrishnan, R. (2019). First principle study of the structural and optoelectronic properties of direct bandgap double perovskite Cs2AgInCl6. *Materials Today: Proceedings*, *33*, 1252–1256. https://doi.org/10.1016/j.matpr.2020.03.489

Meyer, E., Mutukwa, D., Zingwe, N., & Taziwa, R. (2018). Lead-free halide double perovskites: A review of the structural, optical, and stability properties as well as their viability to replace lead halide perovskites. *Metals*, *8*(9). https://doi.org/10.3390/met8090667.

Michael M. Lee, Joël Teuschertsutomu, M. N. M. H. J. S. (2012). Efficient Hybrid Solar Cells Based on Meso-Superstructured Organometal Halide Perovskites. *Science*, *338*, 643–647.

N.K. Noel, S.D. Stranks, A. Abate, C. Wehrenfennig, S. Guarnera, A. A. H., & Petrozza, A. (2014). No. *Energy Environ. Sci.*, *7*(9), 3061–3068.

Nam Joong Jeon, Jun Hong Noh, Woon Seok Yang, Young Chan Kim, Seungchan Ryu, J. S. & S. I. S. (2015). Compositional engineering of perovskite materials for high-performance solar cells. *Nature*, *517*, 476–480.

Nayak, P. K., Mahesh, S., Snaith, H. J., Cahen, D. (2019). Photovoltaic solar cell technologies: analysing the state of the art. *Nature Reviews Materials*, *4*(4), 269–285. https://doi.org/10.1038/s41578-019-0097-0

NREL. (2022). *Best Research-Cell Efficiency Chart*. https://www.nrel.gov/pv/cell-efficiency.html

P.K. Kung, M.H. Li, P.Y. Lin, J.Y. Jhang, M. Pantaler, D.C. Lupascu, G. Grancini, P. C. (2020). Lead-free double perovskites for perovskite solar cells. *Sol RRL*, 190030.

P Giannozzi, S Baroni, N. B. et al. (2017). QUANTUM ESPRESSO: a modular and open-source software project for quantum simulations of materials. *J. Phys.:Condens. Matter*, *29*(465901).

Q. Dong, Y. Fang, Y. Shao, P. Mulligan, J. Qiu, L. Cao, J. H. (2015). Electron-hole diffusion lengths > 175 μm in solution-grown CH3NH3PbI3 single crystals. *Science*, *347*, 967–970.

S.D. Stranks, G.E. Eperon, G. Grancini, C. Menelaou, M.J. Alcocer, T. Leijtens, L., & M. Herz, A. P. (2013). Electron-hole diffusion lengths exceeding 1 micrometer in an organometal trihalide perovskite absorber. *Science*.

Sandeep, Rai, D. P., Shankar, A., Ghimire, M. P., Khenata, R., Bin Omran, S., Syrotyuk, S. V., & Thapa, R. K. (2017). Investigation of the structural, electronic and optical properties of the cubic RbMF3 perovskites (M = Be, Mg, Ca, Sr and Ba) using modified Becke-Johnson exchange potential. *Materials Chemistry and Physics*, *192*, 282–290. https://doi.org/10.1016/j.matchemphys.2017.02.005

Slavney, A. H.; Hu, T.; Lindenberg, A. M.; Karunadasa, H. I. A. (2016). Bismuth-Halide Double Perovskite with Long Carrier Recombination Lifetime for Photovoltaic Applications. *J. Am. Chem. Soc.*, *138*(2138–2141).

T.J. Jacobsson, M. Pazoki, A. Hagfeldt, T. E. (2015). Goldschmidt's Rules and Strontium Replacement in Lead Halogen Perovskite Solar Cells: Theory and Preliminary Experiments on CH3NH3SrI3. *J. Phys. Chem C*, *119*, 25673–25683.

Volonakis, G., Haghighirad, A. A., Milot, R. L., Sio, W. H., Filip, M. R., Wenger, B., Johnston, M. B., Herz, L. M., Snaith, H. J., & Giustino, F. (2017). Cs2InAgCl6: A New Lead-Free Halide Double Perovskite with Direct Band Gap. *Journal of Physical Chemistry Letters*, *8*(4), 772–778. https://doi.org/10.1021/acs.jpclett.6b02682

W. Khan, S. Azam, M.B. Kanoun, S. G.-S. (2016). Optoelectronic structure and related transport properties of BiCuSeO-based oxychalcogenides: First principle calculations. *Solid State Sciences*, *58*.

Waqas Mukhtar, M., Ramzan, M., Rashid, M., Naz, G., Imran, M., Fahim, F., AlObaid, A. A., Al-Muhimeed, T. I., & Mahmood, Q. (2021). New lead-free double perovskites A2NaInI6 (A = Cs, Rb) for solar cells and renewable energy; first principles analysis. *Materials Science and Engineering B: Solid-State Materials for Advanced Technology*, *273*(July), 115420. https://doi.org/10.1016/j.mseb.2021.115420

Wonseok Lee, Seunghwa Hong, S. K. (2019). J. Phys. Chem. C. *J. Phys. Chem. C*, *123*, 2665–2672.

Xin-Gang Zhao, Dongwen Yang, Yuanhui Sun, Tianshu Li†, Lijun Zhang, Liping Yu, and A. Z. (2017). Cu–In Halide Perovskite Solar Absorbers. *J. Am. Chem. Soc.*, *139*, 6718–6725.

Z. Zhang, J. Su, J. Hou, Z. Lin, Z. Hu, J. Chang, J. Zhang, Y. H. (2019). No Title. *J. Phys. Chem. Lett.*, *10*, 1120–1125.

Z. Zhou, M.S. Xia, X. Molokeev, D. Peng Zhang, Q. L. (2017). No Title. *J. Mater. Chem. A*, *5*, 15031–15037.

Zhen Li, Mengjin Yang, Ji-Sang Park, Su-Huai Wei, Joseph J. Berry, and K. Z. (2016). Stabilizing Perovskite Structures by Tuning Tolerance Factor: Formation of Formamidinium and Cesium Lead Iodide Solid-State Alloys. *Chem. Mater*, *28*, 284–292.

pH-Sensitive Biogenic Silica-chitosan modified for Targeted Folic Acid delivery

King J. Akuetteh[1], Bernard O. Asimeng[1*], Najat Inusah[1], Oluwabusola D. Adeologun[1], Woedem S. Atsutse[1], Sheila P. Kyeremeh[1], Edward Amenyaglo[1], and Elvis K. Tiburu[1]

[1]Department of Biomedical Engineering, University of Ghana, Legon, Accra, Ghana.

Corresponding author: boasimeng@ug.edu.gh

ABSTRACT

The drug loading onto silica derived from organic compounds satisfies the need for effective biocompatible carriers for sustained and targeted delivery. Silica is a naturally occurring material that is biocompatible and biodegradable. However, studies reveal silica nanoparticles' drug loading and release capabilities are uncontrolled and erratic. In this paper, biogenic silica (BS) was modified with chitosan to improve the loading and release capabilities in vitro. The BS was prepared by calcining for 4 hours at 600 ℃, and the modification was accomplished by immersing the BS in a chitosan solution overnight. The modified BS (BS-C) was characterised using Fourier transform infrared spectroscopy (FTIR) and X-ray diffractometry (XRD). Folic acid loading and release studies were performed for the BS alone and the BS-C using UV-Vis spectrophotometry analysis at a wavelength of 285 nm. The folic acid loading was done at a pH of 9, and release studies were done at a pH of 7.24 and 10.40. Results from the comparative analysis of the BS and the BS-C showed improvements in drug adsorption efficiency of 29.79 and 73.96%, respectively, in a 2-hour period. Thus, the findings show the potential application of folic acid delivery in the small intestine.

Keywords: Drug delivery, Folic acid, Biogenic silica

1.0 INTRODUCTION

Silica is a material that has become of keen interest in the area of nanomaterials. They have provided a different avenue for biomedical applications in areas such as bio-sensing, cellular uptake, and drug delivery (Devi *et al.,* 2016). Following advancements in research, the use of silica particles as drug delivery systems for sustained drug release is quickly becoming a sought-after application for scientists and engineers due to significant research focused on the design and implementation of biomaterials, which provide a sustained release of therapeutics and

can be modified for the bioavailability of drugs at specific locations in the body (Fenton et al., 2018). The sustained drug release reduces the high consumption of drugs and reduces toxicity in patients (Žid et al., 2020), which has inspired material scientists and engineers to study materials that have high stability and flexibility for the administration of drugs through various pathways (Menon & Pillai, 2022). One of the many materials that have been studied for use as a drug delivery agent is silica particles (Isa et al., 2021; Trzeciak et al., 2021). These particles can be acquired by organic or inorganic means. The use of chemicals such as tetraethyl orthosilicate (TEOS) and cetyl trimethyl ammonium bromide (CTAB), (Song *et al.*, 2019) constitutes the inorganic means, whereas the contrary makes use of natural materials composed of biogenic silica (BS) (de Cordoba et al., 2019).

Rice husk has been found to have the highest amount of silica among all plant-based resources (Chun et al., 2020), with a study reporting that about 95% by weight of amorphous silica can be obtained from rice husk after acid leaching treatment and calcination at 600° (Dorairaj et al., 2022; Suyanta & Kuncaka, 2011). Its use in obtaining BS is rapidly catching the attention of material scientists due to the low cost of production and eco-friendliness of these materials (Prabha et al., 2021). Approximately 148.2 million tonnes of rice husk are produced worldwide each year (Park et al., 2021), which speaks to their availability for utilisation. This allowed the use of rice husks in the production of magnetic Mobil Composition of Matter 41 (magMCM-41) for use as adsorbents and sensor bases (Kamari & Ghorbani, 2021). However, their use in designing drug delivery systems reveals a major challenge: insufficient drug delivery profiles. This was evident when BS was used for targeted release studies at pH above 7 (Salazar Hernández et al., 2014). Subsequent research observed an issue of uncontrolled drug delivery with BS, using Folic acid (FA) as the model drug (Carmen et al., 2017). Folic acid (FA) is an essential vitamin used in the regulation of homocysteine, to mediate the formation of cardiovascular diseases when metabolised (Ganguly & Alam, 2015; Ratajczak et al., 2021). A targeted delivery of FA prevents having an excess amount in the bloodstream and any possible development of cancer (Khan & Jialal, 2022; Tam et al., 2012).

Thus, we propose the use of chitosan for surface modification of BS for controlled folic acid studies at a selected pH of 7 and 10, since FA is mostly absorbed in an alkaline medium in the small intestine. Chitosan, a natural polymer with minimal toxicity, biodegradability, and biocompatibility (Ibrahim et al., 2015), has the presence of hydroxyl and amine functional groups that can interact with organic and inorganic compounds (Lizardi-Mendoza et al., 2016; Zhang et al., 2010). The modified material was characterized using X-ray diffraction spectroscopy and Fourier infrared spectroscopy, while drug loading and release studies were done using an ultraviolet (UV) visible spectrophotometer

2.0 MATERIALS

The rice husk used in this study was obtained from rice fields in the northern region of Ghana. Hydrochloric acid (HCl), nitric acid (HNO_3), and acetic acid (AcOH) were purchased from Sigma Aldrich. Industrial chitosan as well as pharmaceutical folic acid from Sundown® were used. Phosphate buffer saline was also used in the dissolution of the pharmaceutical folic acid.

3.0 METHODS

3.1 Extraction of SiO2 from Rice

A mass of 125g of rice husk was measured and washed with water to remove all organic impurities. Concentrations of 2 M of both hydrochloric acid (HCl) and nitric acid (HNO_3) in volumes of 700 and 150 mL, respectively, were mixed in 150 mL of distilled water to form a solvent. The rice husk was added to the solvent, stirred, and placed in a water bath at 75 °C for 1 h, after which it was dried at room temperature for 48 h. The dried rice husk was then calcined in a muffle furnace at 600 °C for 4 h.

3.2 Surface Modification of Biogenic Silica

A mass of 0.15 g of chitosan was completely dissolved in 25 mL of 10% acetic acid to form a homogenous solution. 1g of biogenic silica (BS) was added to this solution in a beaker and stirred with a magnetic stirrer for 24 h. The solution was centrifuged and dried for 72 h to form a biogenic silica-chitosan composite (BS-C).

3.3 Preparation of Folic Acid (FA)

A mass of 50 mg of pharmaceutical folic acid was dissolved in 100 mL of 1% phosphate buffered saline (PBS) with a pH of 9.131 in a beaker. The solution was stirred for 20 min and filtered to obtain an aliquot with a concentration of 0.5 mg/mL.

3.4 Drug Loading and Release

Folic acid with a concentration of 0.5 mg/mL was added to 0.5 mg of both the BS and the BS-C in separate Eppendorf tubes. A 360° mechanical rotator with a speed of 10 rpm was used to aid in the drug loading process in triplicate for 2 h at intervals of 30 min. The solution was then centrifuged for 5 min at a speed of 1000 rpm. The supernatants from the preparation were pipetted, and absorbance was read using a UV-Vis spectrophotometer at a wavelength of 285 nm. The materials were then dried. Drug release was carried out for both BS and BS-C in PBS at a pH of 7.24 and 10.10. The drug release was studied in triplicate for 2 hours with time intervals of 30 minutes with a 360 mechanical rotator at a speed of 10 rpm. The absorbance was recorded at each time interval using UV-Vis spectrophotometer at a wavelength of 285 nm after centrifugation.

3.5 Characterization Techniques

The BS and BS-C were characterised with an X-Ray Diffractometer (XRD) equipped with Cu-Kα radiation of wavelength 1.54Å. Also, a Fourier transform infrared spectrometer (FTIR) was used to determine functional groups over a wavelength of 400 to 4000 cm^{1}.

4.0 RESULTS AND DISCUSSION

4.1 XRD of BS, chitosan and BS-C

Figure 1 compares the X-ray diffractometry (XRD) patterns of biogenic silica (BS), chitosan, and BS modified with chitosan (BS-C). The BS is seen to have a major peak at the 50 2θ/degrees position, whereas the chitosan shows more peaks at 8.5, 20, 28.9, 38.1, 42.8, 44.4, 47.1, 48.3, 64.8, and 78 2θ/degrees positions (Ghorbani et al., 2015). The profile in Fig. 1 reveals that BS is amorphous while chitosan is semicrystalline. However, when the BS is modified with chitosan, the BS-C forms an amorphous material. The amorphous nature of the BS-C is due to the silica and chitosan polymeric chains being completely mixed at a molecular level (Rajiv Gandhi & Meenakshi, 2012) and masking the minor crystalline peaks in chemical reactions that result in an amorphous structure (Kamari & Ghorbani, 2021).

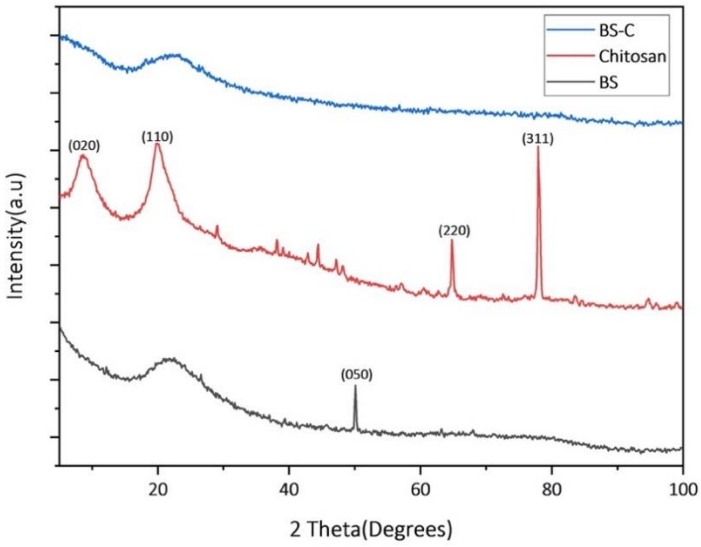

Figure 1: XRD patterns of BS, Chitosan and BS modified with chitosan (BS-C).

4.2 FTIR of BS, chitosan and BS-C Composite

Figure 2 represents the FTIR spectra of BS, chitosan, and BS-C. The broad band between 3610 and 3000 cm^{-1} in BS, chitosan, and BS-C is assigned to the stretching vibration of surface hydroxyl. The stretching vibration of Si-OH is seen in the band between 3610 and 3000 cm^{-1} in the BS. The bands at 1042, 788, and 439 cm^{-1} in both the BS and the BS-C are assigned to the Si-O group and Si-O-Si and

and Si-O-Si, respectively (Yuan et al., 2006). The bending, symmetric, and asymmetric stretching of the Si-O-Si and Si-O at 1042, 788, and 439 cm^{-1} are consistent with the fingerprint region seen for silica particles in literature (Chen et al., 2014). Chitosan reveals a vibrating NH band, which is spotted at 1640 cm^{-1}. Other vibrating C-H groups in the chitosan can be found at 952 and 800 cm^{-1}. From the BS-C, new bands occurred at 1640, 1557, 1408, and 952 cm^{-1}. The new bands are attributed to the N-H bending vibration of the amine group and the C-H stretching bond of the CH_2 and CH_3 groups, respectively, which are characteristic functional groups present in the chitosan structure.

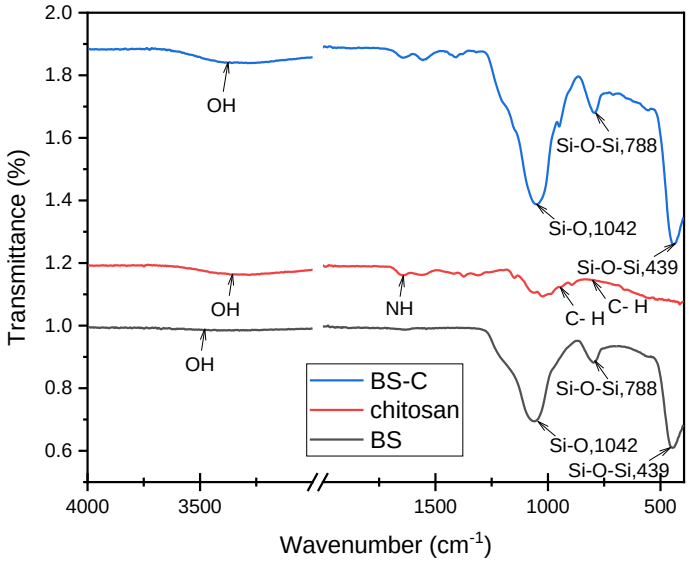

Figure 2: FTIR of BS, chitosan and BS modified with chitosan (BS-C).

4.3 FA Loading of BS And BS-C

FA loading studies were conducted on BS and BS-C at room temperature. The drug adsorption efficiency (DAE), which quantifies the amount of drug loaded onto the material, of BS and BS-C was then calculated using the concentration after 2 hours obtained from the UV-VIS spectrophotometer:

$$DAE = \frac{(C_i - C_f)}{C_i} \times 100\% \quad (1)$$

C_i is the initial concentration and C_f is the final concentration.

The DAE of BS after 2 h was calculated as 29.79%, while that of the BS-C composite was 73.96%, which confirms that the BS-C has a higher drug entrapment efficiency when compared to BS. Figure 3 compares the absorbance readings of the BS and BS-C. It shows irregular drug adsorption by the BS, confirming the inefficient and uncontrolled drug loading characteristic of the BS (Salazar Hernández et al., 2014). On the contrary, there was a steady decrease in drug adsorption by the BS-C. This indicates efficient drug loading onto the material, which could be attributed to the chemical interactions taking place between the FA and the composite.

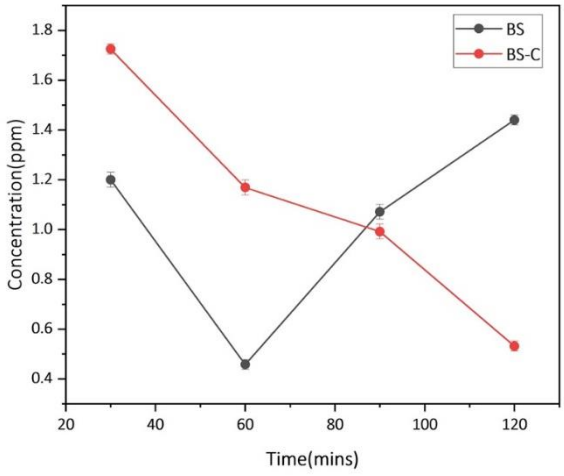

Figure 3. Drug loading of biogenic silica (BS) and BS modified with chitosan (BS-C).

4.4 FA Release and Kinetic model of BS and BS-C

FA release studies were carried out for both the BS and the BS-C composite to analyse their release behaviour at different pH (7 and 10). At a pH of 7.24, FA was released into solution by the BS in the first 30 minutes, and progressively adsorbed again after 90 minutes (at 30 minutes interval), which confirms the poor release character of BS. This could be due to the high surface energy of silica (Bauer et al., 2021; Seied Reza Saeid Jalali et al., 2018), causing minimal release from the BS surface. On the contrary, there was a sustained release of the FA by BS-C composite as seen in *Figure 4.* This is partially due to the character of chitosan reducing the surface energy of BS and the interactions between the FA and chitosan rather than the BS. At a pH of 10.1, FA continued to be released from the BS-C with increased affinity of FA to the OH ions in solution as well as the character of chitosan. In the BS sample, it was suspected that FA released into solution with time as a result of FA affinity for OH ions and solubility of FA at high pH causing it to release from the BS sample.

Based on dependence of the substance amount released with time *Figure 4*, the data was fitted to the Korsemeyer-Peppas kinetic model. Korsmeyer-Peppas equation, also called power law, is a semi-empirical model based on the diffusion phenom that is used to describe in a general way the main transport phenomena involved in release procedures, which occurs by either diffusion or swelling (Salah Eldeen et al., 2019). Although a good fit has been achieved with this model, several authors have shown that Korsmeyer-Peppas is applicable only to the first 60% of the release profile (Heredia et al., 2022; Korsmeyer et al., 1983). The diversity of this process can be summarised by the equation :

$$F = K_m \qquad (2)$$

t^n where K is kinetic constant, t is time, n is diffusion exponent. The diffusion exponent(n) of the Korsmeyer–Peppas model preparation that releases the FA as a result of both diffusion and erosion is 0.384, with an R^2 value of 0.9812. Reference values

value of 0.9812. Reference values for non-fickian transport are between 0.5< n <= 0.89 (Ballantine et al., 1997). It has been clearly shown in *Figure 5* that the process is consistent with this model and was observed only in a period of time between 30 and 120 min.

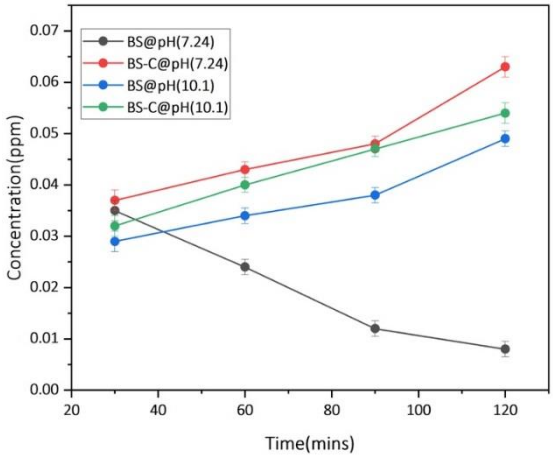

Figure 4. Drug release of biogenic silica (BS) and BS modified with chitosan (BS-C) at pH of 7.24 and 10.10.

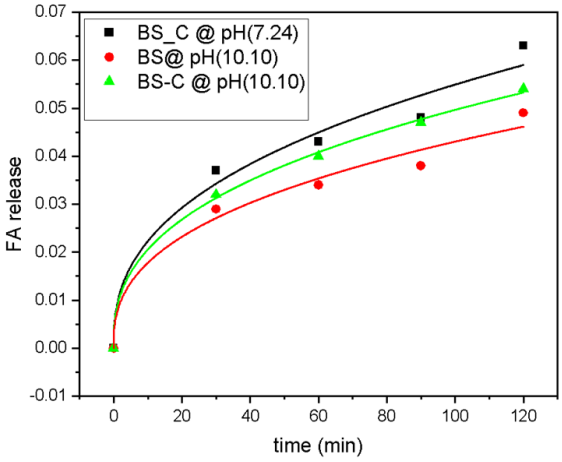

Figure 5. Kosmeyer-Pepper model of biogenic silica (BS) and BS modified with chitosan (BS-C) at pH of 7.24 and 10.10.

5.0 CONCLUSION

The potential of biogenic silica (BS) modified with chitosan (C) (BS-C) was evaluated for the adsorption and release of folic acid (FA) over a period of 120 min. The BS-C displayed better drug loading and release capability for FA as compared to the BS. The release of FA from the BS-C was influenced by the pH of the medium. The pH range was chosen to mimic the pH in the small intestine, where folic acid is absorbed. The release profile of the BS-C agrees with the Kosmeyer-Pepper model. The mechanism of reaction between BS-C and FA, as well as BS and FA, was mainly governed by the adsorption of the functional groups. The study shows the potency of biogenic silica from rice husk modified with chitosan as an effective system for the delivery of FA.

REFERENCES

Ballantine, D. S., Martin, S. J., Ricco, A. J., Frye, G. C., Wohltjen, H., White, R. M., & Zellers, E. T. (1997). Materials Characterization. In D. S. Ballantine, S. J. Martin, A. J. Ricco, G. C. Frye, H. Wohltjen, R. M. White, & E. T. Zellers (Eds.), *Acoustic Wave Sensors* (pp. 150–221). Academic Press. https://doi.org/10.1016/B978-012077460-9/50004-6

Bauer, F., Meyer, R., Bertmer, M., Naumov, S., Al-Naji, M., Wissel, J., Steinhart, M., & Enke, D. (2021). Silanization of siliceous materials, part 3: Modification of surface energy and acid-base properties of silica nanoparticles determined by inverse gas chromatography (IGC). Colloids and Surfaces A: Physicochemical and Engineering Aspects, 618, 126472. https://doi.org/10.1016/J.COLSURFA.2021.126472

Carmen, S.-H., Mercedes, S.-H., Rocío, L.-R., Enrique, E.-R., Agustín Hilario, R.-R., Carmen, S.-H., Mercedes, S.-H., Rocío, L.-R., Enrique, E.-R., & Agustín Hilario, R.-R. (2017). Silica from Rice as New Drug Delivery Systems. Rice - Technology and Production. https://doi.org/10.5772/66723

Chen, X., Jiang, J., Yan, F., Tian, S., & Li, K. (2014). A novel low temperature vapor phase hydrolysis method for the production of nano-structured silica materials using silicon tetrachloride. RSC Advances, 4(17), 8703–8710. https://doi.org/10.1039/C3RA47018K

Chun, J., Mo Gu, Y., Hwang, J., Oh, K. K., & Lee, J. H. (2020). Synthesis of ordered mesoporous silica with various pore structures using high-purity silica extracted from rice husk. Journal of Industrial and Engineering Chemistry, 81, 135–143. https://doi.org/10.1016/J.JIEC.2019.08.064

de Cordoba, M. C. F., Matos, J., Montaña, R., Poon, P. S., Lanfredi, S., Praxedes, F. R., Hernández-Garrido, J. C., Calvino, J. J., Rodríguez-Aguado, E., Rodríguez-Castellón, E., & Ania, C. O. (2019). Sunlight photoactivity of rice husks-derived biogenic silica. Catalysis Today, 328, 125–135. https://doi.org/10.1016/J.CATTOD.2018.12.008

Dorairaj, D., Govender, N., Zakaria, S., & Wickneswari, R. (2022). Green synthesis and characterization of UKMRC-8 rice husk-derived mesoporous silica nanoparticle for agricultural application. Scientific Reports 2022 12:1, 12(1), 1–11. https://doi.org/10.1038/s41598-022-24484-z

Fenton, O. S., Olafson, K. N., Pillai, P. S., Mitchell, M. J., & Langer, R. (2018). Advances in Biomaterials for Drug Delivery. Advanced Materials, 30(29), 1705328. https://doi.org/10.1002/ADMA.201705328

Ganguly, P., & Alam, S. F. (2015). Role of homocysteine in the development of cardiovascular disease. Nutrition Journal, 14(1). https://doi.org/10.1186/1475-2891-14-6

Ghorbani, F., Sanati, A. M., & Maleki, M. (2015). Production of Silica Nanoparticles from Rice Husk as Agricultural Waste by Environmental Friendly Technique. 2(1), 56–65.

Heredia, N. S., Vizuete, K., Flores-Calero, M., Katherine Pazmiño, V., Pilaquinga, F., Kumar, B., & Debut, A. (2022). Comparative statistical analysis of the release kinetics models for nanoprecipitated drug delivery systems based on poly(lactic-co-glycolic acid). PLoS ONE, 17(3 March). https://doi.org/10.1371/journal.pone.0264825

Ibrahim, H. M., Zairy, E. M. R. E.-, Ibrahim, H. M., & Zairy, E. M. R. E.-. (2015). Chitosan as a Biomaterial — Structure, Properties, and Electrospun Nanofibers. Concepts, Compounds and the Alternatives of Antibacterials. https://doi.org/10.5772/61300

Isa, E. D. M., Ahmad, H., Rahman, M. B. A., & Gill, M. R. (2021). Progress in Mesoporous Silica Nanoparticles as Drug Delivery Agents for Cancer Treatment. Pharmaceutics 2021, Vol. 13, Page 152, 13(2), 152. https://doi.org/10.3390/PHARMACEUTICS13020152

Kamari, S., & Ghorbani, F. (2021). Extraction of highly pure silica from rice husk as an agricultural by-product and its application in the production of magnetic mesoporous silica MCM–41. Biomass Conversion and Biorefinery, 11(6), 3001–3009. https://doi.org/10.1007/S13399-020-00637-W/METRICS

Khan, K. M., & Jialal, I. (2022). Folic Acid Deficiency. StatPearls. https://www.ncbi.nlm.nih.gov/books/NBK535377/

Korsmeyer, R. W., Gurny, R., Doelker, E., Buri, P., & Peppas, N. A. (1983). Mechanisms of solute release from porous hydrophilic polymers. In international Journal of Pharmaceutics (Vol. 15).

Lizardi-Mendoza, J., Argüelles Monal, W. M., & Goycoolea Valencia, F. M. (2016). Chemical Characteristics and Functional Properties of Chitosan. Chitosan in the Preservation of Agricultural Commodities, 3–31. https://doi.org/10.1016/B978-0-12-802735-6.00001-X

Menon, A. A., & Pillai, R. G. (2022). Source optimization, characterization, assessing biocompatibility and drug loading efficiency of biogenic silica particles from agro wastes. Chemical Biology Letters, 9(1), 311–311. https://www.pubs.thesciencein.org/journal/index.php/cbl/article/view/311

Park, S. J., Son, S. H., Kook, J. W., Ra, H. W., Yoon, S. J., Mun, T. Y., Moon, J. H., Yoon, S. M., Kim, J. H., Kim, Y. K., Lee, J. G., Lee, D. Y., & Seo, M. W. (2021). Gasification operational characteristics of 20-tons-Per-Day rice husk fluidized-bed reactor. Renewable Energy, 169, 788–798. https://doi.org/10.1016/J.RENENE.2021.01.045

Prabha, S., Durgalakshmi, D., Rajendran, S., & Lichtfouse, E. (2021). Plant-derived silica nanoparticles and composites for biosensors, bioimaging, drug delivery and supercapacitors: a review. In Environmental Chemistry Letters (Vol. 19, Issue 2, pp. 1667–1691). Springer Science and Business Media Deutschland GmbH. https://doi.org/10.1007/s10311-020-01123-5

Rajiv Gandhi, M., & Meenakshi, S. (2012). Preparation and characterization of silica gel/chitosan composite for the removal of Cu(II) and Pb(II). International Journal of Biological Macromolecules, 50(3), 650–657. https://doi.org/10.1016/J.IJBIOMAC.2012.01.012

Ratajczak, A. E., Szymczak-Tomczak, A., Rychter, A. M., Zawada, A., Dobrowolska, A., & Krela-Kaźmierczak, I. (2021). Does Folic Acid Protect Patients with Inflammatory Bowel Disease from Complications? Nutrients 2021, Vol. 13, Page 4036, 13(11), 4036. https://doi.org/10.3390/NU13114036

Salah Eldeen, T., Ahmed, L., Atif, R., Yahya, I., Omara, A., & Eltayeb, M. (2019). Study the Using of Nanoparticles as Drug Delivery System Based on Mathematical Models for Controlled Release. In International Journal of Latest Technology in Engineering: Vol. VIII. www.ijltemas.in

Salazar Hernández, M., Salazar Hernández, C., Gutiérrez Fuentes, A., Elorza, E., Carrera-Rodríguez, M., & Puy Alquiza, M. J. (2014). Silica from rice husks employed as drug delivery for folic acid. Journal of Sol-Gel Science and Technology, 71(3), 514–521. https://doi.org/10.1007/S10971-014-3378-5/METRICS

Seied Reza Saeid Jalali, Sobat, S., & Farzi, G. (2018). Surface modification of silica nanoparticle using dichlorodimethylsilane for preparation of self-cleaning coating based on polyurethane and polydimethylsiloxane. Materials Research Express, 5(9), 095311. https://doi.org/10.1088/2053-1591/AAD607

Suyanta, S., & Kuncaka, A. (2011). UTILIZATION OF RICE HUSK AS RAW MATERIAL IN SYNTHESIS OF MESOPOROUS SILICATES MCM-41. Indonesian Journal of Chemistry, 11(3), 279–284. https://doi.org/10.22146/IJC.21393

Tam, C., O'Connor, D., & Koren, G. (2012). Circulating Unmetabolized Folic Acid: Relationship to Folate Status and Effect of Supplementation. Obstetrics and Gynecology International, 2012, 1–17. https://doi.org/10.1155/2012/485179

Trzeciak, K., Chotera-ouda, A., Bak-sypien, I. I., & Potrzebowski, M. J. (2021). Mesoporous Silica Particles as Drug Delivery Systems—The State of the Art in Loading Methods and the Recent Progress in Analytical Techniques for Monitoring These Processes. Pharmaceutics 2021, Vol. 13, Page 950, 13(7), 950. https://doi.org/10.3390/PHARMACEUTICS13070950

Yuan, W. Z., Peng, M., Yu, Q. M., Tang, B. Z., & Zheng, Q. (2006). Synthesis and Characterization of Polystyrene/Nanosilica Organic-Inorganic Hybrid. Chemical Research in Chinese Universities, 22(6), 797–802. https://doi.org/10.1016/S1005-9040(06)60215-8

Zhang, J., Xia, W., Liu, P., Cheng, Q., Tahirou, T., Gu, W., & Li, B. (2010). Chitosan Modification and Pharmaceutical/Biomedical Applications. Marine Drugs, 8(7), 1962. https://doi.org/10.3390/MD8071962

Žid, L., Zeleňák, V., Almáši, M., Zeleňáková, A., Szücsová, J., Bednarčík, J., Šuleková, M., Hudák, A., & Váhovská, L. (2020). Mesoporous Silica as a Drug Delivery System for Naproxen: Influence of Surface Functionalization. Molecules 2020, Vol. 25, Page 4722, 25(20), 4722. https://doi.org/10.3390/MOLECULES25204722

Reducing Postharvest Losses in Plantain through Sodium Alginate/Essential oil coatings

Emmanuel Nettey[1], Richard Ngmenyelle[1], Jessica Juweriah Ibrahim[1], Enoch Dankyi[2], Firibu Kwesi Saalia[1], Abu Yaya[3], and Vitus Atanga Apalangya[1*]

[1]Department of Food Process Engineering, University of Ghana, Legon, Ghana.
[2]Department of Chemistry, University of Ghana, Legon, Ghana.
[3]Department of Material Science and Engineering, University of Ghana, Legon, Ghana.

***Corresponding author:** vapalangya@ug.edu.gh

ABSTRACT

Matured plantain fruits undergo postharvest physiological deterioration in the food supply chain contributing to food loss/waste and economic losses. However, available plantain preservation techniques are ineffective, cost intensive and unsustainable. The aim of the study was to evaluate effective, low-cost, and sustainable plantain preservation techniques by harnessing the potential of sodium alginate and cellulose nanocrystals to produce a film blended with cinnamon essential oil in varying proportions (10%, 15%, and 20%) and to determine the extended shelf-life of fresh plantain under the tested treatment conditions. The film produced exhibited good molecular interaction and thermal stability as elucidated by the Fourier Transform and Infrared (FTIR) spectroscopy and thermogravimetric analysis respectively. The samples of plantain coated with film-forming solution and stored up to 8 days were examined for their physiochemical parameters (pulp moisture content, ^{o}Brix, weight loss, firmness, and colour changes) during eight-day storage at room temperature (25 ±1°C). There was a significant ($p<0.05$) reduction in moisture production, ^{o}Brix, weight loss rate, and softening rate for coated plantains relative to the uncoated samples. Increasing proportion of the essential oil in the film was effective in delaying the unset of ripening and deterioration by one week. Therefore, by optimizing the level of cinnamon essential oil in the film, this innovative technique can serve as an effective, sustainable and inexpensive way of preserving plantain to maintain it nutritional and functional qualities while enhancing its economic value in the food supply chain.

1.0 INTRODUCTION

The issue of Food Loss and Waste (FLW) has engendered significant interest worldwide. Estimate by FAO's State of Food and Agriculture (2019) report indicates that about 14% of the food produced get lost or wasted. This figure, in monetary terms, is nearly $400 billion dollars yearly. According to FAO projection, the food that is wasted and lost is enough to cater for 1.26 billion hungry people every year. Food losses are associated with the food supply chain, i.e., from the growing, harvesting, transportation, storage, processing, and retailing to the final consumer. Consequently, the Sustainable Development Goal (SDG) target 12.3, which seeks to

to halve per capita global food waste at the consumer and retail levels and further cause a reduction of food losses along food supply chains, including post-harvest losses (UNEP Food Waste Index Report, 2021). In Ghana, food crops such as cereals, grains, and legumes rank high, with a predicted 30%-50% annual losses, whilst fruits, vegetables, roots, and tubers follow with an estimated yearly loss of 20-50%. These losses are mainly caused, among others, by lack of technical and/or financial capacity of the players along the food supply chain to preserve the food (Xue et al., 2019). Because of the huge economic losses associated with FLW, much attention and research are being focused on reducing food losses and waste in major food crops such as cereals, grains, and legumes and to some extent fruits and vegetables (Rutten & Verma, 2014) to the neglect of food crops such as plantain which ripens easily and if not quickly utilized get wasted posing economic losses to farmers and other actors in the food supply chain.

Plantain (genus *Musa*) falls under banana as a monocotyledonous perennial and important crop in the tropical and sub-tropical regions of the world (Baiyeri et al., 2011). Plantain is a staple crop with significant economic value based on its high nutritional value. In Africa, Cameroon leads in plantain production with 4.3 million tonnes, followed by Ghana (about 4 million tonnes) annually (Adi et al., 2019). In Ghana, the production approximates 13% of GDP, representing a unit annual consumption of about 100kg per person (Adi et al., 2019). Nutritionally, plantain is a major source of energy for the body and therefore utilized as food at every stage of its life cycle (immature to overripe). The main methods used in plantain processing in West and Central parts of Africa are boiling/steaming, frying, roasting or drying of plantain fruits. Food products such as fried plantain, roasted plantain, boiled plantain, pounded plantain and plantain chips in Ghana (Dadzie & Wainwright, 1995), Cameroon (Newilah et al., 2005), Ivory Coast (Kouamé et al., 2015), Nigeria (Akinyemi et al., 2008), Benin (Marcellin et al., 2018) and Democratic Republic of Congo (Ekesa et al., 2012). Despite the high nutritional and economic benefits obtainable from plantain utilization, it economic value reduces considerably along the fruit maturation cycle. The average shelf life of mature plantain after harvest is below two weeks (Adi et al., 2019) due to rapid ripening resulting in product deterioration and economic losses. The projected plantain loses in Ghana is between 10-30% representing 200-400 thousand tonnes of annual production (Adu-Amankwa & Boateng, 2011). These losses represents 100-300 million US dollars yearly (Dzomeku et al., 2011) and occur from production to consumption raising the need for effective post-harvest management strategies to preserve the fruit. Plantain is mostly preserved to prolong its shelf-life and enhance freshness using various preservation strategies including cold refrigeration, using modified atmosphere packaging, and storage on counters or floors under room temperature and processing into plantain chips. However, these

available rudimentary methods often fail to enhance the shelf-life of plantain particularly during storage and distribution and still contributes to huge economic losses.

As a climacteric fruit, plantain produces ethylene gas at maturity that induces ripening. The process of ripening is characterized by distinctive color changes (green to pale yellow), texture changes (firm to soft), conversion of complex polysaccharides (starches) to simple sugars with sweet taste, and the development of a unique flavour compounds. Other noticeable changes include pulp-to- peel ratio, ethylene production, changes in ^{o}Brix, pulp moisture, pulp pH, total titratable acidity, dry matter content, and changes in respiration rate (Adi et al., 2019; Subedi & Walsh, 2009, 2011). Therefore, it is important to understand the physiological process involved in plantain ripening and adopt appropriate control strategy to slow down the processes and delay early ripening. Little attention has been paid to the use of active packaging system in extending the shelf-life and maintaining the freshness of plantain along the supply chain. Active packaging controls the respiration of fruit and vegetables, lipid oxidation, loss of moisture, and microbial activity (Youssef & El-Sayed, 2018). It also preserves the nutritional value of food and decrease the wastage of food. Therefore, the objectives of the study were to: 1) fabricate and characterize active packaging coatings from sodium alginate, cellulose nanocrystals blended with cinnamon essential oil using calcium chloride as a crosslinking agent, and 2) investigate the effect of the coatings on shelf-life extension of plantain. This active sustainable packaging technique is expected to have the potential to deliver fresh and nutritive plantain to the ever rapidly growing population in Ghana and beyond while enhancing its economic benefits in the food supply chain.

2.0 MATERIALS AND METHODS

2.1 Materials

Sodium alginate and glycerol (both extra pure) were obtained from Daejung Chemicals and Metals in Gyeonggi-do, Korea. Calcium chloride was purchased from Merck KGaA, Germany, the Cinnamon Essential Oil was sourced from Hemani Herbal LLC, USA, and Tween 80 obtained from Jinan Future Chemical company, China. Cellulose nanocrystals (CNC) (12.2wt% batch no-2015-FLP-71) was acquired from University of the Maine.

2.2 Film Preparation procedure

To investigate physical, mechanical, and thermal characteristics of the coats formed on the plantains, films were prepared using different coating solutions. The film-forming solution was prepared by using 4g of sodium alginate powder mixed in 200ml of distilled water.

Furthermore, 2g weight of glycerol, 1.68g of cellulose nanocrystals (CNCs), and 0.12g of $CaCl_2$ were added as plasticizers, reinforcement, and cross-linking agents. Following this process, an emulsion consisting of Cinnamon Essential Oil and Tween-80 were added at three varying concentrations (10%, 15%, and 20%). Stirring was done to the final solution to obtain a consistent mixture. Part of the final film-forming solution, 30.0g, was delivered into a 9cm diameter Petri Dish and made to dry in a 60^{o}C in an oven for a period of 24 hrs. The fabricated films were cooled, peeled off from the Petri Dishes ready for characterization.

2.3 Thermal properties of the film

Analysis of the thermal properties were done using Differential Scanning Calorimeter (DSC, Q2000, TA Instruments, Delaware, USA) under a 30 mL/min nitrogen flow rate. Nearly 15mg of the fabricated films, in triplicates, was weighed in aluminum pans, sealed, and then heated from 20^{o}C to 400^{o}C at a heating rate of 5^{o}C/min (Pankaj et al., 2014).

2.4 Thickness of film

Film thickness was measured using a Micrometer (Mitutoyo dial thickness gauge, Mitutoyo Co., Japan) at a 0.01-mm accuracy at five random position of the film. The mean of recorded data was found using statistical averages (Rhim, 2004).

2.5 Moisture content of films

The films were subjected to weighing using an electronic balance, and the values of the initial weight recorded as W1. The films were subsequently placed in an oven at constant temperature of 105°C for 24 hours. Second weighing was done almost immediately after the films were out from the oven to prevent the films reabsorbing moiture from the atmosphere (Cazón et al., 2020) and this weight represented as W2. The percentage moisture was estimated using the equation below.

$$\text{Moisture Content} = \frac{W1-W2}{W2} \times 100\%$$

Where: W1 = Initial weight of the film

W2 =Second weigh of film (weight of film after it was dried in the oven)

2.6 Fourier Transform and Infrared Spectroscopy (FTIR)

Fourier Transform and Infrared Spectroscopy (FTIR) Analysis was done with the help of Perkin Elmer UATR Two Spectrometer with an attenuated total reflectance accessory. The measurement range was 450 – 4000 cm^{-1}, with a 4 cm^{-1} resolution. The process encompassed wiping the holding crystal with ethanol, after which films were arranged for spectral analysis. The analysis of the data was done using Origin Pro 2019 software, with which the FTIR spectra were obtained.

2.8 ºBrix of coated plantain

To determine the soluble solid contents of the plantain, samples pulp were first blended with distilled water to form a consistent solution. Following this, a drop of the solution was placed on an Abbey 60 Refractometer (Bellingham and Stanley Ltd, Kent, United Kingdom) with the aid of a pipette to determine the ^{o}Brix. This experiment was done three times to obtain the statistical average value of the ^{o}Brix.

2.9 Pulp moisture of coated plantains

Approximately 10g of each sample of plantain pulp was weighed and represented by P1. Afterward, the weighed samples were placed in an oven at a constant heat of 105°C for 24 hours and weighed again presenting P2. Finally, the moisture content of the samples was calculated as a percentage using the equation:

Moisture Content (MC) of plantain = $\frac{P1-P2}{P2}$ x 100%

2.10 Firmness of coated plantain pulp

The firmness of the pulp was determined using a Brookfield Texture Analyzer Model CT3 10K (Middleboro, MA 02346, U.S.A) operating in a normal mode. The experiment was conducted using a needle probe (1.0mm D, 43mm L) at a penetration depth of 20mm at three randomly selected positions of the plantain pulp and a speed of 2mm/s(Owolabi et al., 2021).

2.11 Pulp to peel ratio of coated plantain

This ratio was determined by weighing the pulp and peel separately on the third day, sixth and eighth day on an electronic scale. The experimental process was done in triplicate and the ratio of the pulp relative to the peel determined for each of the measure. The weight loss was also estimated from the measurements.

2.15 Visual observation of the coated and uncoated plantain

Visual images were taken using a high-resolution Digital Camera to detect visual variabilities of the plantains with time.

2.16 Statistical Analysis

The data gathered was analyzed using GraphPad Prism software Version 8.0.2 (263) for Windows (GraphPad Software, San Diego, CA, USA) for all descriptive and inferential statistics. One-way ANOVA inferential statistics was done to compare means between different groups of numerical continuous variables for at least 3 different groups at 5% significance level.

3.0 RESULTS AND DISCUSSION

3.1 Characterization of the Films

The characterization of the films included thermographic analysis, FTIR analysis, moisture adoption capacity, and film thickness.

3.1.1 Thermogravimetric Analysis

The Thermogravimetric Analysis (TGA) was applied to detect variations in weight relative to temperature changes and to observe the impact of cinnamon essential oil (CEO) and other components of the film-forming solution, on the film's thermal stability. The TGA thermogram of the different films were studied, and the outcome signaled a multistage decomposition (three stages of weight loss) for films (Figure 1). The first change in the weight of the film depicts loss of free water and other low molecular weight volatile compounds from the films corresponding to temperatures of 50^{o}C and 75^{o}C. The second weight lost corresponds to temperature of 175^{o}C and 190^{o}C explaining thermal degradation of substance of low molecular weight like glycerol and bonded water. Furthermore, significant mass loss of the film was observed occasioned by thermal decomposition of the sodium alginate within the temperature range 200^{o}C and 250^{o}C, and then remain stable with temperature with no significant weight loss. In comparison, the control film (Film 1) showed higher weight loss as relative to the films containing cinnamon essential oil (Film 4, Film 5, and Film 6). It was observed that the essential oils caused an increase in the thermal stability of the film. However, the films with different cinnamon essential oil concentration gave different thermal stability on the basis of discontinuous structure formation resulting in a rise in free volume spaces and a less dense structure.

3.1.2 Fourier-transform Infrared Spectroscopy (FTIR) Analysis

The FTIR profile, Figure 2, presents the spectra of the different kinds of films showing the chemical and/or physical interactions between the participating compounds and bonding entities in the coatings or films. Usually, the films, regardless of their chemical makeup, show unique peaks. The high absorption peak at 3000-3683cm^{-1} is characteristic of stretching vibration of OH. The OH stretching absorption peak in all the films is broad ranging from 3000cm^{-1} to 3700cm^{-1} compare to free standing OH group which absorbs within 3200-3600cm^{-1} wavenumber. The increased intensity and broadening of OH stretching vibration is attributed to H-bonding. This may be due to strong intermolecular interactions between hydroxyl (OH) groups present in sodium alginate and cellulose nanocrystals or intramolecular interaction of molecules of the sample compounds. This is consistent with studies that indicated that H-bonding cause an increase in absorption peak intensity.

Figure 1: Thermogravimetric Analysis (TGA) profiles of the different films

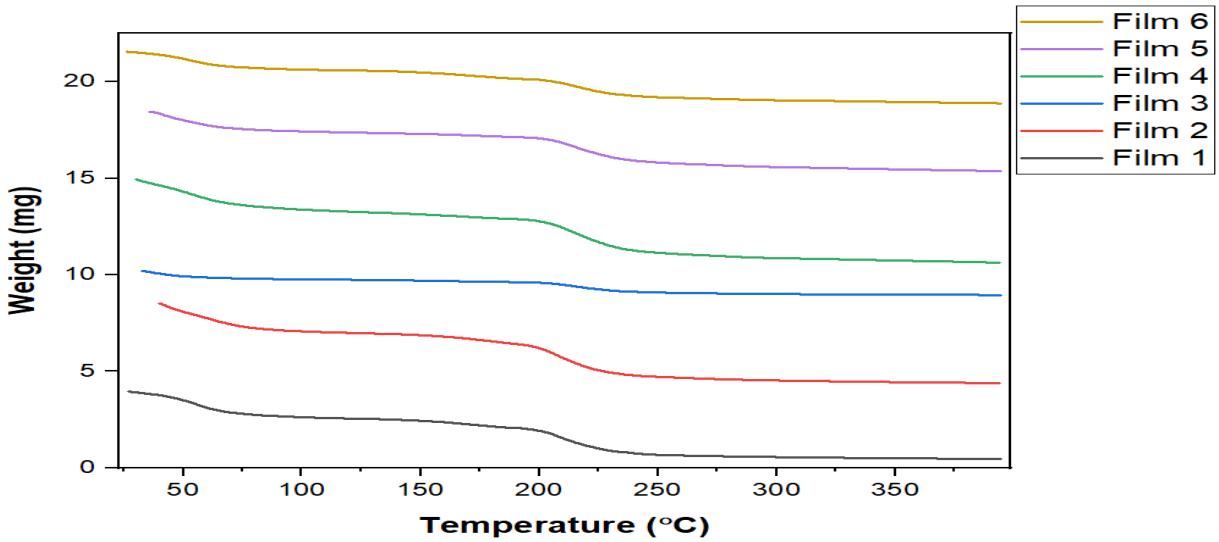

Film 1 - Sodium alginate (SA)/Glycerol, Film 2 - SA/Glycerol, Cellulose Nano Crystals (CNC), Film3 -SA/Glycerol/CNC/Calcium Chloride (CC), Film 4-SA/Glycerol/CNC/CC/Tween 80 (T80)/10% Cinnamon Essential oil (CEO), Film 5- SA/Glycerol/CNC/CC/T80/15% CEO, Film 6 - SA/Glycerol/CNC/CC/ T80/20%CEO.

Figure 2B shows an overlap plot comparing individual components of the film with different fabricated films. The two prominent peaks at 2925cm−1 and 2857cm−1 shoulder to the OH peak are assignable to stretching vibration C-H bond in the film.

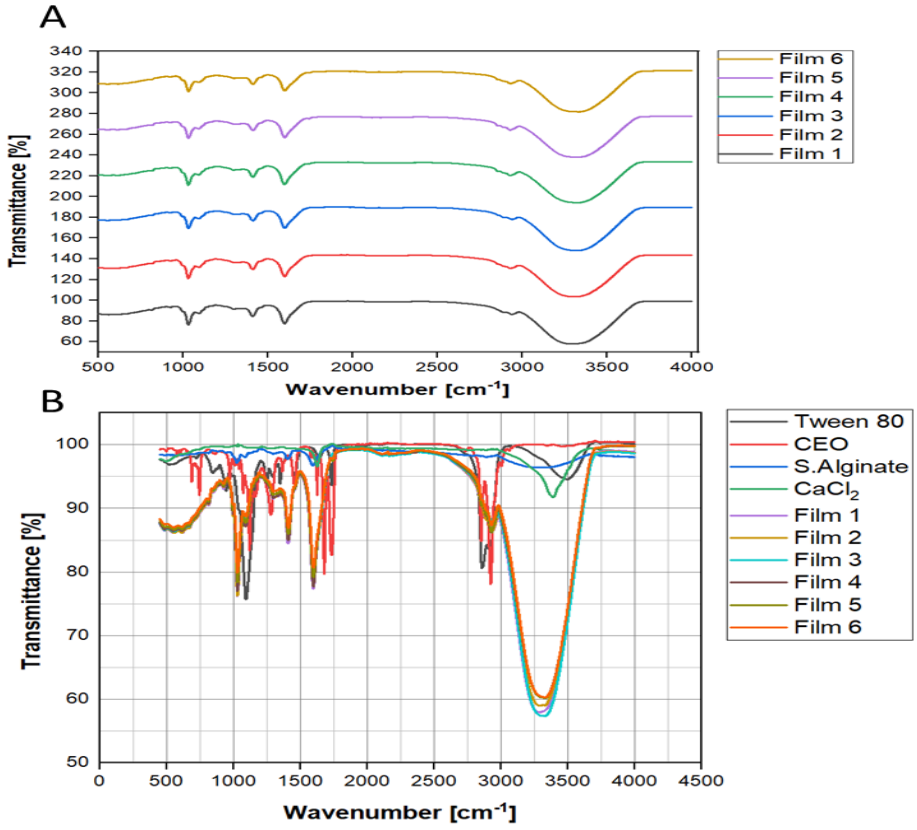

Figure 2: A: FTIR profile of Film 1, Film 2, Film 3, Film 4, Film 5, and Film 6.

The FT-IR spectra of Film 1-Sodium alginate (SA)/Glycerol, Film 2-SA/Glycerol, Cellulose Nano Crystals (CNC), Film 3-SA/Glycerol/CNC/Calcium Chloride (CC), Film 5-SA/Glycerol/CNC/CC/Tween 80 (T80)/10% Cinnamon Essential oil (CEO), Film 6- SA/Glycerol/CNC/CC/T80/15%CEO, Film 6-SA/Glycerol/CNC/CC/ T80/20% CEO, characterized as film 1 to 6 respectively.

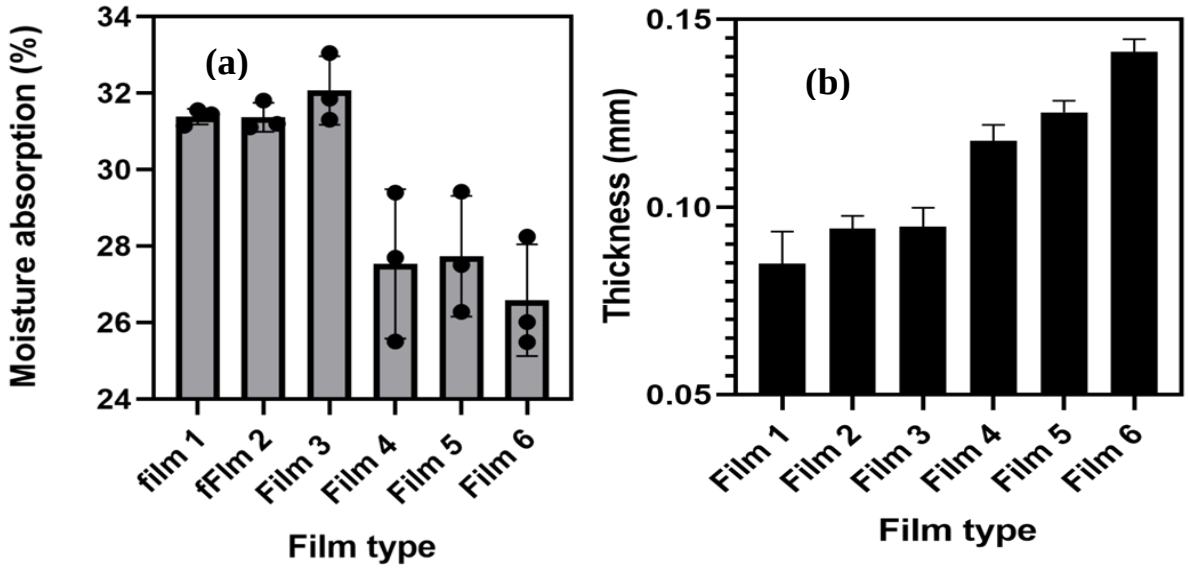

Figure 3a. Moisture absorption capacity film. **Figure 3b: Thickness of film**

Error bars indicate standard deviation at 95% Confidence interval

3.1.3 Moisture adoption capacity and thickness of the films

The moisture absorption capacity of the various films is shown in Fig. 3a. Film 1, 2 and 3, which did not contain the essential oil, absorbed moisture more than 30% of their dry weight. Whereas films 4, 5, and 6 which contain essential oil absorbed moisture of at least 27 % of their dry weight. The films without the essential oil had significant water absorption capacity than the films with essential oils ($p<0.05$). The presence of essential oil in the film therefore limited the water absorption capacity of the film. The thickness of the various films as presented in Figure 3b was largely influenced by variation in the amount of the cinnamon essential oils present in the film. The films with the essential oil had significant greater thickness than those with the film ($p<0.05$). Film 6 with 20% of the essential oil had significant higher thickness than both Film 5 (15% essential oil) and Film 4 (10% essential oil) but the two also had significant greater thickness than those without the essential oils ($p<0.05$). The essential oils decreased water adoption capacity of the films, rendering them denser (less volume of film per unit area) than the films without the essential oils which tended to absorb more moisture from the atmosphere leading to significant rise in volume of film per unit areas.

3.2 Preservation of plantain by films

The protective effect of the coating against plantain ripening and deterioration, was examined on pieces of plantain and the properties of the pulp such as moisture, ^{o}Brix, firmness, weight loss and visualization determined. The results of the pulp moisture of the plantains both coated and uncoated with initial moisture content of about 57% increased after the 8th day (Figure 4b) with the pulp of uncoated plantain (control) producing significant moisture content than coated plantains ($p<0.05$). For example, on day 8, the pulp of the uncoated plantain produced 65.0% moisture content, a significant increase of about 7% from its initial value whilst the plantains coated with 10% and 15% cinnamon essential oil also had significant rise in their pulp moisture content to about 62% each but significantly lower than that of the uncoated sample. The plantain coated with the 20% cinnamon essential oil with initial pulp moisture content of 57% produced insignificant increase in pulp moisture content to about 59% ($p>0.05$). The coating of the plantain with essential oils therefore helps to lower the pulp moisture content of the plantain pulp.

The coating controlled the rate of respiration of the plantain by limiting gas exchange (O_2 uptake, CO_2 and ethylene production) and reducing plantain ripening rate. Reduced rate of ripening could be due to the reduction in the rate of enzyme-catalyzed hydrolysis of starches (amylose and amylopectin) present in the plantain pulp into simple soluble sugars (sucrose, glucose, and fructose) used for cellular respiration to produce energy and water thereby increasing the moisture content of the pulp. This observation is in agreement with the results of the study conducted by (Sojinu et al., 2021) and found that ripening of plantain produces a higher pulp moisture content than unripe plantain with a recorded value of 50.66 ± 0.50 for unripe plantain and that of the naturally ripened plantain to be 62.53±0.20. ^{o}Brix is an estimated of total soluble solids (TSS) content of the pulp, which is indicative of the amount of sugars (fructose, glucose, sucrose) present, corresponding to the degree of ripeness and taste of fruits. Therefore, TSS represents nutritional constituents such as sugars, organic acids, and soluble amino acids present in the plantain fruit (Phan, Chaliha, Sultanbawa, & Netzel, 2019). The results showed that both coated (treated) uncoated plantain (control) showed a significant ($p<0.05$) increase in ^{o}Brix content from the initial value (1.03%) up to Day 8 with the uncoated plantain producing a significant higher ^{o}Brix (7.5%) than the coated samples, 10% CEO (4.12%), 15%CEO (3.82%) and 20% CEO (1.53%).

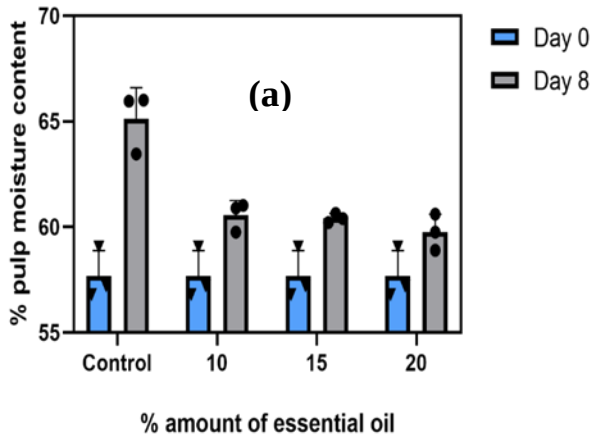

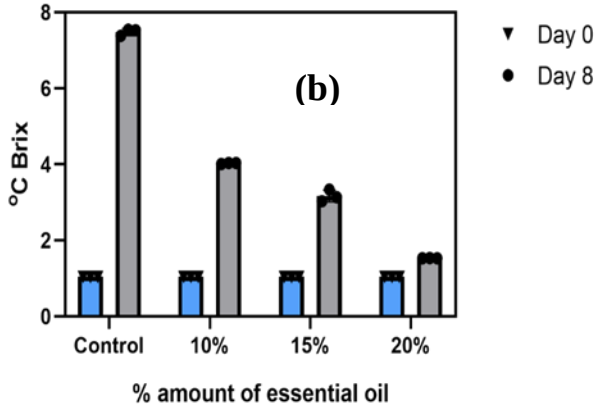

Figure 4 (a): Moisture content plantain pulp; **Figure 4 (b): °Brix of plantain pulp**

Error bars indicate standard deviation at 95% Confidence interval

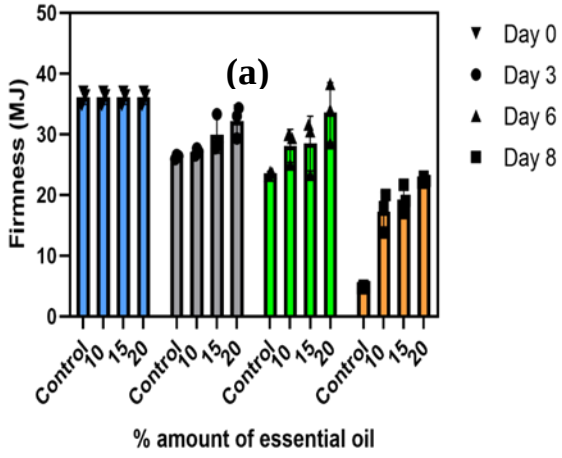

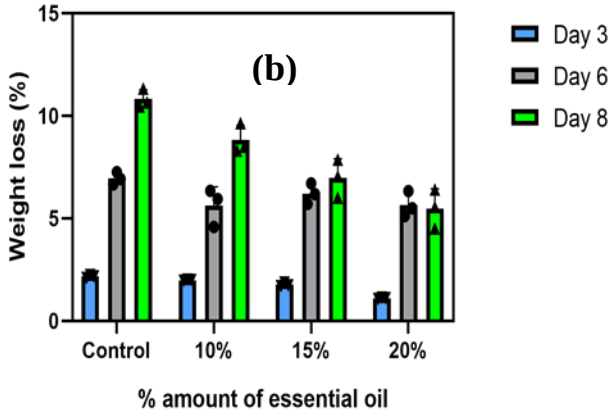

Figure 5 (a): Firmness of plantain pulp; **Figure 5 (b): Weight loss of plantain pulp**

Error bars indicate standard deviation at 95% Confidence interval

The plantains coated with cinnamon essential oils showed a slow rise in °Brix content. The result further showed that °Brix content decreased with increasing essential oil content in the coated plantain. Therefore, the presence of essential oil is effective in suppressing a rise in the °Brix content. The rise in °Brix content is attributable to enzyme-catalyzed hydrolysis of starch to sugars like sucrose, glucose, and fructose (Sojinu et al., 2021).

Firmness is one of the most important characteristics of fruit quality and softening is an indicator of fruit ripening and deterioration which is the main obstacle for long distant shipments of fruits like plantain. The results of the firmness of uncoated and coated plantains are depicted in figure 4.10. The results confirmed that, generally, firmness of plantains reduced as the number of days storage increased. The firmness of the uncoated plantain reduced from 36.07 MJ to 4.8 MJ on Day 8, whereas the firmness of the plantain coated with 10%, 15%, and 20% cinnamon essential oil reduced to 17.27 MJ, 19.23 MJ, and 22.4 MJ, respectively after the eighth day. Therefore, increasing proportion of cinnamon essential oil in the coasted samples caused a delay in the softening of the plantain. The softening of the plantain pulp can be ascribed to enzyme-catalyzed degradation of starches into simple sugars and the changes in cell wall polysaccharides. As previously explained, the fruit softening process is mainly caused by the disintegration of primary cell wall of the fruit causing a disentanglement of intercellular association (Shi et al., 2022; Wang & Seymour, 2022). Biomolecules such as cellulose, hemicelluloses, and pectin are the three main constituents of the primary cell wall in fruits, which undergo enzymatic hydrolysis and transformation during fruit ripening by a group of cell wall hydrolytic enzymes causing disintegration of the middle lamella, enhancing pectin solubilization, facilitating loss of pectin side chain neutral sugars, and engineering the depolymerization of polysaccharides of hemicellulose (Shi et al., 2022; Wang & Seymour, 2022). The enzyme-mediated degradation process of these biomolecules constitutes a vital source of carbon for the formation of sucrose and flavour-producing volatile molecules (Saraiva et al., 2013).

Fig 4b also present the results of the moisture loss from both coated (treated) and uncoated (control) samples of the plantain. Moisture loss in fruit is intricately linked to changes in firmness during storage (Moggia & Lobos, 2023). The outcome of the investigation showed that both the control and coasted samples of plantain produced significant weight losses during storage from the initial weighs equivalent of about 11% (uncoated), 8.5% (10% CEO), 7.0% (15% CEO) and 5% (20% CEO) on Day 8. Cinnamon essential oil had significant influence in reducing the weight of loss in the plantain. Weight loss during storage may be mainly due to water loss

through transpiration process or weight loss could be due to carbon loss in respiration (Liu et al., 2003; Onwuka & Onwuka, 2005; Ranasinghe et al., 2019). Aerobic respiration contributes to overall fruit weigh loss by three main processes: (a) carbon loss in the form of carbon dioxide gas, (b) water generated during respiration getting lost as water vapour during transpiration, and (c) the heat energy produced during respiration becomes source of latent heat for more water vapourization. As observed by Xanthopoulos et al. (2017) respiratory water loss contributes to about 39% total water loss by transpiration in a study of pear.

3.3 Color Changes in Plantain

The changes in pigments are indicative of the development stage and the physiological condition of the fruit which are critical for optimal storage and postharvest management (Solovchenko et al., 2019) . Figure 5 shows colour changes associated with the coated and uncoated plantain peels during storage. Fruit color is indicative of its stage of maturity, freshness and quality, and provides the basis for classification (Wrolstad & Culver, 2012). From the results, no colour change in the peels of the plantain was observed for both coated and uncoated samples up to Day 2. The onset of colour change (green to light yellow) was observed in Day3 for only the uncoated sample. While the fourth day marked the beginning of colour change for the coasted samples particularly for the samples coated with 10% and 15% cinnamon essential oil, the colour change was almost completely dominant for the uncoated sample. The coasted samples did not show dominant colour change up to the 8^{th} Day while the peels of the uncoated sample had dark patches signifying over-ripening and marking the unset of plantain deterioration. The results portray that the amount of cinnamon essential oil in the coated samples is influential in the delay of unset of colour changes associated with ripening of plantains.

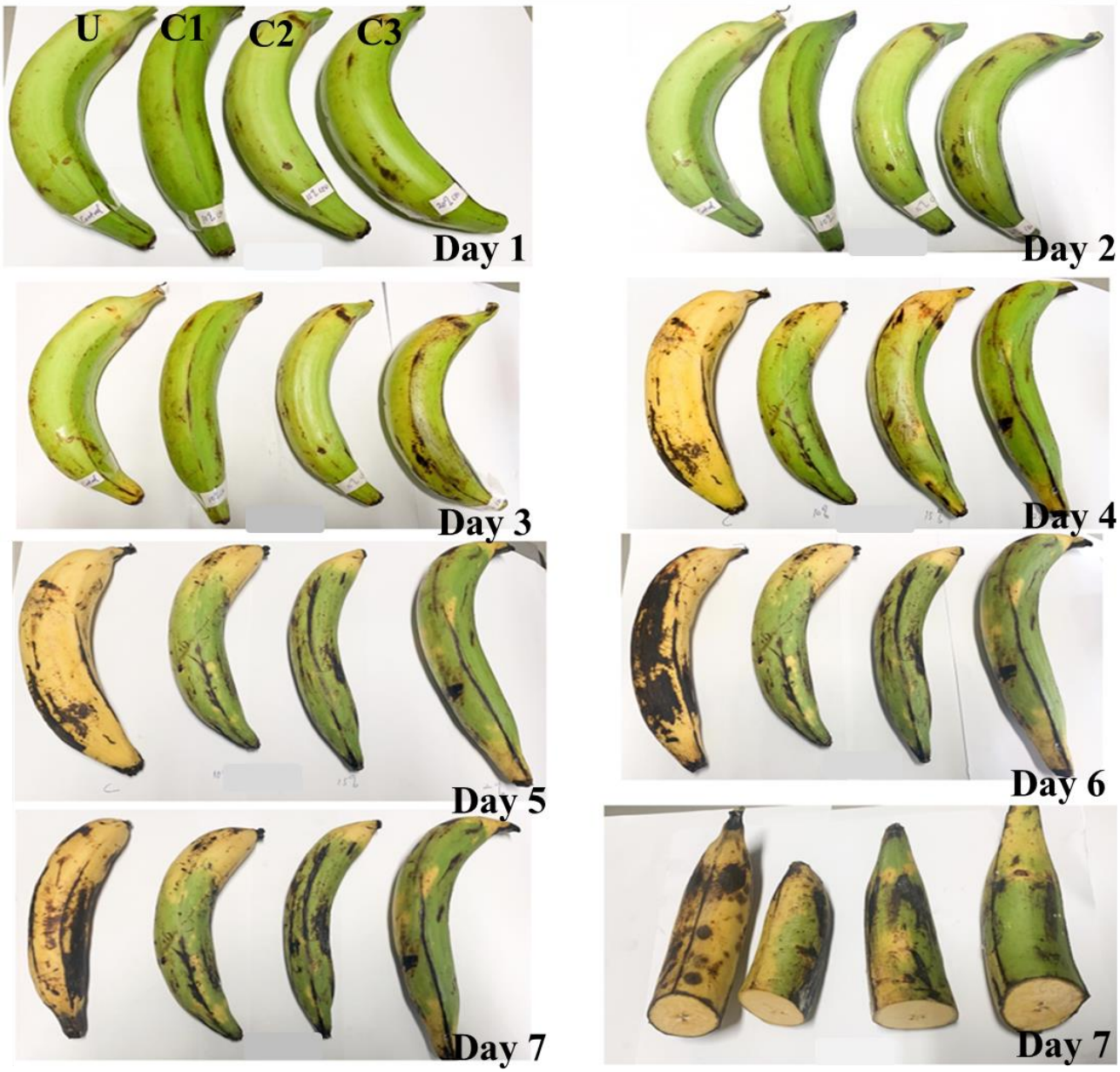

Figure 3: Images of coated and uncoated plantain during the storage for Day 1, 2,3,4,5,6,7 and 8

U=Uncoated, C1=Coated film (10% CEO), C2=Coated Film (15% CEO), and C3=Coated film (20% CEO)

The colour changes in fruit during ripening is caused by biosynthesis and degradation of pigments during the growth and maturation stages of the fruit. The buildup of pigments is influenced mostly by the various maturation stages, during fruit ripening, which is also influenced by biotic and abiotic factors as well as the genetic constitution of the plant species. In the process of maturation, various biochemical and physiological transformations take place in the fruit that tend to affect the type and composition of bioactive substances in the fruit (Belwal et al., 2019).

4.0 CONCLUSION

The study investigated the potential of harnessing sodium alginate and cellulose nanocrystals blended with cinnamon essential oil in varying proportions to produce an effective, low-cost, and sustainable film coatings to examine their suitability of preserving fresh plantains by extending shelf-life of the produce under the tested treatment conditions. Characteristically, the film coatings produced exhibited good molecular interaction and thermal stability based on the results of Fourier Transform and Infrared (FTIR) spectroscopy and thermogravimetric analysis respectively. The samples of plantain coated with film-forming solution and stored for 8 days were examined for their physiochemical parameters (pulp moisture content, ^{o}Brix, weight loss, firmness, and colour changes) during eight-days storage at room temperature (25 ±1°C). There was a significant ($p<0.05$) reduction in moisture production, ^{o}Brix, weight loss rate, and softening rate for coated plantains relative to the uncoated samples. Increasing proportion of the essential oil in the film was effective in delaying the unset of ripening and deterioration by one week. This investigation demonstrates that cinnamon essential oil incorporated in sodium alginate polymer and cellulose film is effective in delaying the postharvest physiological ripening and deterioration of fresh plantain and can contribute to extending the shelf life of fresh mature plantain in distribution and storage. Therefore, by optimizing the level of cinnamon essential oil in the film, this innovative technique can serve as an effective sustainable way of preserving plantain to maintain it nutritional and functional qualities while enhancing its economic value in the food supply chain.

ACKNOWLEDGEMENT

Authors, are grateful to the University of Ghana Building a New Generation of African Academics (BANGA-AFRICA) Project funded by the Carnegie Corporation of New York for Financial support.

REFERENCES

Adi, D. D., Oduro, I. N., & Tortoe, C. (2019). Physicochemical changes in plantain during normal storage ripening. *Scientific African*, *6*, e00164.

Adu-Amankwa, P., & Boateng, B. A. (2011). Postharvest status of plantains in some selected markets in Ghana.

Akinyemi, S., Aiyelaagbe, I., & Akyeampong, E. (2008). Plantain (Musa spp.) cultivation in Nigeria: a review of its production, marketing and research in the last two decades. IV International Symposium on Banana: International Conference on Banana and Plantain in Africa: Harnessing International 879,

Baiyeri, K., Aba, S., Otitoju, G., & Mbah, O. (2011). The effects of ripening and cooking method on mineral and proximate composition of plantain (Musa sp. AAB cv.'Agbagba') fruit pulp. *African Journal of Biotechnology*, *10*(36), 6979-6984.

Belwal, T., Pandey, A., Bhatt, I. D., Rawal, R. S., & Luo, Z. (2019). Trends of polyphenolics and anthocyanins accumulation along ripening stages of wild edible fruits of Indian Himalayan region. *Scientific Reports*, *9*(1), 5894.

Dadzie, B. K., & Wainwright, H. (1995). Plantain utilization in Ghana. *Tropical Science*, *35*(4), 405-410.

Dzomeku, B., Dankyi, A., & Darkey, S. (2011). Socioeconomic importance of plantain cultivation in Ghana.

Ekesa, B., Kimiywe, J., Davey, M. W., Dhuique-Mayer, C., Van den Berg, I., Karamura, D., & Blomme, G. (2012). Banana and plantain (Musa spp.) cultivar preference, local processing techniques and consumption patterns in Eastern Democratic Republic of Congo.

Kouamé, A. C., Kouassi, K. N., N'dri, Y. D., & Amani, N. g. G. (2015). Glycaemic index and load values tested in normoglycemic adults for five staple foodstuffs: pounded yam, pounded cassava-plantain, placali, attieke and maize meal stiff porridge. *Nutrients*, *7*(2), 1267-1281.

Liu, Y. S., Gur, A., Ronen, G., Causse, M., Damidaux, R., Buret, M., Hirschberg, J., & Zamir, D. (2003). There is more to tomato fruit colour than candidate carotenoid genes. *Plant biotechnology journal*, *1*(3), 195-207.

Marcellin, F., EWEDJE, E.-E. B., ADEOTI, K., DJEDATIN, G. L., AFFOKPON, A., Farid, B.-M., & TOUKOUROU, F. (2018). Diversity of local varieties of banana and plantain cultivated in Benin. *International Journal of Biodiversity and Conservation*, *10*(12), 497-509.

Moggia, C., & Lobos, G. A. (2023). Why measuring blueberry firmness at harvest is not enough to estimate postharvest softening after long term storage? A review. *Postharvest Biology and Technology*, *198*, 112230.

Newilah, G. N., Tchango, J. T., Fokou, É., & Etoa, F.-X. (2005). Processing and food uses of bananas and plantains in Cameroon. *Fruits*, *60*(4), 245-253.

Onwuka, G., & Onwuka, N. (2005). The effects of ripening on the functional properties of plantain and plantain based cake. *International Journal of Food Properties*, *8*(2), 347-353.

Owolabi, I. O., Songsamoe, S., & Matan, N. (2021). Combined impact of peppermint oil and lime oil on Mangosteen (Garcinia Mangostana) fruit ripening and mold growth using closed system. *Postharvest Biology and Technology*, *175*, 111488.

Pankaj, S. K., Bueno-Ferrer, C., Misra, N., O'Neill, L., Jiménez, A., Bourke, P., & Cullen, P. (2014). Characterization of polylactic acid films for food packaging as affected by dielectric barrier discharge atmospheric plasma. *Innovative Food Science & Emerging Technologies*, *21*, 107-113.

Ranasinghe, R., Maduwanthi, S., & Marapana, R. (2019). Nutritional and health benefits of jackfruit (Artocarpus heterophyllus Lam.): a review. *International journal of food science*, *2019*.

Rhim, J.-W. (2004). Increase in water vapor barrier property of biopolymer-based edible films and coatings by compositing with lipid materials. *Food Science and Biotechnology*, *13*(4), 528-535.

Rutten, M., & Verma, M. (2014). *The Impacts of Reducing Food Loss in Ghana: A scenario study using the global economic simulation model MAGNET*.

Saraiva, L. d. A., Castelan, F. P., Shitakubo, R., Hassimotto, N. M. A., Purgatto, E., Chillet, M., & Cordenunsi, B. R. (2013). Black leaf streak disease affects starch metabolism in banana fruit. *Journal of Agricultural and Food Chemistry*, *61*(23), 5582-5589.

Shi, Y., Li, B. J., Su, G., Zhang, M., Grierson, D., & Chen, K. S. (2022). Transcriptional regulation of fleshy fruit texture. *Journal of Integrative Plant Biology*, *64*(9), 1649-1672.

Sojinu, O., Biliaminu, N., Mosaku, A., Makinde, K., Adeniji, T., & Adeboye, B. (2021). The implications of ripening agents on chemical compositions of plantain (Musa paradisiaca). *Heliyon*, *7*(6).

Solovchenko, A., Yahia, E. M., & Chen, C. (2019). Pigments. In *Postharvest physiology and biochemistry of fruits and vegetables* (pp. 225-252). Elsevier.

Subedi, P., & Walsh, K. (2009). Non-invasive techniques for measurement of fresh fruit firmness. *Postharvest Biology and Technology*, *51*(3), 297-304.

Subedi, P., & Walsh, K. (2011). Assessment of sugar and starch in intact banana and mango fruit by SWNIR spectroscopy. *Postharvest Biology and Technology*, *62*(3), 238-245.

Wang, D., & Seymour, G. B. (2022). Molecular and biochemical basis of softening in tomato. *Molecular Horticulture*, *2*(1), 5.

Wrolstad, R. E., & Culver, C. A. (2012). Alternatives to those artificial FD&C food colorants. *Annual review of food science and technology*, *3*, 59-77.

Xanthopoulos, G. T., Templalexis, C. G., Aleiferis, N. P., & Lentzou, D. I. (2017). The contribution of transpiration and respiration in water loss of perishable agricultural products: The case of pears. *Biosystems Engineering*, *158*, 76-85.

Xue, S., Zhang, X., Ngo, H. H., Guo, W., Wen, H., Li, C., Zhang, Y., & Ma, C. (2019). Food waste based biochars for ammonia nitrogen removal from aqueous solutions. *Bioresource technology*, *292*, 121927.

Youssef, A. M., & El-Sayed, S. M. (2018). Bionanocomposites materials for food packaging applications: Concepts and future outlook. *Carbohydrate polymers*, *193*, 19-27.

Green Synthesized Iron Nanoparticles from *Tetrapleura tetraptera* for Fluoride Mitigation in Aqueous Media

Abideen Umar Mohammed[1], Ebenezer Annan[1*], Grace Karikari Arkorful[1], and Stephen Kofi Armah[1,2]

[1]Department of Materials Science and Engineering, University of Ghana, Legon, Ghana.
[2]Ashesi University, 1 University Avenue, Berekuso, PMB CT 3, Cantonments Accra, Ghana

***Corresponding author**: ebannan@ug.edu.gh

ABSTRACT

The utilization of better remediation methods is required due to the growing concerns of environmental protection and sustainability. In this regard, the use of biosynthesized offers a viable path. This research describes the synthesis of stabilized iron nanoparticles using the fruit of *Tetrapleura tetraptera* as a source of extract. Due to the combination of different phytochemicals confirmed present in the extract through phytochemical screening, reduction and capping of Iron/iron oxide nanoparticles were produced. The change in colour of the extract solution from light brown to dark black verified the presence of iron oxide nanoparticles. X-Ray Diffraction analysis confirmed peaks of Iron/iron oxide nanoparticles and estimated particle size of 30 nm. Fourier Transform Infrared Spectroscopy (FTIR) of both extract and Iron/iron oxide nanomaterial confirmed functional groups associated with the phytochemicals in the extract. The ultra-violet-Visible spectroscopy (UV-Vis) peak of 300 nm was observed which was within the range for iron nanoparticles. Fluoride removal studies show high removal efficiency of 94 % by the iron nanoparticles. kinetic and isotherm modeling undertaken shows that the adsorption occurred by chemisorption on multiple active sites. The results show the successful synthesis of Iron/iron oxide nanoparticles from *Tetrapleura tetraptera* extract and its effect on fluoride removal, therefore providing a sustainable water treatment design system.

Keywords: Fluoride Removal, Green synthesis of magnetite, Water treatment, *Tetrapleura tetraptera*

1.0 INTRODUCTION

Fluoride is naturally embedded in rocks and gets released into water, soil, and air due to volcanic and anthropogenic activities. Major sources of fluoride ingestion by humans are from water, dental products, food, and beverages (Yadav et al. 2007). Fluoride is non-degradable and its presence in water above accepted limits is detrimental. In drinking water, fluoride levels between 1-1.5 mg/L are favourable to teeth and bones, long exposure to levels above 4 mg/L leads to health risks such as dental and skeletal

fluorosis (Fouladkhah, Thompson, and Camp 2019). As a result, the need for more effective and efficient methods to deal with this problem continues to be a topic of interest for researchers.

The main water treatment methods documented for fluoride reduction include Adsorption (Mondal and George 2015), coagulation, precipitation, ion exchange (Gandhi, Kalaivani, and Meenakshi 2011), electrodialysis (Hichour et al. 1999) and nanofiltration (Simons 1993). However, adsorption has been documented as the most favorable because of it cost effectiveness, simple and an environmentally friendly approach (Onyango and Matsuda 2006). It is important to note that most of these adsorption processes are being engineered for real-life application. Among the different materials (activated and impregnated alumina, hydroxyapatite, quick lime, hydrated cement activated carbon , waste residue, ion-exchanger, various types of activated clay, impregnated silica, and plaster of Paris) reported to have been used for fluoride removal, metal nanoparticles have shown far greater performance. The comparative high removal efficiency by metal nanoparticles is due to their excellent magnetic, physical, optical, electrical, and chemical properties which differ marginally from most materials including their bulk counterparts (Liang et al. 2021).

In recent years, nanotechnology has become a cutting-edge technology in microbiology, optics, environmental remediation, and various engineering applications. It involves nanoparticles which are materials with reduced size and high surface area to volume ratio, higher stability, biological compatibility, high reactivity, and photocatalytic activity making them the perfect photocatalyst for fluoride removal and other environmental remedies (Bishnoi, Kumar, and Selvaraj 2018). For specific defluorination purposes, various metal and metal oxide-based nanoparticles have been utilized to study their removal efficiencies but unfortunately, they require expensive centrifuging for separation. Iron and iron oxide nanoparticles (FeNPs/FeONPs) on the other hand are easy to separate with excellent recoverability, reactivity, and photocatalytic properties (Annan et al. 2021). Additionally, iron is abundant and therefore the most suitable nanoparticles for environmental remediation (O'Carroll et al. 2013). Bulk iron oxide and iron oxide nanoparticle has been reported to give moderate adsorption of fluoride in water and its nanoparticle reportedly removed fluoride completely (Deliyanni et al. 2004) (Zhao et al. 2016). The removal efficiency or performance of iron nano particles depends on the size and morphology. Chemical synthesis techniques such as chemical reduction, sol gel process, co-precipitation, hydrothermal synthesis (McNeil 2005) involve the use of toxic reagents such as hydrazine hydrate (Adhikari et al. 2020),

N N-dimethylformamide (Aryal et al. 2019), and the borohydride and/or hydroxide of sodium as reducing agents (Adhikari et al. 2020), N N-dimethylformamide (Aryal et al. 2019), and the borohydride and/or hydroxide of sodium as reducing agents for the synthesis of nanoparticles and, form hazardous by-products (Jing et al. 2020). This has led to research into sustainable or green, less expensive, and less sophisticated approaches over the past decade (Jadoun et al. 2021; Ying et al. 2022). Synthesis of FeNPs via plant sources offers significant benefits over other biological techniques in terms of simplicity and cost, with the reduction of precursors occurring at a faster rate. The presence of a plethora of poly-phenolic compounds in the plant extracts affords them the ability to cap the individual nanoparticles, simultaneous reduction and stabilization during the synthesis of nanoparticles (Izadiyan et al. 2020).

In the last decade, green synthesis has been the sustainable approach adopted by many researchers. Published research works have proven the successful synthesis of Iron nanoparticles (FeNps) and Iron Oxide nanoparticles (FeONPs) using leaves and fruits of plants such as *Carica papaya, Persea americana, Punic granatum*, andleaves of *Tetrapleura tetraptera*, etc (Ogunsile, Seyinde, and Salako 2020; Castillo-Henríquez et al. 2020; Bouafia and Laouini 2021). Silver nanoparticles has been green synthesized from Tetrapleura tetaptera (Ogunsile, Seyinde, and Salako 2020).

Tetrapluera tetaptera is a flowering plant which belonging to the family *Fabaceae* and mostly found in West African countries. It has been reported to contain several phytochemicals which include, tannins, flavonoids, and starch which enables them to reduce iron salts and are able to adequately cap metal nanoparticles because of their numerous hydroxyl groups which confer on them higher reduction potential and chelating powers. This research adopts green approach in the synthesis of iron nanoparticles (FeNPs) from *Tetrapleura tetraptera* extract and examine its efficacy in the removal of fluoride from aqueous media.

2.0 MATERIALS AND METHODS

The reagents used in this research were all analytical grade and were supplied by Sigma-Aldrich. The reagents used include: 0.1 M hydrochloric acid (HCl), sodium hydroxide (NaOH), ferric chloride ($FeCl_3$), ethanol (C_2H_6O), chloroform ($CHCl_3$), sodium ferrocyanide $[Fe(CN)6]^{4-}$ and sulfuric acid (H_2SO_4). Fluoride solution was prepared from 22.2 mg of sodium fluoride**.** TISAB 1 solution was used to dissolve any complexes of the fluoride prior reading of UV-Vis. Fluoride concentrations were measured using Iron Selective Electrode HI4110 (HANNA Instruments, Inc., Woonsocket, USA)

2.1. Extract Preparation and Screening

The fruits of *Tetrapleura tetraptera* were purchased from a local market in Accra, Ghana. *Tetrapleura tetraptera* fruit sample was washed with water, dried under the sun for a week and further dried in an oven at 60 ^{0}C for the removal of any excess moisture. The dried fruits were pulverized and sieved into particle size of 150 microns. A solution of Ethanol and water was made in a ratio of 2:1 to obtain a total volume of 750 mL. A mass of 166.9 g of the powdered *Tetrapleura tetraptera* sample was added to the ethanol-water mixture in a beaker. The mixture in the beaker was heated at 60° C for an hour at constant stirring speed of 700 rpm. Following the settlement of mixture, the mixture was filtered using a filter paper (150 microns) to obtain liquid portions and stored in a refrigerator. The flow diagram for the process is provided in supplementary information 1(SI 1).

Phytochemical screening was undertaken to ascertain their availability in the *Tetrapleura tetraptera* extract. Chemical structures for some of the phytochemicals are in supplementary information 2 (SI 2). Braymer's test for tannin was conducted where 20 mL the plant extract was diluted with 5 mL of distilled water. The diluted extract solution was heated, filtered, and 2 mL ferric chloride solution was added dropwise. A change of colour from light brown to blue-black confirms the availability of tannin. In a ferric chloride test for polyphenols, few drops of 0.1M ferric chloride solution was added to 5 mL of the extract. Positive result is confirmed by the appearance of a blue colouration for the ferric chloride test. Salkowki's test for terpenoid was also conducted. For this, 5 mL of the extract, 5 mL of H_2SO_4 solution and 2.5 mL of chloroform were mixed, where the appearance of a reddish-brown layer signifies a result for terpenoid. The flavonoid test was undertaken by adding 5ml of dilute NaOH and by 5mL of HCl to a tube containing 2.5 mL of the extract in an alkaline reagent. Colour change from yellow to colourless shows presence of flavonoids. The experimental process for nanoparticles synthesis and the colour changes of the solutions are provided in supplementary information 3(S I3) and supplementary information 4(SI 4) respectively.

2.3. Characterization

FTIR analysis was undertaken on powdered dried fruit samples and iron nanoparticle solution to study the chemical bonds present in the phytochemicals which are responsible for the reduction of iron. X-ray diffraction (XRD) analysis was run on the powdered iron oxide nanoparticles to study the crystallographic nature of the iron oxide nanoparticles. Ultraviolet-visible spectroscopy (UV-Vis) of the synthesized iron nanoparticle solution was obtained.

2.4 Batch adsorption Experiment

The batch adsorption experiment as carried out using 5 mg, 10 mg and 14 mg of the adsorbent and 15 mg of the adsorbent and added to 250 ml of the adsorbate. To ensure uniform mixing, orbital shaker was used at constant speed of 250 rpm. The concentrations of fluoride were determined for each contact time and for each adsorbent dosage. The removal efficiency values, kinetic and isotherm modelling plots were analysed to fully describe the adsorption mechanism. Adsorption capacity and removal efficiency equations are represented in equations (1) and (2) respectively.

$$q=(C_o-C_t)\frac{V}{m}, \quad (1)$$

$$A\%=(\frac{Co-Ct}{Co})\times 100 \quad (2)$$

where 'v' represents the volume of the solution, m represents adsorbent dosage, C_o represents initial concentration of fluoride ions and C_t represents the fluoride concentration at any given time(t)

3.0 RESULTS AND DISCUSSIONS

3.1. Phytochemical screening

Polyphenols, flavonoids, saponins and tannins were all present in the extract of the Tetrapleura tetraptera. A negative test result was obtained for terpenoids as presented as indicated in Table1. However, this has no significant effect on the reduction process because polyphenols confirmed to be available in the extract are the most prominent phytochemicals for capping and stabilization of iron nanoparticles (Bouafia and Laouini 2021).

Flavonoids also have good reduction and complexing properties aided by hydroxyl groups present in their structure (Bouafia and Laouini 2021). The proof of these phytochemicals' presence in the extract indicates the collective reducing properties which aided in the capping of Fe^{3+}ions and stabilization of iron nanoparticles.

Table 1: Phytochemical screening of *Tetrapleura tertraptera* extracts

Phytochemical	TEST Results
Polyphenols	Positive
Saponin	Positive
Flavonoid	Positive
Tannin	Positive
Terpenoids	Negative

3.2. Synthesis of Iron Nanoparticles (FeNps)

The extract solution upon addition of $FeCl_3$ solution changed color to deep black implying the capping of the precursor iron solution and formation of nanomaterials. This confirms collective reduction by the different phytochemicals present in the extract. Additionally, the development of a stable, dark colored colloidal solution that did not alter over time showed that there were enough nucleation agents present to control the production of nanoparticles (SI 3 and SI 4).

3.3. Characterization of extract and FeNps

The most popular and accepted method being utilized to describe the optical characteristic of nanomaterials is UV-Vis absorption spectroscopy. The surface plasmon resonance band of nanomaterials gives an idea about their morphology (Guo et al. 2020). The green synthesized nanoparticles showed a maximum peak at 300 nm which indicate that, the green synthesized nanoparticles absorbs the UV light and it's a characteristic surface plasmon resonance band for metallic iron nanoparticles (Shafey 2020; Kiwumulo et al. 2022). Figure 1(a) and Figure 1(b) shows the UV-Vis spectroscopy and X-ray diffraction studies spectra of the synthesized iron nanoparticles respectively.

The crystallography of the powdered nanomaterial was studied via XRD studies. The peaks from figure 1(b) were observed at 2θ = 22.1°, 29.4°, 36.2°, 39.4° and 47.3° corresponded to cubic (220), (311), (400), (422) and (511) crystal planes of Fe_3O_4 nanoparticles (Shafey 2020). Machado et al have reduced Fe^{3+} to zero-valent FeNPs and observed predominant peak at 2θ = 46° (Machado et al. 2015). The peak at 2θ = 46° which signifies capping of iron nanoparticles to the zero-valent iron was absent and proposed that the absence was due to coating of the iron core by compounds from the extract rendering it undetectable. Average particle size was of 30 nm as estimated from the Scherrer's equation (Chaki et al. 2015):

$$D=\frac{K\lambda}{\beta\cos\theta}, \qquad (3)$$

where D = crystalline size, K= 0.9 (Scherrer constant), λ =0.15673 nm, β= Full Width at Half Minimum(radians) and θ represents Peak Position (radians).

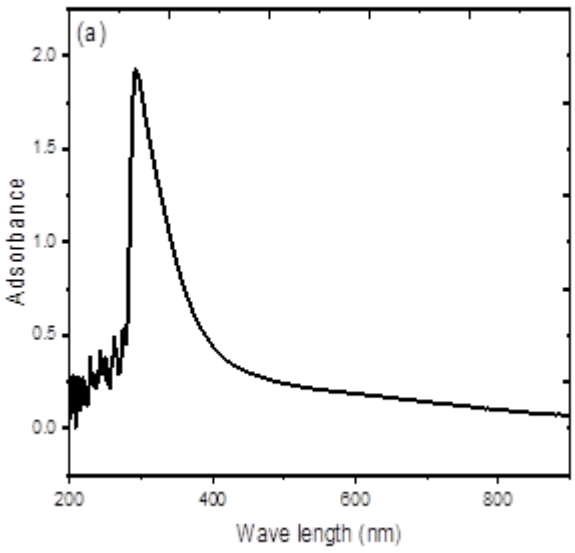

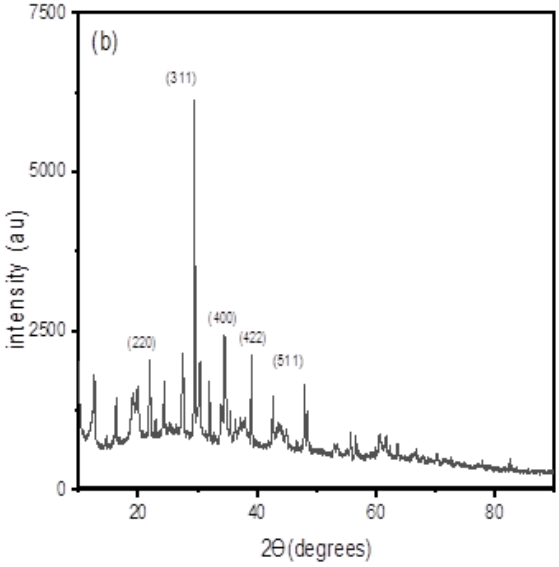

Figure 1(a): UV-Vis Spectrum for FeNps,

Figure 1(b): XRD spectrum for FeNps.

Table 2 (a) Absorption bands from FTIR spectrum of Tetrapleura tetraptera extract and their functional groups.

Wavelength (cm^{-1})	Functional Groups
3302	O-H (hydroxyl group)
2921	C-H and CH_2 (aliphatic Hydrocarbon)
1602	C=C (ketone)
1047	C-O (alcohol stretch)

Table 2 (b) Absorption bands for FeNp spectrum and their functional groups

Wavelength (cm^{-1})	Functional Group
3394	O-H
2921	C-H & CH_2
1602	C=C
1098	C-O

FTIR spectra for both the extract and FeNPs possessed similar functional groups with slight differences in absorption peaks and intensities as shown in Tables 2(a) and 2(b) respectively (complemented by Figure 2). The extract and nanoparticles displayed comparable adsorption bands which might be explained by the fact that the main phytochemicals in the extract have identical functional groups. These represent the predominant functional groups associated with the dominant phytochemicals available in the extract for the capping and stabilization of iron nanoparticles.

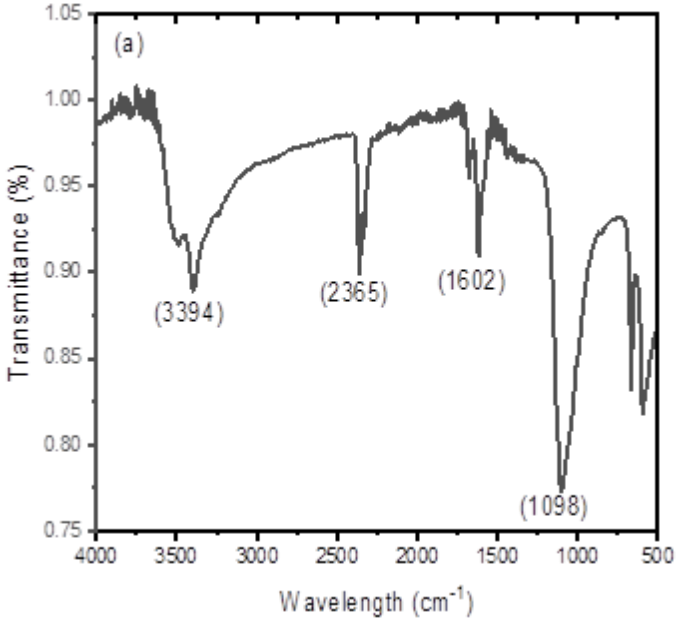

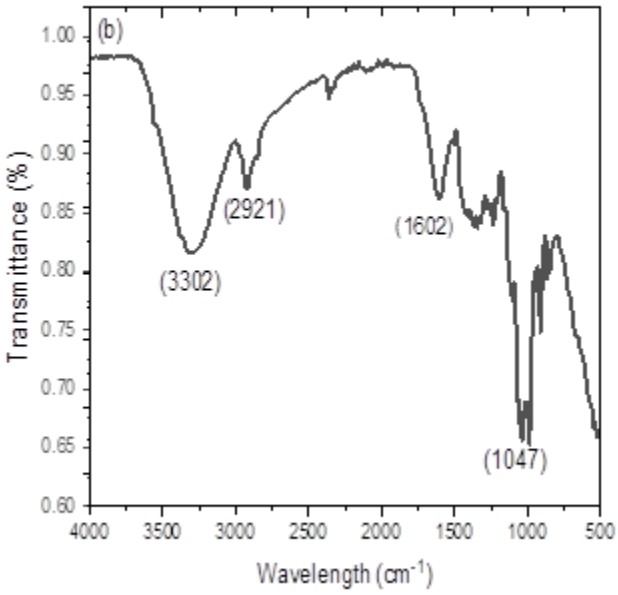

Figure 2: FTIR plot for (a)Tetrapleura tetraptera Extract, (b) FeNp

3.4. Effect of Dosage and Time

Fluoride removal efficiency as time varies for the three doses of the synthesized nanoparticles were plotted (Figure 3). The average removal percentages for 5 mg, 10 mg and 15 mg adsorbent were 42%, 64%, and 81% respectively. For the three different doses, as contact time was increased, defluorination also increased until maximum removal percentages for the 5 mg, 10 mg, and 15 mg which were 62%, 83% and 94% respectively were reached at 180 minutes. This has been explained to be due to numerous vacant sites initially available when the adsorbate concentrations are high (Annan et al. 2021; Appiah et al. 2022). The removal efficiency values are observed to hardly vary form a fixed value, indicating that the adsorption process has reached equilibrium. This may be due to lack of any more active sites for either recombination or adherence.

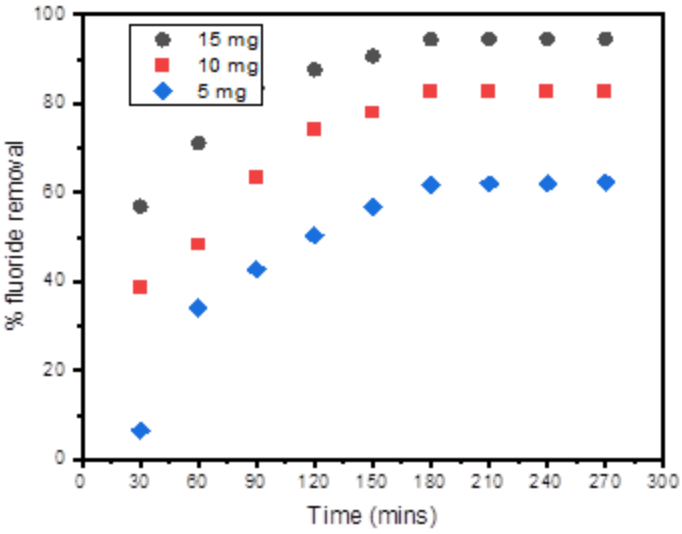

Figure 3: Effect of contact time on removal efficiency

There could also be reduced adsorbate for remaining available site. In the latter case, further agitation, depending on the type and strength of the binding/adherence to the active site, may detach and recombination may occur later. In this research, higher dose was found to show more adsorption capability than lower doses at all the contact times investigated. For each dose, gradual increase is observed as time in contact prolongs.

3.5 Kinetic and Isotherm Model

The adsorption data for the adsorbent doses were fit to the pseudo- first order (equation 4) and pseudo-second order (equation 5) kinetic models as shown in figure 8. The rate of solute uptake is described by the process of kinetics, which in turn enables the specific level of defluorination to be determined.

$$\log(q_e - q_t) = \log qe - \frac{K_1}{2.303}t, \quad (4)$$

$$\frac{t}{q_t} = \frac{1}{(k_2 q_e^2)} + \frac{t}{q_e}, \quad (5)$$

Table 3.0 shows the values for estimated parameters for kinetic modeling analysis. The plots fitted to the models are provided in supplementary information, SI 5. The use of R-square (R2) is the popular and accepted approach in determining better fit. The Pseudo- second order had higher R^2 value than the pseudo-first order. This implies that removal of fluoride ions by the synthesized nanomaterial is characterized by chemical adsorption which involves ion exchanges (Appiah et al. 2022; Annan et al. 2021). The fundamental principles describing the mechanism for the adsorption process was explained in the current work using the Langmuir (equation 6) and Freundlich (equation 7) models. Langmuir model assumes that the adsorption occurs on a monolayer. This is due to the assumption that the adsorption sites on the surface of the adsorbent have comparable affinities for only one molecule of the adsorbate. Also, concentration difference between sites of proximity does not affect rate of adsorption (Habuda-Stanić, Ergović Ravančić, and Flanagan 2014). The Freundlich model is empirical, and it assumes that adsorption occurs on a multilayer. This imposes availability of numerous dissimilar active sites for adsorption.

Original form: $q_e = \frac{q_m K_L C_e}{1 + K_L C_e}$, (6)

Linearized form: $\frac{C_e}{q_e} = \frac{1}{K_L q_m} + \frac{1}{q_m} \times C_e$

Original form: $q_e = K_F \times C_e^{1/n}$ (7)

Linearized form: $\log q_e = \log K_F + \frac{1}{n} \log C_e$

Adsorption mechanism is influenced by the Langmuir model when separation factor (K_L) is within the range of $0 < K_L < 1$. However, when and the heterogeneity factor (n) is greater than 1, the Freundlich isotherm model is favoured. From the experimental results in Table 4, it was found that the heterogeneity factor (n) for the three adsorbent masses was greater than 1.

Table 3: Kinetic models' parameters for adsorption of fluoride.

Adsorbent Mass(mg)	Pseudo First Order (PFO)			Pseudo Second Order (PSO)		
	K_1 (min^{-1})	q_e (mg/g)	R^2	K_2 (g/mg/min)	q_e (mg/g)	R^2
5.0	0.087	0.37	0.94	15.68	0.40	0.97
10.0	0.091	0.25	0.96	13.77	0.27	0.98
15.0	0.116	0.19	0.95	11.36	0.20	0.99

Table 4: Adsorption isotherm model parameters for adsorption of fluoride

Adsorbent Mass (mg)	Lanqmuir Model			Freundlich Model		
	K_L (L/mg)	q_{max} (mg/L)	R^2	K_F (mg/g)	n	R^2
5.0	11.66	0.44	0.90	0.042	5.47	0.99
10.0	21.81	0.25	0.82	0.082	6.13	0.98
15.0	29.55	0.18	0.98	0.015	6.86	0.995

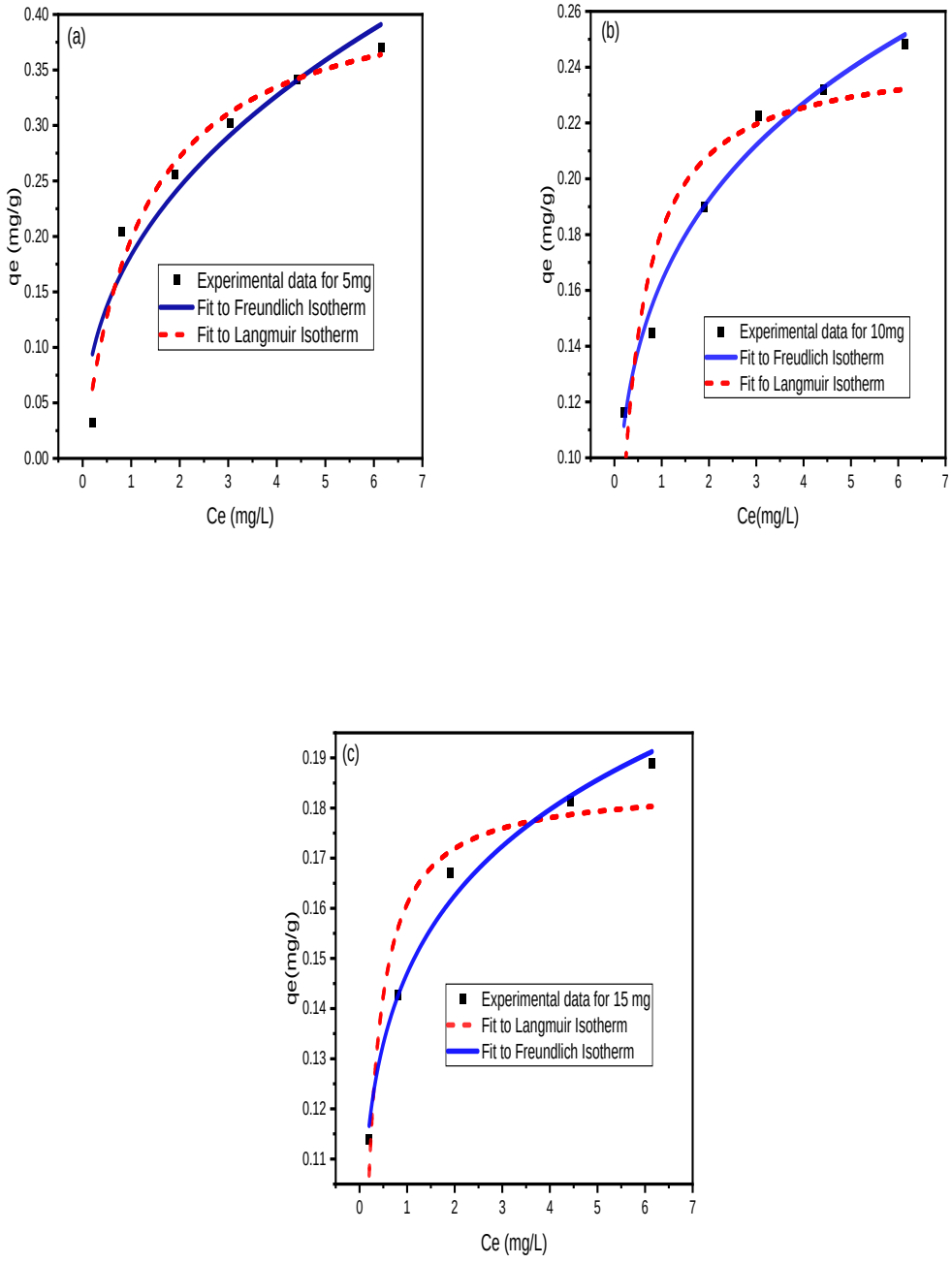

Figure 4: Isotherm modelling for (a) 5mg, (b) 10 mg and (c) 15 mg adsorbent.

4.0 CONCLUSION

Iron nanoparticles were successfully synthesized using the fruits of *Tetrapleura tetraptera.* Plant Phytochemicals acted as aided reducing agent of Fe^{3+}ions from the precursor solution to metallic FeNps. The most essential phytochemicals for capping and stabilizing the iron nanoparticles, polyphenols (with hydroxyl groups) were confirmed present from the FTIR analysis. Other predominant functional groups were also confirmed and aided in the collective reduction process. The FeNps showed a significant removal efficiency of 94 % towards the fluoride ions in the aqueous media. The kinetic process for fluoride adsorption by FeNps suits the pseudo-second order which implies chemisorption of fluoride ions. The experimental results suggest that the adsorption process fits Freundlich adsorption model implying that adsorption occurred on a multilayer. Therefore, the synthesized FeNps have proven to be very good candidate for the treatment of fluoride contaminated water. Further work should be undertaken on the further characterization of FeNps using Transmission Electron microscopy, regeneration undertaken, and reuse of the FeNps. Also, functionalization of the nanoparticles to investigate it efficacy towards other contaminants are equally paramount.

REFERENCES

Adhikari, Menuka, Elena Echeverria, Gabrielle Risica, David N McIlroy, Michael Nippe, and Yolanda Vasquez. 2020. 'Synthesis of Magnetite Nanorods from the Reduction of Iron Oxy-Hydroxide with Hydrazine', *ACS omega*, 5: 22440-48.

Annan, Ebenezer, Emmanuel Nyankson, Benjamin Agyei-Tuffour, Stephen Kofi Armah, George Nkrumah-Buandoh, Joanna Aba Modupeh Hodasi, and Michael Oteng-Peprah. 2021. 'Synthesis and characterization of modified kaolin-bentonite composites for enhanced fluoride removal from drinking water', *Advances in Materials Science and Engineering*, 2021: 1-12.

Appiah, Augustine Nana Sekyi, Lucas Nana Wiredu Damoah, Yaw Delali Bensah, Peace Korshiwor Amoatey, Daniel Nukpezah, Aubin Aholouvi, and Ebenezer Annan. 2022. 'Evaluation of adsorption properties of organic wastes in aqueous media for arsenic removal', *International Journal of Energy and Environmental Engineering*: 1-11.

Aryal, Susmita, Hyungkyu Park, James F Leary, and Jaehong Key. 2019. 'Top-down fabrication-based nano/microparticles for molecular imaging and drug delivery', *International journal of nanomedicine*: 6631-44.

Bishnoi, Shahana, Aarti Kumar, and Raja Selvaraj. 2018. 'Facile synthesis of magnetic iron oxide nanoparticles using inedible Cynometra ramiflora fruit extract waste and their photocatalytic degradation of methylene blue dye', *Materials Research Bulletin*, 97: 121-27.

Bouafia, Abderrhmane, and Salah E Laouini. 2021. 'Plant-mediated synthesis of iron oxide nanoparticles and evaluation of the antimicrobial activity: A review', *Mini-Reviews in Organic Chemistry*, 18: 725-34.

Castillo-Henríquez, Luis, Karla Alfaro-Aguilar, Jeisson Ugalde-Álvarez, Laura Vega-Fernández, Gabriela Montes de Oca-Vásquez, and José Roberto Vega-Baudrit. 2020. 'Green synthesis of gold and silver nanoparticles from plant extracts and their possible applications as antimicrobial agents in the agricultural area', *Nanomaterials*, 10: 1763.

Chaki, SH, Tasmira J Malek, MD Chaudhary, JP Tailor, and MP Deshpande. 2015. 'Magnetite Fe3O4 nanoparticles synthesis by wet chemical reduction and their characterization', *Advances in Natural Sciences: Nanoscience and Nanotechnology*, 6: 035009.

Deliyanni, E, D Bakoyannakis, A Zouboulis, and K Matis. 2004. 'Development and study of iron-based nanoadsorbents', *Journal of Mining and Metallurgy B: Metallurgy*, 40: 1-9.

Fouladkhah, Aliyar Cyrus, Brian Thompson, and Janey Smith Camp. 2019. "Safety of food and water supplies in the landscape of changing climate." In, 469. MDPI.

Gandhi, M Rajiv, Govindasamy Kalaivani, and S Meenakshi. 2011. 'Sorption of chromate and fluoride onto duolite a 171 anion exchange resin–a comparative study', *Elixir Pollution*, 32: 2034-40.

Guo, Yuchen, Chunhong Liu, Rongke Ye, and Qingling Duan. 2020. 'Advances on water quality detection by uv-vis spectroscopy', *Applied Sciences*, 10: 6874.

Izadiyan, Zahra, Kamyar Shameli, Mikio Miyake, Hirofumi Hara, Shaza Eva Binti Mohamad, Katayoon Kalantari, Siti Husnaa Mohd Taib, and Elisa Rasouli. 2020. 'Cytotoxicity assay of plant-mediated synthesized iron oxide nanoparticles using Juglans regia green husk extract', *Arabian Journal of Chemistry*, 13: 2011-23.

Jadoun, Sapana, Rizwan Arif, Nirmala Kumari Jangid, and Rajesh Kumar Meena. 2021. 'Green synthesis of nanoparticles using plant extracts: A review', *Environmental Chemistry Letters*, 19: 355-74.

Jing, Feng, Bai Hui, Xue Yudan, Zhang Rui, Zhu Puli, Bu Duo, Dan Zeng, Li Wei, and Lu Xuebin. 2020. 'Recycling of iron and aluminum from drinking water treatment sludge for synthesis of a magnetic composite material (ALCS-Fe-Al) to remove fluoride from drinking water', *Groundwater for Sustainable Development*, 11: 100456.

Kiwumulo, Henry Fenekansi, Haruna Muwonge, Charles Ibingira, Michael Lubwama, John Baptist Kirabira, and Robert Tamale Ssekitoleko. 2022. 'Green synthesis and characterization of iron-oxide nanoparticles using Moringa oleifera: a potential protocol for use in low and middle income countries', *BMC Research Notes*, 15: 1-8.

Liang, Li, Weiying Li, Yue Li, Wei Zhou, and Jiping Chen. 2021. 'Removal of EDTA-chelated CdII by sulfidated nanoscale zero-valent iron: Removal mechanisms and influencing factors', *Separation and Purification Technology*, 276: 119332.

Machado, S, JG Pacheco, HPA Nouws, José Tomás Albergaria, and Cristina Delerue-Matos. 2015. 'Characterization of green zero-valent iron nanoparticles produced with tree leaf extracts', *Science of the total environment*, 533: 76-81.

A Review of Ghana's National Legal and Regulatory Framework for Nuclear Power and the way Forward

Shirazu Issahaku[1, 2*] and David Asumda[3]

[1]Radiological and Medical Sciences Research Institute, Ghana Atomic Energy Commission
[2]Department of Medical Physics, School of Nuclear and Allied Sciences, University of Ghana, Legon, Ghana
[3]Faculty of Law, Pentecost University College, Accra, Ghana

***Corresponding author**: sissahaku@ug.edu.gh / shirazu.issahaku@gaec.gov.gh

ABSTRACT

Ghana's interest in nuclear power dates back to the 1950s and has continued under successive governments. Recently, the government of Ghana has renewed its commitment to establish a nuclear power programme and use nuclear power to drive economic transformation and development. Hence, Ghana has aligned its nuclear programme closely with the recommendations and guidelines of the International Atomic Energy Agency (IAEA), especially as outlined in the IAEA Milestones Approach. The Statute of the IAEA authorizes the IAEA to promote the safe and peaceful use of nuclear energy. The safe and peaceful use of nuclear energy in any given State can only be assured with the promulgation and implementation of an effective national nuclear legal framework and infrastructure. Over the past two decades, the IAEA's Office of Legal Affairs has provided assistance to Ghana in the development of its national nuclear legal infrastructures and training of professionals. The legislative framework for nuclear power generation has two main aspects: international and national legislative framework. At the international level, Ghana has ratified some basic international legal instruments, which, when implemented, will show Ghana's commitment to peaceful use and application of nuclear energy. At the national level, Ghana has enacted legislation to deal with radiation, waste, transport safety, environmental protection; among others, which, is relevant and is being taken into account in the development of its legal and regulatory infrastructure. In addition, Ghana has established an independent regulatory body, the Nuclear Regulatory Authority (NRA) to provide for the regulation and management of activities and practices for the peaceful use of nuclear material or energy, radioactive material or radiation; the protection of persons and the environment against the harmful effects of radiation hazards; to ensure the effective implementation of Ghana's international obligations, and for related matters. Also, Ghana has started the development of its Nuclear Power Program through the establishment of its nuclear infrastructure and the training of personnel to mount this program. The Nuclear Power Planning Committee (NPPC) comprising Stakeholder Institutions was established by the President of Ghana in 2008 for the formulation of the Nuclear Power Policy and development of the basic elements of nuclear infrastructure. Despite all this, more work lies ahead. Ghana will need long term commitment and planning, large scale financial and human capital investment, and effective implementation of its national legal framework, if its nuclear power programme is to succeed. Therefore, this study aims to review available international, national legal and regulatory frameworks and the extent to which these frameworks will enhance the establishment of a functional and sustainable nuclear power programme in Ghana.

Keywords: Nuclear Energy, Nuclear Power Programme, Legislative Framework, Regulatory Framework

1.0 INTRODUCTION

The Statute of the International Atomic Energy Agency (IAEA) authorizes the IAEA to promote the safe and peaceful uses of nuclear energy. The safe and peaceful use of nuclear energy in any given State can only be assured with the promulgation and implementation of an effective national nuclear legal infrastructure. The legislative framework for nuclear power generation has two main aspects; national and international legislative framework. At the national level, the existing legislative framework for radiation, waste, transport safety, environmental protection, etc, is relevant and is been taken into account in the legal and regulatory infrastructure development. Ghana though has started the development of its Nuclear Power Program through the establishment of its nuclear infrastructure and the training of personnel to mount this program. Nuclear Power Planning Committee (NPPC) involving Stakeholder Institutions was established by the President of Ghana in 2008 for the formulation of the Nuclear Power Policy and development of the basic elements of nuclear infrastructure. The Committee made recommendations on key issues to Government, including Economics of nuclear power, Legal, regulatory and legislative aspects on nuclear power, Environmental and siting aspects of nuclear Power, Selection of type of reactor, Nuclear fuel cycle including waste management, Role of government and private sector in the development of the programme, Additionally, after the Legislations dealing with establishing effectively independent regulatory authorities, with clear mandate on the responsibility for safety, security and safeguards. Ghana's emerging nuclear power programme is the culmination of nearly 60 years of socio-economic and political developments under successive governments. As far back as 1961, the Nkrumah government instituted a major atomic policy initiative, the Kwabenya Nuclear Reactor Project. Although the nuclear programme never took off as intended, for both political and economic reasons, the government of Ghana recently decided to renew its commitment to establish a nuclear power programme and use nuclear power to drive economic transformation and development. Ghana has demonstrated its commitment to responsible nuclear behavior and standards by ratifying relevant international nuclear instruments, entering into bilateral agreements with responsible nuclear partners, and joining major multilateral nuclear organisations. Ghana has ratified or acceded to several international treaties, conventions and protocols related to nuclear no-proliferation and nuclear safety and security as well as the civil liability regime. Since it joined the IAEA in 1960, Ghana has been a cooperative member of a number of international initiatives with the potential to enhance human resource

development, transfer of nuclear science and technology know-how, and the implementation of the nuclear power programme in the country. To comply with its obligation and benefit from privileges provided ounder the international instruments, Ghana has enacted several laws, formulated policies and worked to institutionalized them. These national laws and policies cover the core issues of nuclear non-proliferation and nuclear safety and security.The legislative framework for nuclear power generation in Ghana has two main aspects: national and international legislative framework. At the national level, there is existing legislative framework for radiation, waste, transport safety, and environmental protection; which is relevant and is being taken into account in the legal and regulatory infrastructure development. These include local land use controls, environmental matters (e.g. air and water quality and wildlife protection), the economic regulation of electric power utilities, the occupational health and safety of workers, general administrative procedures of governmental bodies, transport, the export and import of nuclear material, intellectual property rights, insurance and liability for nuclear damage, emergency management, criminal laws and taxation. At the international level, Ghana has ratified some basic international legal instruments, which, when implemented, will show Ghana's commitment to peaceful use and application of nuclear energy.

In addition, Ghana has enacted the Nuclear Regulatory Authority Act, 2015 (Act 895) which has established NRA to provide for the regulation and management of activities and practices for the peaceful use of nuclear material or energy, radioactive material or radiation, to provide for the protection of persons and the environment against the harmful effects of radiation hazards, to ensure the effective implementation of Ghana's international obligations, and for related matters. The NRA comprises three directorates and 10 Departments. Two of these departments – Nuclear Safety, Security and Safeguard; and, Emergency Preparedness and Response – have been taxed with overseeing the development of nuclear power-related regulations. The drafting of regulations by the NRA contributes to its mission of guaranteeing the implementation of the provisions of the NRA Act 895. Since 2017, 20 regulations relating to different categories were under development. These ranged from nuclear safeguards, siting of nuclear installations, nuclear power generation in Ghana and ration of a nuclear and radioactive waste management facility; to the education, training, qualification and certification of personnel of a nuclear installation. The regulations cover a wide range of factors that have to be taken into account in a nuclear power programme and as such represent an important step in its development. Apart from these regulations, the NRA is also preparing a number of 'guidance documents' that correspond to the general focus areas of the regulations. A number of stakeholders will play a part in the development of Ghana's nuclear power programme.

These consist of government ministries, nuclear regulatory bodies, key players from the energy sector and development partners. Ghana has taken significant steps to establish a viable and sustainable nuclear programme, but much work lies ahead. There will be need for long term commitment and planning; as well as large-scale financial and human capital investment, if the programme is to be successful. This paper discusses available international, national legal and regulatory frameworks and the extent to which these frameworks will enhance the establishment of a financial and sustainable nuclear programme in Ghana

2.0 ASSESSING LEGAL FRAMEWORK

This study reviewed the current legal framework state of the Ghana Nuclear Programme, and the way forward. In addition, to examine the available international legal and regulatory frameworks and the extent to which these frameworks will enhance the establishment of a functional and sustainable nuclear programme in Ghana.

The paper employed two comprehensive data collection methodological tools. The first source of data collection methodology was interviews and questionnaires conducted with randomly selected stakeholders of the nuclear programme in Ghana. Secondly, the paper also relied on qualitative research design by utilizing texts of existing primary and secondary sources of information on the nuclear programme in Ghana. These included international treaties, conventions and protocols; relevant domestic legislation and subsidiary legislation, and legislative instruments. In addition, the paper relied on information from textbooks, professional journals and periodicals, research papers, official reports, official government and policy papers, the internet and online library materials. All information and data were collated, coded, reviewed, analyzed and interpreted to clarify issues, to answer the relevant questions and finally provide the basis for recommendations and the way forward. The results of the review data were based on two studies done. Table 1 represent national legislative framework undertaken for the establishment of nuclear power program in Ghana and Table 2 represent international legislative framework that support the national laws for the nuclear power project. The protection of people and the environment in countries with nuclear installations relies on the existence of a solid regulatory framework that oversees the safety of these installations. The IAEA promotes and supports the establishment of comprehensive regulatory frameworks to ensure the safety of nuclear installations throughout their lifetime.

These regulatory frameworks consist of relevant legislation, regulations and guidance and a robust leadership and management programme for safety. It is essential to ensure that an operational and effectively independent regulatory body is established and maintained for the regulatory control of nuclear installations.

This body needs sufficient resources and suitably qualified and competent staff that are enabled to fulfil their regulatory responsibilities and functions. The IAEA's Safety Standards and the Code of Conduct on the Safety of Research Reactors lay out the international requirements and recommendations for enhancing existing or developing regulatory systems for the control of nuclear installations throughout their lifetime until they are released from regulatory control, and any subsequent period of institutional control. The Convention on Nuclear Safety also provides to its contracting parties a set of obligations, including those relative to their legislative and regulatory framework and regulatory bodies. To accomplished these two international regulatory frameworks as prerequisite for the use of nuclear technology, Ghana in 1960 signed on to IAEA status for peaceful use of nuclear for economic development. This led to the established of Ghana Atomic Energy commission in 1963. Subsequent to this, Ghana signed to the non-proliferation treaty and this allows her to utilize nuclear technology for peaceful purposes. The first president of the country cut the sod for the Ghana Nuclear Reactor Project (GNRP) in 1964, unfortunately this was abandoned after the 1966 coup d'état. However, since 1993 a number of legislative frameworks has been established that paved way for the establishment of nuclear power in Ghana. This includes the establishment of Radiation Protection Instrument, LI 1559, National Nuclear and Radiological Emergency Response Plans, Act 517, 1996, Nuclear Power Programme Organization, Regulatory Strategy, NPID-11521-STG-001, 2014 and Nuclear Regulatory Authority, Act 895, 2015. Additionally, the regulator provided a draft Safeguards Regulation, NRA SGR DV1/16, 2016, the establishment of Nuclear power institute (NPI) to provide a leading role in research and the Nuclear Power Ghana (NPG) which was set up to manage Ghana's first nuclear power project. NPG has been designated to be the eventual owner and operator of Ghana's first Nuclear Power Plant. Activities of the organisation began in 2018 when some staff of Volta River Authority (VRA), Bui Power Authority (BPA), and the Ghana Atomic Energy Commission (GAEC) were co-opted to form an initial core staff.

Table 1: Development of National Legal Framework

Laws	**Est Year**	**Agency**
GAEC Instrument, Act 204	1963	GOG
Radiation protection instrument, LI 1559	1993	GAEC
National Nuclear and Radiological Emergency Response Plans, Act 51	1996	NADMO/GAEC
Nuclear Power Programme Organization, Regulatory Strategy, NPID-11521-STG-001	2014	GAEC
NRA, Act 895	2015	GAEC
Draft Safeguards Regulation, NRA_SGR_DV1/16	2016	NRA
Nuclear Power Institute (NPI)	2016	NPI
U.S. Nuclear Regulatory Commission-Ghana Nuclear Regulatory Auth Action Plan, NPID-127540-TNT-005	2016	NPI
Nuclear power Ghana (NPG)	2018	NPG

Table 2: International legal framework ratified by Ghana

Laws/Treaties	**Year depos**	**Agency**	**Instrument**	**Year Entry into force**
Agreement on the Privileges and Immunit of the IAEA	1963	IAEA/GoG	Acceptance	1963
The Convention on Nuclear Safety (INFCIRC/449)	2011	IAEA/GoG	Ratification	2011
Joint Convention on the Safety of Spent F Management and the Safety of Radioactiv Waste Management (INFCIRC/546)	2011	IAEA/GoG	Accession	2011
Convention on Assistance in the Case of a Nuclear Accident or Radiological Emerge (INFIRC/336)	2016	IAEA/GoG	Accession	2016
The Convention on the Early Notification Nuclear Accident (INFCIRC/335)	2016	IAEA/GoG	Accession	2016
Convention on the Physical Protection of Nuclear Material (INFCIRC/274)	2002	IAEA/GoG	Accession	2002
Convention for the Suppression of the Financing of Terrorism, UNSCR Resolution 1373	2001	IAEA/GoG	Accession	2001
Treaty on Non-Proliferation of nuclear weapons (INFCIRC/153),	1972			1972
Convention on the Physical Protection of Nuclear Material (GOV/INF/2005/10-GC (49)/INF/6).	2012	IAEA/GoG	Ratification	2016
Vienna Convention on Civil Liability for Nuclear Damage (INFCIRC/500) and (INFCIRC/556) and (INFCIRC/567)	1963	IAEA/GoG	Ratification	1977
African Regional Co-operative Agreemen Research, Development and Training rela to Nuclear Science and Technology (AFR	2020	IAEA/GoG	Acceptance	2020

3.0 DISCUSSIONS

Ghana has demonstrated its commitment to responsible nuclear behavior and standards by ratifying relevant international nuclear instruments, entering bilateral agreements with responsible nuclear partners, and joining major multilateral organisations; as well as enacted national laws on nuclear power and established the relevant regulatory bodies. This section reviews the most important international, national and regulatory frameworks relevant to the Ghanaian context.

3.1 International Nuclear Instruments

To advance its nuclear programme, Ghana has ratified or acceded to several international treaties, conventions and protocols. The Convention on Nuclear Safety (INFCIRC/449), the Joint Convention on the Safety of Spent Fuel Management and the Safety of Radioactive Waste Management (INFCIRC/546) are instruments on nuclear safety and radiological protection, and seek to promote adherence to nuclear safety principles based on a common interest of the international community to achieve higher levels of safety. State Parties are obliged to submit reports on the implementation of the safety principles with arrangements for "peer review" at meetings.

The Convention on the Early Notification of a Nuclear Accident (INFCIRC/335) and the Convention on Assistance in the Case of a Nuclear Accident or Radiological Emergency (INFIRC/336) are conventions on Emergency Response and were adopted after the Chernobyl accident. They create a system for notifying the IAEA and neighbouring countries of a nuclear accident with potential transboundary consequences, and also set up a framework for prompt assistance and support for nuclear accidents or radiological emergencies.

The main legal instruments on nuclear security and physical protection are: Convention on the Physical Protection of Nuclear Material (INFCIRC/274) and Amendment to the Convention on the Physical Protection of Nuclear Material (GOV/INF/2005/10-GC (49)/INF/6). They aim to promote principles that are designed to prevent, detect and respond to criminal and other unauthorised acts involving or directed to nuclear or other radioactive material and associated facilities or activities. Other conventions include the Suppression of Unlawful Acts against the Safety of Maritime Navigation, Protocol for the Suppression of Unlawful Acts against the Safety of Fixed Platforms located on the Continental Shelf, International Convention for the Suppression of Terrorist Bombings, International Convention for the Suppression of the Financing of Terrorism, UNSCR Resolution 1373 on Prevention/Suppression of Financing and of Preparation of Terrorist Acts, and International Convention on the Suppression of Acts of Nuclear Terrorism. Legal instruments that empowers and requires that the IAEA ensures that safeguards and measures area applied to all nuclear materials in the territory, jurisdiction or control of

State, for the exclusive purpose of verifying that such materials are not diverted for nuclear weapons or other nuclear explosive devices are: the Treaty on the Non-Proliferation of Nuclear Weapons (NPT), The Structure and Content of Agreements Between the Agency and States Required in Connection with the Treaty on Non-Proliferation onf Nuclear Weapons (INFCIRC/153), Small Quantities Protocol (GOV/INF/276), Model Protocol Addition to the Agreement(s) between the State and IAEA for the application of Safeguards (INFCIRC/540), UNSC Resolution 1540 on Preventing theAcquisition of Weapons of Mass Destruction (Including Nuclear) by Terrorist/ Criminal Groups. Acquisition of Weapons of Mass Destruction (Including Nuclear) by Terrorist/ Criminal Groups.

However, two conventions are not yet in force: The Comprehensive Nuclear-Test-Ban Treaty and the Treaty on the Prohibition of Nuclear Weapons. Once these conventions enter into force, they will buttress the legal regime for non-proliferation and safeguards. Another relevant legal instrument is the Revised Supplementary Agreement Concerning the Provision of Technical Assistance by the IAEA.

The Nuclear Liability Conventions ensure that there is no ambiguity as to who bears liability in the event of a nuclear incident and also makes provision for compensation for victims of nuclear damage. Nuclear damage includes transboundary damage caused by a nuclear incident at a nuclear installation, or in the course of transporting of nuclear materials to or from an installation. The Nuclear Liability Conventions include: The Paris Convention on Third Party Liability in the Field of Nuclear Energy, Brussels Convention Supplementary to the Paris Convention, Vienna Convention on Civil Liability for Nuclear Damage (INFCIRC/500), the Joint Protocol Relating to the Application of the Vienna Convention (INFCIRC/402), the Paris Convention and the Protocol to Amend the Vienna Convention on Civil Liability for Nuclear Damage (INFCIRC/556) and the Convention on Supplementary Compensation for Nuclear Damage (INFCIRC/567).

The Protocol to Amend the Paris Convention on Third Party Liability in the Field of Nuclear Energy, and the Protocol to Amend the Brussels Convention Supplementary to the Paris Convention seek to improve the compensation provisions in the Paris Convention on Third Party Liability in the Field of Nuclear Energy. These two conventions are yet to enter into force.

3.2 Ghanaian Nuclear Legal Framework

The Nuclear Regulatory Authority Act 2015 (Act 895) applies to all activities and practices involving the peaceful uses of radiation, nuclear and radioactive material conducted under the jurisdiction of Ghana. The Act establishes the Nuclear Regulatory Authority and provides for the regulation and management of activities and practices for the peaceful use of nuclear material or energy, radioactive material or radiation; to provide

peaceful use of nuclear material or energy, radioactive material or radiation; to provide for the protection of persons and the environment against the harmful effects of radiation hazards, to ensure the effective implementation of the Country's international obligations and to provide for other related matters. for the protection of persons and the environment against the harmful effects of radiation hazards, to ensure the effective implementation of the Country's international obligations and to provide for other related matters.

The Act deals with Nuclear Installations, Radioactive Waste Management, Transportation of Radioactive Materials and Decommissioning of Nuclear Facilities, and ensures the independence and separation of regulatory functions from those of other organisations concerned with the promotion and or utilization of nuclear energy. The Act addresses all relevant non-proliferation and safeguards undertakings of Ghana and clearly spells out the responsibilities and liabilities for the operation of nuclear facilities and the handling and safeguarding of nuclear materials; and establishes a system of licensing as well as the terms of licenses (i.e. suspension, modification and revocation of a license), a system of regulatory inspection and assessment to ascertain compliance with the applicable laws and regulations. The sector minister is empowered by the Act to make subsidiary legislation in the form of Legislative Instruments for the efficient and effective implementation of the Act. The Act is very comprehensive and covers all aspects of nuclear safety, security and safeguards. It also establishes an independent regulatory authority to regulate the industry and has put in place measures to ensure that the regulatory authority is independent and financially stable. This is in conformity with international legal requirements and best practices. Subsidiary legislation is yet to be passed as required by the law. The Environmental Protection Agency Act 1994 (Act 490) amends and consolidates all the laws relating to environmental protection, pesticides control and regulation, as well as related activities.

The Act establishes the Environmental Protection Agency, which is governed by a Board, as the Agency, mainly charged with the execution of the duties spelt out in the Act. The Act is generally silent on Nuclear Power or Nuclear waste. It rather deals with Industrial waste as well as other hazardous chemicals. It provides for a hazardous chemicals committee which has a representative of the Ghana Atomic Energy Commission as a member. The Act requires any person who wishes to undertake any activity which has or is likely to have an adverse effect on the environment to submit an environment impact assessment report. Apart from this requirement, there is no other compliance requirement that has to be met. However, the functions of the Agency and the Hazardous Committee both create an avenue through which issues on nuclear energy and nuclear waste can be dealt with pending an amendment of the EPA Act to cater for peculiar needs of the nuclear requirements of the nuclear industry.

In addition, the Act does not contain a comprehensive definition of key concepts such as pollution, hazardous substances, waste materials or substances and the environment. There is a need to include a clear and comprehensive definition of these concepts, and also amend the existing EPA Act to include nuclear energy and nuclear waste. Minerals and Mining Act 2006 (Act 703) consolidates all the laws relating to minerals and mining and also to cater for related purposes. The Act covers all minerals in its natural state in, under or upon land in Ghana, rivers, streams, water-courses throughout the Country. The Act also applies to radio-active minerals mined or discovered within the territory of Ghana.

The present scope of the Act is wide enough to cover the mining and milling of radio-active materials which may be mined locally to be processed as nuclear fuel or for other purposes. The Act at the moment need not be amended. National Disaster Management Organisation Act 1996 (Act 517) establishes a National Disaster Management Organization (NADMO) to be responsible for disaster management and other similar emergencies, to provide for the rehabilitation of persons affected by disaster and for related matters.

NADMO is mandated to prepare national disaster plans for preventing and mitigating the consequences of disasters. It is also to monitor, evaluate and update national disaster plans. NADMO is also tasked with ensuring that there are appropriate and adequate facilities for the provision of reliefs, rehabilitation and reconstruction after a disaster or any emergency incidence; and also responsible for coordinating local and international support for disaster or emergency control relief services and reconstruction. NADMO is also to ensure the establishment of adequate facilities, technical training and the institution of educational programmes to provide public awareness, warning systems and general preparedness of its staff and the general public; and to perform any other function that is incidental to disaster management and related matters NADMO is governed by the National Security Council which is responsible for determining its policies. It has the mandate to establish a national, regional and district management committees which carry out and implement the policies and functions of the organization at each level. NADMO is funded by moneys provided by parliament and by way of grants, donations and gifts. Hazardous and Electric Waste Control and Management Act 2016 (Act 917) provides for the control, management and disposal of hazardous waste, electrical and electronic waste for related purposes. The Act, among others, covers waste chemical substances arising from research and development or teaching activities which are not identified and/or are new and whose effects on man and/or the environment are not known, wastes of an explosive nature not subject to other legislation, wastes from production, formulation and use of

of photographic chemicals and processing materials; wastes resulting from surface treatment of metals and plastics and residues arising from industrial waste disposal operations. The main implementation organization is the EPA established under the Environmental Protection Agency Act, 1994 (Act 490). Though the Act contains provisions on the Control and management of hazardous wastes and other wastes, there is no specific mention of nuclear or radioactive waste substances. The Act makes it an offence to import, export, sell, purchase or deal in hazardous or other waste without lawful authorization from either the Minister or EPA . One criterion for granting such authorization is whether or not the State that desires to export the waste is a party to the Basel Convention on the Control of Transboundary Movements of Hazardous Wastes and their Disposal or is a party to a bilateral, multilateral or regional agreement or arrangement regarding transboundary movement of hazardous waste or other wastes in accordance with Article 11 of the Basel Convention; The Act defines "wastes" to mean substances or objects, which are disposed of or are intended to be disposed of or are required to be disposed of and "waste electrical and electronic equipment" to mean electrical or electronic equipment that is waste, including all components, sub-assemblies and consumables which are part of the equipment at the time the equipment becomes waste. Looking at the scope of Act 917, it will appear that nuclear waste is best catered for by Act 895.

Energy Commission Act 1997 (Act 541) establishes the functions relating to the regulation, management, development and utilization of energy resources, provide for the granting of licenses for the transmission, wholesale supply, distribution and sale of electricity, among other things. The objects of the Commission are to regulate and manage the utilization of energy resources in Ghana and co-ordinate policies in relation to them. More particularly, the Commission shall, among other things: recommend national policies for the development and utilization of indigenous energy resources; advice the Minister on national policies for the efficient economical and safe supply of electricity and natural gas transmission, wholesale products considering the national economy; prepare, review and update periodically indicative national plans to ensure that reasonable demands for energy are met; secure a comprehensive data base for national decision making on the extent of development and utilization of energy resources available to the nation; receive and assess applications, and grant licenses under this Act to public utilities for the transmission, wholesale supply distribution, and sale of electricity and natural gas; establish and enforce, in consultation with the Public Utilities Regulatory Commission, standards of performance for public utilities engaged in the transmission, wholesale supply, distribution and sale of electricity and natural gas; and, promote and ensure uniform rules of practice for the transmission, wholesale supply , distribution and sale of electricity

products considering the national economy; and natural gas; and, promote and ensure uniform rules of practice for the transmission, wholesale supply, distribution and sale of electricity and natural gas. The NRA Act needs to be amended to ensure that the Energy Commission no longer plays a role in the licensing of electricity generation sources from nuclear energy resources.

Renewable Energy Act, 2011 (Act 832) provides for the development, management, utilization, sustainability and adequate supply of renewable energy for generation of heat and power and for related matters.The object of this Act is to provide for the development, management and utilization of renewable energy sources for the production of heat and power in an efficient and environmentally sustainable manner.The Act defines "renewable energy" to include energy obtained from non-depleting sources such as wind, solar, hydro, biomass, bio-fuel, landfill gas, sewage gas, geothermal energy, ocean energy and any other energy source designated in writing by the Minister. The Act provides a framework to support the development and utilization of renewable energy sources, an enabling environment to attract investment in renewable energy sources, the promotion for the use of renewable energy, the diversification of supplies to safeguard energy security; improved access to electricity through the use of renewable energy sources, the building of indigenous capacity in technology for renewable energy sources; public education on renewable energy production and utilization, and the regulation of the production and supply of wood fuel and bio-fuel.The Act also provides for requirements, qualifications and application for a license to engage in a commercial activity in the renewable energy industry. Even though there are ongoing arguments as to whether nuclear energy is a form or type of renewable energy, the Act, however, gives the Minister the discretion to designate any other energy source as a renewable energy source and this is one way or the other places nuclear energy directly or indirectly within the purview of this Act. In the event where a specific Act on nuclear energy does not make express provision on a subject or matter affecting nuclear energy, the Minister in exercise of his discretionary powers under the Act can make provision for same. The Act therefore does not need any amendment. Ghana Atomic Energy Commision Act, 2000 (Act 588) amends and consolidates the law relating to the establishment of the Atomic Energy Commission and for related matters in Ghana, and provides for establishment of the Energy Commission, functions of the Commission, committees of the Board, Funds and the general governance of nuclear energy in Ghana. The functions of the Commission include, among others: proposals to the Government for legislation in the field of nuclear radiation and radio-active waste management; to advise the Government on questions relating to nuclear energy, science and technology; to establish, for the purposes of research and in furtherance of its functions, institutes of the Commission and to exercise

of management of the institutes to encourage and promote the commercialization of research and development results through its Institutes; to supervise the carrying out of all requirements designed to secure the safety and health of nuclear radiation workers and the environment; to engage in research and development activities, as well as in the publication and dissemination of research findings and other useful technical information; to oversee and facilitate the development of human resources in the fields of nuclear science and technology, and to promote the training of scientific, technical and non-scientific personnel of the Commission; to maintain relations with the IAEA and other similar international and national organizations, and to collaborate and liaise with those organizations on matters of research and development of nuclear energy and nuclear technology. Under the Act, the Minister may, on the recommendation of the Commission, by legislative instrument, make regulations for the purpose of securing the safe operation of a nuclear installation under the supervision of the Commission and by any other organization; securing the safe transport of nuclear fuel, radio-active products or waste; regulating and controlling the collection, segregation, treatment, conditioning, storage and disposal of radio-active waste generated in facilities of the Commission and in the mining, milling, gas production and other uses of radio-active materials and sources; securing the maintenance of efficient systems for personnel and environmental monitoring and for medical surveillance and treatment of radiation related sickeness; harmonizing the interests of state agencies concerned with the utilization of radiation; and ensuring the operations relating to irradiating devices and radio-active materials are carried out without risk to public health and safety and that devices, plants, installations and facilities are designed, constructed, calibrated and operated in accordance with standards prescribed by the Minister. The Act is very instructive on nuclear energy in Ghana, setting up and Atomic Energy Commission in Ghana and provides expert knowledge on the nuclear power generation. Provision is also made for the safe keeping and transportation of radioactive materials as well as the safe disposal of radioactive waste. There is also a possible duplication of the provisions of the NRA Act. Collaboration between GAEC and NRA is therefore suggested. No amendment is however needed. Emergency Powers Act, 1994 (Act 472) provides for powers to be exercised in cases of state of emergency and for related matters. The Act states the circumstances under which a state of emergency may be declared to include a natural disaster and any situation in which any action is taken or is immediately threatened to be taken by any person or body of persons which, is calculated or likely to deprive the community of the essentials of life or renders necessary the taking of measures which are required for securing the public safety, the defence of Ghana and the maintenance of public order and of supplies and services essential to the life of the community. The Act provides immediate action in dire situations where necessary measures have to be

immediate action in dire situations where necessary measures have to be taken, or is required for securing the public safety, in the defence of the Republic and the maintenance of public order and of supplies and services essential to the life of the community. Furthermore, the Act makes provision for the removal of persons from emergency areas where the emergency relates only to a part of the country. The President in these emergency situations may be exercise these emergency powers through the issuance of Executive Instruments (EI) or Orders etc. These EIs or Orders may empower persons or authorities to take certain actions specified in the instruments. This Act, needs no amendment since it could be applied to an emergency situation arising from a nuclear disaster. Public Utilities Regulatory Commission, Act 1997, (Act 538) establishes the Public Utilities Regulatory Commission (PURC) as a multi-sectorial public utility regulator. Functions of the PURC among others is to provide guidelines for rates to be charged for the provision of utility services; examine and approve water and electricity rates; advise any person or authority in respect of any public utility; receive and investigate complaints and settle disputes between consumers and public utility. The Act deals largely with the administration of the Commission, providing for its governing body, staff, funding sources etc. and also deals with regulatory matters like standards of performance and rate setting for public utilities. Public Utilities Regulatory Commission Act, 2010 (ACT 800) As amended was amended in 2010, to include levies payable to on electricity and natural gas transmission services, to be part of the funding sources for the Commission. In my view, there is no need to amend the PURC Act to cater for a nuclear power programme. From the above review and analysis of the current laws of the country, it is important to note that the available framework is enough and very little amendments are required for the development of nuclear power plant program.

3.3 Ghanaian Nuclear Regulatory Framework

The regulatory framework established under Act 895 provides for the regulation of nuclear installations, establishing a licensing regime, safeguards and prohibitions, inspections, enforcement, liability for nuclear damage, among others The main approach adopted by the NRA is to set standards and requirements for the licensee and provide guidance by which the applicant will meet its license obligations. The NRA is responsible for the regulation of nuclear safety, security and safeguards, and also emergency preparedness and environmental considerations for nuclear and radiological related matters. The NRA was established in 2016; when, preparation for the introduction of nuclear power had started. Subsequently, it is developing regulations and guides; recruiting and developing the competency of its staff. The work of the NRA is guided by the IAEA Safety Series and Nuclear Security Series document. Meaning, it's work is

guided by the ten Fundamental Safety Principles provided for in the IAEA Fundamental Safety Principles document, and the twelve Essential Nuclear Security Elements provided for in the Objectives and Essential Elements of a State's Nuclear Security Regime document. The NRA follows the IAEA proposed 4-quadrant approach for the systematic training of its staff. Level I capture basic professional training in nuclear technology, nuclear security, safeguards and non-proliferation. Level II addresses technical competencies in nuclear safety, nuclear security, safeguards and non-proliferation; while Level III addresses the core functions of NRA work including inspections, review and assessment and development of regulatory tools, etc. The fourth level addresses management and leadership competencies. The above training requirements are conducted through a combination of both internal and external training programmes, including foreign training programmes. For local training, apart from in-house training of staff, the School of Nuclear & Allied Sciences (SNAS) of the University of Ghana offers training in various Level I, II and III topics. Considerable external foreign training support is provided by the IAEA and other multilateral organisations, bilateral partners, and other foreign regulatory bodies. Some of these include the Regulatory Cooperation Forum (RCF), Global Nuclear Safety and Security Network (GNSSN), the Forum on Nuclear Regulatory Bodies in Africa (FNRBA), the European Commission Instrument of Nuclear Safety (INSC), the United States Nuclear Regulatory Commission (US NRC), the Canadian Nuclear Safety Commission (CNSC), Moroccan Agency for Nuclear & Radiological Safety & Security (AMSSNUR) of Morocco, etc. In developing regulations for the nuclear power programme, the NRS adopts a hybrid approach of prescriptive and performance-based approaches. This approach is considered an optimal position between providing explicit regulatory requirements, that requires the licensee to follow a well-developed methodology, and generic requirements, that gives room for the licensee to innovate and use approaches that are well-founded and internationally accepted. The legal hierarchy of documents that govern the work of the NRA is presented in Figure 1.

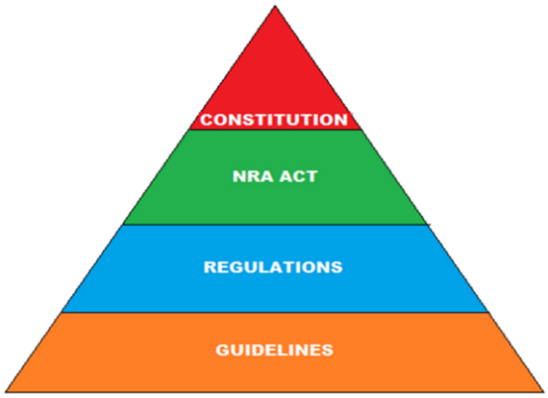

Figure 1: Ghana's Legal Hierarch

The NRA has experience with review and assessment for research reactors. Specifically, the NRA conducted a review and assessment for the change of the core of the Ghana Research Reactor -1 (GHARR-1) from highly enriched uranium to low enriched uranium. The NRA, however, does not have experience in conducting review and assessments for nuclear power plants.

The review and assessment process is a critical appraisal of a proposed reactor project design, with the objective of determining whether the information submitted by the prospective licensee demonstrates that the facility complies with safety and security objectives, throughout its lifetime. The process consists of examining the prospective operator's submissions on all aspects relating to the safety, security and safeguards of the facility. This includes considerations of both normal operation and under accidental conditions, and events including human errors that have the potential for causing exposure of workers, the public, or environment to radiological hazards.

Figure 2 presents a brief on the process that will lead to a series of regulatory decisions including granting an authorisation/license, which if appropriate, imposes conditions or limitations on a facility operator's subsequent activities; or the refusal of such an authorization or license.

Prepare programme of review and assessment	• This allows for streamlining activities during the review and assessment. With this, the NRA will be able to follow the development of facility, as applicable, from initial selection of site, through all activities until removal from regulatory control.
Acceptance review	• This is to ascertain if the document(s) submitted is complete and contains all necessary information to conduct an indepth review and assessment.
Conduct preliminary review	• Findings from this process allows for prioritizing review on the basis of potential implication on overall safety of the facility which inturn will support effectiveness of the Authority.
Systematic plan	• To provide assurance that all topics significant to safety will be covered and all operators of similar facilities are trated equally.
Conduct of review	• Subject matter experts assess information presented to ascertain its trueness/ appropriatness in meeting the requirements of the Authority

Figure 2: Brief description of review and assessment process

Authorisation by licensing broadly represents a graded approach to regulatory control based on levels of risk, or nature of the facility or activity. Authorisation is thus required by any licensee. It is the principal means by which the Authority can apply the legal and regulatory framework, and by which the responsibilities of an applicant are clearly spelt out. This is the practice used by the NRA for all radiological facilities within the country and the GHARR-1 facility. Building on the experience gained so far, steps are being developed for authorisation for nuclear power plants. For this case, authorisation is required to take the form of licensing. A license is given when the Authority has confirmed through review and assessment that a prospective licensee's activities and operations are going to be conducted in a manner that does not pose any unacceptable risk to people and or the environment. Licensing covers all stages of the lifetime of the nuclear power plant, including siting, construction, commissioning, operation, decommissioning and release from regulatory control.

Act 895 of 2015 makes provision for the NRA to undertake enforcement actions against any facility that is found to be in non-compliance with requirements. The objective of enforcement is to provide a high level of assurance that authorised parties comply with all requirements at all steps and stages of the lifetime of the facility, ultimately ensuring safety. There is an established enforcement policy for the NRA which is also applied in a graded approach. Enforcement actions within the policy include; verbal notification, written notification, imposition of additional regulatory requirements and conditions, written warnings, penalties and ultimately revocation of authorisation. Extreme situations may entail prosecution.

Figure 3: Steps for authorisation process/Licensing Life Cycle

4.0 CONCLUSION

In conclusion, Ghana has the necessary legislative and regulatory framework to ensure the success of its nuclear power programme. At the international level, Ghana has ratified relevant international nuclear instruments, entered into bilateral agreements with responsible nuclear partners, and joined major multilateral nuclear organisations; which, when properly implemented, will show Ghana's commitment to peaceful use and application of nuclear energy.

At the national level, Ghana has passed several national laws and formulated policies to cover the core issues of nuclear non-proliferation and nuclear safety and security, and has worked to institutionalized them. Also, it has existing legislation to cover radiation, waste, transport safety, environmental protection, among others; which is being taken into account in the development of its legal and regulatory infrastructure.

In addition, Ghana has established the NRA to provide for the regulation and management of activities and practices for the peaceful use of nuclear material or energy, radioactive material or radiation; to provide for the protection of persons and the environment against the harmful effects of radiation hazards; and, to ensure the effective implementation of Ghana's international obligations, and for related matters.

Despite Ghana's comprehensive legislative and regulatory framework, more work lies ahead. Ghana will need long term commitment and planning, large scale financial and human capital investment, effective implementation of its national legal framework, and amendment of some of its laws, if its nuclear power programme is to succeed.

ACKNOWLEDGEMENTS

My sincere thanks go to the entire staff of the Nuclear Regulatory Authority, Nuclear Power Institute of Ghana Atomic Energy Commission, Environmental Protection Agency, School of Nuclear and Allied Sciences, Energy Commission, National Disaster Management Organization and the Minerals Commission for their support and cooperation. Additionally, our sincere acknowledgment goes to International Atomic Energy Agency (IAEA) for most of the review material used and International Center for Theoretical Physics (ICTP) who provided me with the necessary support through the Associate programme (2020 – 2025)

REFERENCES

[1] Basic Infrastructure for a Nuclear Power Project, IAEA-TECDOC-1513, IAEA, Vienna (2006).

[2] GAEC, (2006). Ghana Atomic Energy Commission at a Glance, Fifth edition (revised), p.1.

[3] Potential for Sharing Nuclear Power Infrastructure between Countries, IAEA-TECDOC-1522, IAEA, Vienna (2006).
[4] Handbook on Nuclear Law (STOIBER, C., BAER, A., PELZER, N., TONHAUSER, W., Eds), IAEA, Vienna (2003).
[5] Comprehensive Safeguards Agreement pursuant to INFCIRC/153 (Corr.).
[6] Additional Protocol pursuant to INFCIRC/540 (Corr.).
[7] Convention on Early Notification of a Nuclear Accident (INFCIRC/335).
[8] Convention on Assistance in the Case of a Nuclear Accident or Radiological Emergency (INFCIRC/336).
[9] Convention on Nuclear Safety (INFCIRC/449).
[10] Joint Convention on the Safety of Spent Fuel Management and on the Safety of Radioactive Waste Management (INFCIRC/546).
[11] Convention on Physical Protection of Nuclear Material (INFCIRC/274), and Amendment.
[12] Vienna Convention on Civil Liability for Nuclear Damage (INFCIRC/500).
[13] Joint Protocol Relating to the Application of the Vienna.
[14] Convention and the Paris Convention (INFCIRC/402)
[15] Protocol to Amend the 1963 Vienna Convention on Civil Liability for Nuclear Damage and Convention on Supplementary Compensation for Nuclear Damage, IAEA, (1997).
[16] Sustainable Development and Nuclear Power, INIS-XA-055, pp.
[17] Revised Supplementary Agreement Concerning the Provision of Technical Assistance by the IAEA.
[18] The Nuclear Regulatory Act 2015 (Act 895).
[19] The Environmental Protection Agency Act 1994 (Act 490).
[20] Minerals and Mining Act 2006 (Act 703).
[21] National Disaster Management Organisation Act 1996 (Act 517).
[22] Hazardous and Electronic Waste Control and Management Act 2016 Act 917).
[23] Energy Commission Act 1997 (Act 541).
[24] Renewable Energy Act 2011 (Act 832).
[25] Ghana Atomic Energy Commission Act 2000 (Act 588).
[26] Emergency Powers Act 1994 (Act 472).
[27] Public Utilities Regulatory Commission Act 1997 (Act 538) a amended

Silver Nanoparticles, stabilized by *Tetrapleura tetraptera* from food waste, influence of extract on Nanoparticles' Surface Morphology and Antimicrobial properties

Vitus A. Apalangya[1*], Enock Dankyi[2], Jerry J. Harrison[2], Leticia Donkor[1], Samuel Darko[3], Angela Parry-Hanson Kunadu[4], Nicole S. Affrifah[1], and Abu Yaya[5]

[1]Department of Food Process Engineering, University of Ghana, Legon, Ghana
[2]Department of Chemistry, University of Ghana, Legon, Ghana
[3]School of Arts and Sciences, Florida Memorial University, USA
[4]Department of Nutrition and Food Science, University of Ghana, Legon, Ghana
[5]Department of Materials Science and Engineering, University of Ghana, Legon, Ghana

***Corresponding author:** vapalangya@ug.edu.gh

ABSTRACT

Plant extracts provide a sustainable and eco-friendly route to forming silver (Ag) nanoparticles (NPs). Synthesizing stabilized and monodisperse Ag NPs using plant extracts is challenging as several and various polyhydroxy compounds of extracts produce non-uniform dispersed NPs. In this study, stabilized Ag NPs were biosynthesized from environmentally friendly, non-toxic, novel aqueous *Tetrapleura tetraptera* fruit extract. The role of synthetic conditions like concentration of silver nitrate and pH were also investigated. Phytochemical and FT-IR analyses revealed that the extract contained polyphenols, flavonoids, and other polyhydroxy compounds. UV-Vis spectra indicated a surface plasmon resonance band at 420 nm typical of Ag NPs, and together with X-ray diffraction (XRD), X-ray photoelectron spectroscopy (XPS), and Energy Dispersive Spectroscopy (EDS), the patterns confirmed the formation of Ag NPs. The UV-Vis spectra and TEM micrographs showed that smaller, homogeneous, stabilized Ag NPs had an average particle size of 50 – 120 nm and 65 – 240nm (beyond 120nm is out of the range of nanoparticles). The *Tetrapleura tetraptera* extract made using 2.5 mM of $AgNO_3$ at a pH of 11.5 exhibited superior antibacterial properties depicted by enhanced growth inhibition and significantly lower ($P<0.05$). The minimum inhibition concentration (MIC) was determined against gram-negative and positive bacteria relative to the synthesized NPs at different pHs. The studies demonstrated the potential of deploring *Tetrapleura tetraptera* extract stabilized Ag NPs as potential antimicrobial agents in packaging and biomedical applications.

Keywords: *Tetrapleura tetraptera* fruit extract, green synthesis, silver nanoparticles, antibacterial properties, biomedical applications

1.0 INTRODUCTION

Beyond their enduring and aesthetic appeal, the great novel applications of noble metal nanoparticles (NPs), Such as gold (Au) and silver (Ag), in medicine, sensing, electronics, food, water, and

catalysis have been reported since antiquity [1-11]. Among metal nanoparticles, Ag and its nanoscale forms, for millennia, have been used to treat and disinfect bacterial infections due to their broad-spectrum biocidal effect towards a wide range of bacteria strains implicated in routine industrial and domestic processes[12, 13]. However, the behavior of Ag NPs as effective antimicrobial agents depends on their composition, shapes, and sizes [14-16]. Raza *et al.* noticed that smaller, spherical-shaped Ag NPs exhibited better antibacterial effects than triangular and larger spherical-shaped Ag NPs against gram-positive and negative bacteria strains [17]. However, due to their small size and high reactivity, uncapped metal nanoparticles are inclined to recombine, forming undesirable bulk forms, and reducing their activity. Ag NPs, due to their large surface-area-to-volume ratio, provide better contact with bacteria than bulk forms [16].

Solution-based methodologies have therefore been used to effectively stabilize and control shapes and sizes of Ag NPs, albeit requiring the use of expensive and potentially environmentally hazardous chemicals such as thiols, amines, polyols and acids due to their high reactivity [18-22]. Plant extracts have been proposed as environmentally safe alternatives as they contain diverse moderately reactive polyhydroxy compounds capable of reducing and capping Ag NPs [13, 23-25]. Extracts are biocompatible, and their usage produces Ag NPs with bioactive properties suitable for biological applications [26-28]. Moreover, the variety of polyhydroxy compounds in plant extracts could act cooperatively to confer suitable shapes, which may be challenging to obtain with single surfactant systems [29]. However, diverse polyhydroxy compounds in plant extracts lead to nanoparticle mixtures with varying sizes, shapes, and wide dispersity, diminishing their antibacterial activity. Narrowing down the spectrum of phytochemicals in the plant extracts through purification could present fewer suitable active compounds that come with increased process cost. Since NPs nucleation and stabilization are not only affected by stabilizers, choosing relevant plant extracts, and using appropriate experimental conditions could lead to stabilized and monodispersed colloidal NPs with desirable shapes and sizes. Recently, novel plant extracts and optimized conditions have been developed to obtain stabilized and well-dispersed green Ag NPs.

Tetrapleura tetraptera, locally known as "prekese" in Ghana, is a tropical flowering plant. Its fruits are consumed as food due to its pleasant aroma, appealing color , carbohydrate and protein content, and as medicine due to their abundant polyphenols, flavonoids, carotenoid, lactic acid and vitamin C contents [30, 31]. The fruit, root, and stem extract of this plant have been used and documented as food, and as traditional medicine in tropical African customs for managing a host of ailments including inflamaion, hypertension, epilepsy, diabetes mellitus, and arthritis; however, no study exploits the great phytochemical content of this plant extract for

the biosynthesis of bioactive metal NPs including Ag [32]. The study hypothesized that *Tetrapleura tetraptera* aqueous fruit extract can reduce and stabilize Ag NPs due to its great phytochemical content. The physicochemical characteristics of the synthesized Ag NPs under various experimental conditions were investigated using crystallographic, spectroscopic and microstructural techniques. In addition, the antimicrobial activities of the as-synthesized Ag NPs obtained at different pH and $AgNO_3$ concentrations were investigated against common gram-positive and negative bacterial food contaminants.

2.1. MATERIALS AND METHODS

All analytical chemicals were purchased from their respective sources and used without further purification. Silver nitrate ($AgNO_3$, 99.9%), sodium hydroxide (NaOH, 97%), hydrochloric acid (HCl, 37%) were purchased from Sigma Aldrich.

2.1. Preparation of *Tetrapleura tetraptera*

Fresh *Tetrapleura tetraptera* fruits were obtained from the Madina market and transported to the laboratory. They were cut into smaller pieces, washed thoroughly with tap water, rinsed with deionized water, and air-dried for two weeks. For easy and effective grinding, the air-dried samples were dried in an oven at 60 ^{o}C overnight to ensure complete dehydration. Next, the cut dried samples were milled for 1 hour using an attrition mill (Retsch, Rheinische StraBe 36.D-42781, Haan Germany). The samples were sieved using a sieve shaker with stainless steel sieves stacked from coarse to fine mesh (80, 60, 20 µm). Subsequently, 10 g of the milled powdered samples was mixed thoroughly in 25 ml ethanol and water solution (2:1 v/v). The resulting mixture was boiled at 60 ℃ for 30 minutes under constant stirring to obtain highly viscous extracts and subsequently kept at room temperature to cool. The cooled mixture was filtered using a Whatman No.1 filter paper to get a clearer solution of the extract. The extracts were then stored in a refrigerator until further use.

2.2. Phytochemical screening of extracts

The phytochemical content of the plant extracts was analyzed according to the method adopted by Bashair *et al.* [33]. The availability of phytochemicals such as polyphenols, flavonoids, saponins and tannins in the *Tetrapleura sp* extracts were determined. The detailed procedure for analyzing each phytochemical is shown in the supplementary information (section 1)

2.3. Synthesis of Silver Nanoparticles

All reagents used were of analytical grade. Ag nitrate ($AgNO_3$) solution was prepared by dissolving an appropriate amount of $AgNO_3$ salt in 100 mL deionized water to obtain approximately 0.1 M stock solution. The following reactions were performed to determine the effect of AgNO3 concentration on the properties of the Ag NPs. Aliquots of the stock solution were pipetted and added dropwise to Erlenmeyer flasks containing 25 ml diluted *Tetrapleura tetraptera* fruit extract, which was composed of 5 ml of plant extract and varying amounts of deionized water, to obtain a prepared final reaction solution containing 25-, 50- and 100-mM concentrations of $AgNO_3$. To evaluate the effect of pH on the properties of the Ag NPs during synthesis, the reaction was performed at three different pH values (4.2, 7.4 and 11.2) using final $AgNO_3$ concentrations of 25, 50 and 100 mM. The effect of changing concentration of $AgNO_3$ salt and pH during the synthesis was monitored and analyzed using UV-Vis spectroscopy and TEM analyses.

2.4. Characterization of Biosynthesized Colloidal Silver Nanoparticles

2.4.1. UV-Vis Spectroscopy

The UV-Vis absorption patterns were obtained and analyzed using a Shimadzu UV-3600 UV-Vis-NIR spectrophotometer. The effect of $AgNO_3$ concentration on the UV-Vis spectra of the colloidal Ag NPs synthesized was investigated at three different concentrations of $AgNO_3$ (2.5, 50 and 100 mM). In addition, the influence of pH (at 4.2, 7.4 and 11.2) on the UV-Vis spectra of the Ag NPs was also studied using two concentrations of $AgNO_3$ (25 and 100 mM).

2.4.2. Fourier transform infra-red spectroscopy, X-Ray Diffraction and X-ray photoelectron spectroscopy

The Fourier transform infra-red Spectroscopy (FTIR) patterns were measured and recorded using a PerkinElmer Spectrum 100 spectrophotometer. X-Ray Diffraction (XRD) analyses were performed using Rigaku DMAX 2100 diffractometer (Rigaku, Tokyo, Japan) with monochromatic CuK α radiation ($\lambda = 0.154056$ nm) at 40 kV and 30 mA. The surface chemistry and elemental composition of the colloidal Ag NPs were studied using X-ray photoelectron spectroscopy (XPS) measurements. A load-locked Kratos XSAM 800 surface analysis system was used to acquire the XPS spectra.

2.4.3. Transmission Electron Microscopy

The surface morphological analysis of the biosynthesized colloidal Ag NPs was conducted using high-resolution transmission electron microscopy (H-8000 TEM microscope). In a sonication bath, the colloidal samples were prepared by sonicating 5 ml of the biosynthesized Ag NPs for 5 minutes. A drop of the colloidal Ag NPs solution

made from two concentrations of $AgNO_3$ (2.5 and 100 mM) at pH of 11.2 was deposited on a carbon grid (carbon-coated copper grid and the excess solution was removed using tissue paper) and enough time was allowed for drying of prepared sample grids at room temperature.

2.5. Antimicrobial assays

2.5.1. *In vitro* antimicrobial assay

S. Typhimurium was used in this study. Each stock bacteria species was sub-cultured on a Mueller-Hinton agar (Park Scientific Limited) plate and incubated overnight at 37ºC to obtain pure cultures. About 3-4 single colonies from the bacteria plate were selected, inoculated into Mueller-Hinton broth and incubated at 37 ºC overnight, for the bacteria to reach the log phase of growth. The log phase bacteria were diluted with sterile saline to achieve a turbidity of 0.5 McFarland standard, an approximate concentration of 2 x 10^8 CFU/ml.

Log phase bacteria at a concentration range of 1 x10^2 to 1x10^7 CFU/ml were incubated with different concentrations of the test agents (0 % -100 %) and 10% Alamar Blue® reagent at 37ºC for 6-8 hrs. Absorbance was read at 540 nm, reference 595 nm, using a spectrophotometer (TECAN Sunrise Wako). In determining the bactericidal and bacteriostatic properties of concentrations of the Ag NPs (6 – 60 µg/mL) and 10 % Alamar Blue®. The reducing power of cells to convert the Alamar Blue component resazurin to the pink resorufin was used to determine the Minimum Inhibitory Concentration (MIC) of the samples. The least concentration of compounds with no observable color change was noted as the MIC.

3.0 RESULTS AND DISCUSSION

3.1. Phytochemical Analysis

The phytochemical analysis indicated that the aqueous *Tetrapleura tetraptera* fruit extract contained polyphenols, saponins, glycosides, tannins, and flavonoids as shown in Table 1which constituent with reported study.

Table 1: Phytochemical analysis of aqueous *Tetrapleura tetraptera* fruit extract

Name of test	Phytochemicals	Tetrapleura
Ferric chloride test	Polyphenols	+
Alkaline reagent test	Flavonoids	+
Braymer's test	Tannins	+
Foam test	Saponins	+
Salkowki's test	Terpenoids	-
Keller killiani test	Glycosides	+

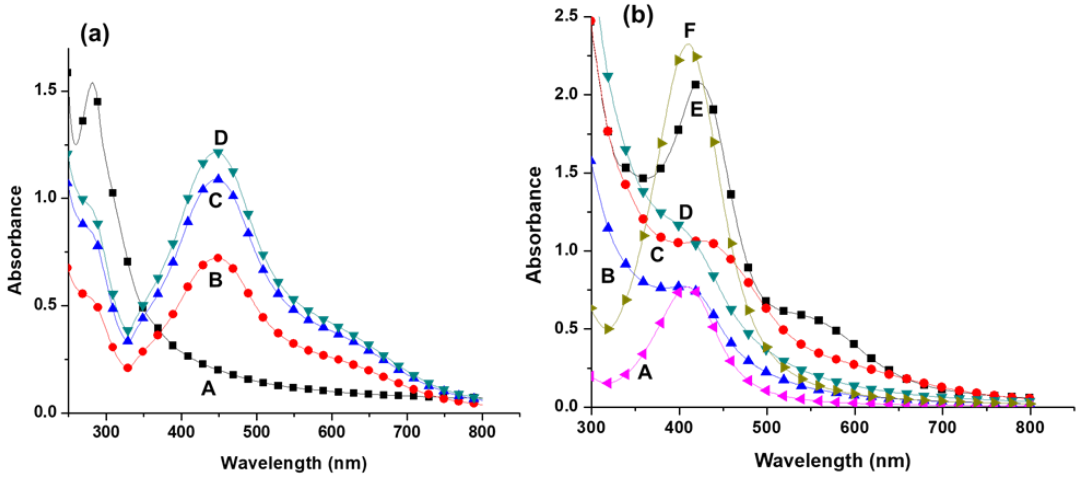

Figure 1. UV-Vis patterns (a) A: pure *Tetrapleura terapleura* extract (TTE), B: Ag NPs 25 nM $AgNO_3$, C: 50 mM $AgNO_3$ D: 100 mM $AgNO_3$ (b) Ag NPs synthesized at A: pH 7.4 & 25 mM $AgNO_3$, B: pH 7.4 & 100 mM $AgNO_3$, C: pH 4.2 & 100 mM $AgNO_3$, D: pH 4.2 & 25 mM $AgNO_3$, E: pH 11.2 & 100 mM $AgNO_3$ and F: pH 11.2 and 25 mM $AgNO_3$

3.2. UV-Vis spectroscopy analysis

The bioreduction of Ag^+ ions to Ag (Ag^0) nanoparticles were observed by monitoring the distinct color changes and the appearance of a typical Ag surface plasmon resonance (SPR) band in UV–Vis spectroscopy measurements accompanying the reactions. The biosynthesis proceeded with distinct change of the solution color from pale brown to dark brown as depicted in the supplementary information (section 2). The appearance of a characteristic SPR band at 420 nm and together with microstructural studies confirmed the formation of Ag NPs (figure 1).

3.3. FT-IR, XRD and XPS Analysis

FT-IR studies were performed to confirm the presence of polyphenolic phytochemicals in the *Tetrapleura tetraptera* fruit extract and as well as on the surface of biosynthesized colloidal Ag NPs. Fig. 2(a)A and fig. 2(a)B depict the FT-IR patterns of pure fruit extract and biosynthesized Ag NPs respectively. Both exhibited similar molecular vibrational patterns. However, the patterns showed strong sharp band at 3320 cm^{-1} which is typical of -OH stretching vibration associated with polyols which can be related to the polyphenols and other polyhydroxy phytochemicals present in the extract. A relatively more robust band around 2912 cm^{-1} and a weak shoulder at about 2800 cm^{-1} are characteristic symmetric and asymmetric stretching vibrations of CH respectively of an aliphatic hydrocarbon attributable to the polysaccharide or terpenoid phytochemicals present in the fruit extract. The band around 1635 cm^{-1} is the bending vibrational mode typical of water in the extract as well as in the colloidal Ag NPs. Finally, the band at 1087 cm^{-1} can be related to the C-O-C stretching vibration of the CH_2OH group on a polysaccharide compound in the extract [37]. These observations are consistent with earlier study that plant extracts possess suitable functional groups which capped the surface of the Ag NPs stabilizing them as stable colloidal solutions [38].

X-ray diffraction (X-RD) pattern of the biosynthesized colloidal Ag NPs is depicted in Fig. 2 (b). Typical of Ag NPs, four characteristic peaks are indexed at 2θ = 38.1°, 44.2°, 64.4°and 77.3° and correspond to the following Bradley crystal faces of (1 1 1), (2 0 0), (2 2 0) and (3 1 1) of Ag with JCPDS card (file No JCPDS # 04-0783). The surface chemical composition of the biosynthesized Ag NPs is depicted by XPS patterns in the Fig. 2 (c) and (d) showing the structure and the chemical identity of the species involved. It is evident that the as-synthesized sample is composed of carbon (C), oxygen (O_2) and Ag with no other chemical or elemental impurities. There is a doublet with binding energies at about 363 and 379 eV which can be associated with Ag3d3/2 and Ag3d5/2 characteristic of Ag. The intensity ratio of this doublet peak is 2:1 and is consistent with similar literature report (6).

The elemental composition of Ag on the surface of the sample is 17.7%, relative to the other elements in the synthesized sample. This lower percentage composition relative to the amount quantified by the EDS may be due to the lower depth of measurement of the XPS technique [6].

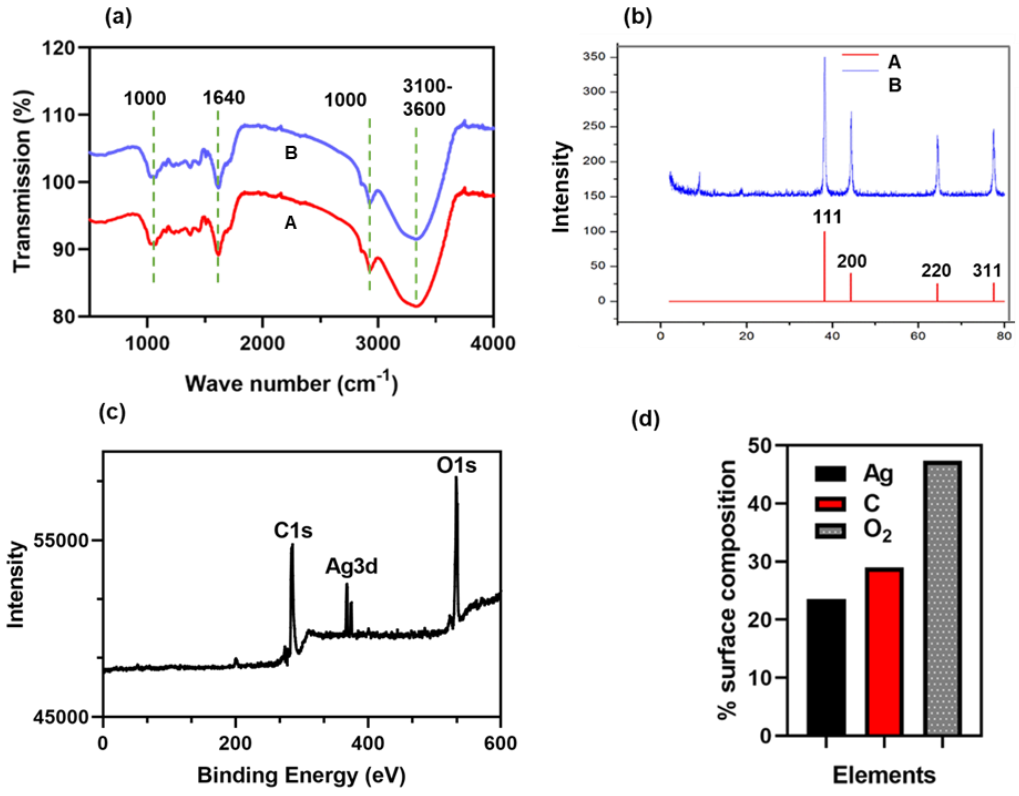

Figure 2. (a) FT-IR patterns of A: Tetrapleura tetraptera fruit extract and B: synthesized Ag NPs (b) XRD pattern of synthesized Tetrapleura tetraptera fruit extract stabilized Ag NPs (c) XPS pattern of *Tetrapleura tetraptera* fruit extract stabilized Ag NPs (d) percentage elemental composition from XPS studies.

3.4. Scanning Electron Microscope and EDX Analysis

The surface morphology of Ag NPs which were synthesized at a pH of 11.2 was acquired and analyzed by FETEM and EDX, as depicted in fig.3. The nanoparticles exhibited uniform morphology with spherical shapes and an average size of 60 nm (fig. 4(b)). NPs appeared well dispersed with little agglomeration. The NPs were well stabilized on the surface of the fruit extract phytochemicals which likely played a role in minimizing particle to particle interaction resulting in reduced particle combination. Moreover, the abundance of polyphenols, flavonoids and polysaccharides in the extract likely adsorbed onto the surface of the nanoparticles. This phenomenon has the tendency to significantly reduce the surface energy of the particles minimizing their reactivity in the process thereby preventing particle agglomeration.

Finally, the significant reduction of $AgNO_3$ concentration drastically shortens the time for the concurrent formation and growth of the Ag NPs with the benefit of promoting the production of monodispersed Ag NPs with less particle recombining. As shown in fig. 4(c), there is a 3keV intense spectral peak which is indicative of the formation of Ag NPs as shown in the EDX pattern. Fig. 3(b) is a depiction of the surface morphology of Ag NPs synthesized at a pH of 11.2 using 100 mM $AgNO_3$ concentration. It is evident that there is a wide particle size variation ranging from 70 – 240 nm. The particle shapes vary from spherical to other complicated morphologies. The particles appeared to be coalescing. Compared to the particles formed at the same pH of 11.2 but at 2.5 mM $AgNO_3$ concentration, it can be observed that more nanoparticles are formed for the same amount of plant extract with reduced mono-dispersity. The agglomeration of the NPs is a result of insufficient stabilizing agents. Mono-dispersity of the NPs can be attained by having particles surfaces well stabilized immediately they are formed. This will minimize undesirable particle interactions reducing nucleation outpacing particle growth. It is therefore prudent to increase the amount of plant extract to provide more stabilizing agents.

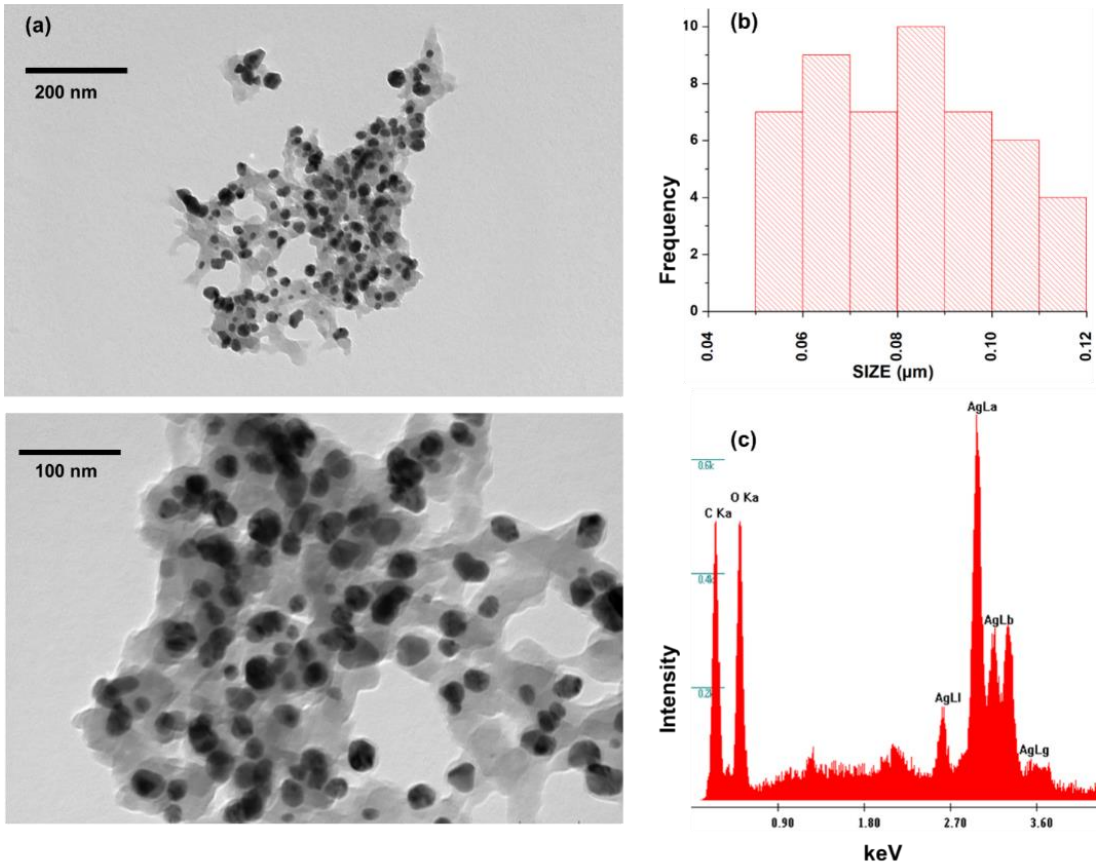

Figure 3. (a) Low and high magnification TEM image of Ag NPs synthesized from 2.5 mM of $AgNO_3$ at pH of 11.2 (b) average size of Ag NPs (c) EDX pattern of Ag NPs

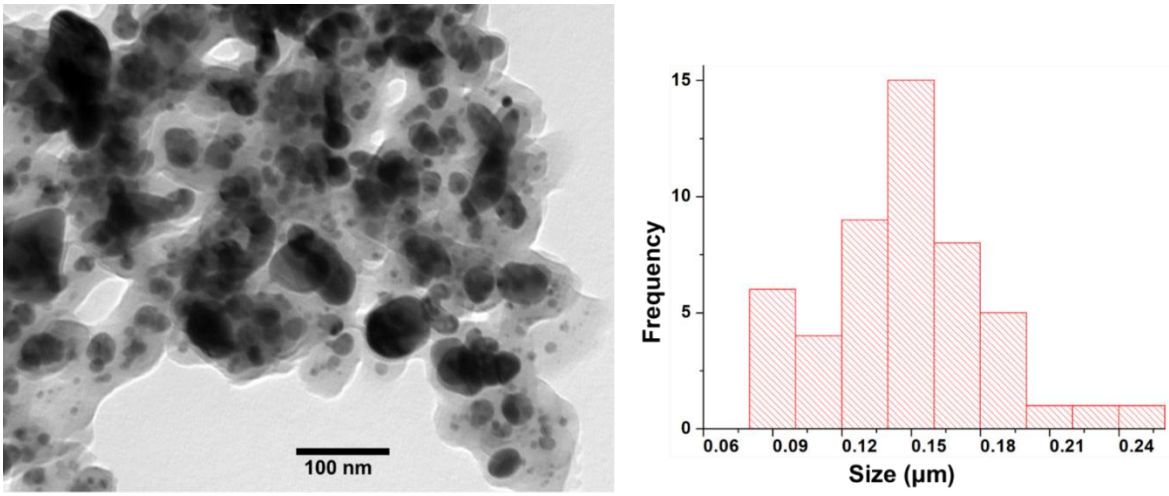

Figure 4: (a) TEM image of Ag NPs at 100 mM of $AgNO_3$ at pH of 11.2 (b) average size of Ag NPs

3.5. Mechanism of formation and stabilization of Silver Nanoparticles

Most plant extracts are weak or moderate reducing agents compared to stronger synthetic oxidizing agents such as sodium borohydride, sodium dodecyl sulfate, and poly (vinyl pyrolidone) [39, 40]. As a result, their rate of reduction of Ag ions to Ag NPs is slow, this inadvertently enables concurrent nucleation and growth of metal nanoparticles. The new and old nuclei readily recombine due to their high surface energy and closeness in space and time, therefore yielding polydisperse NPs. To overcome polydispersity, metal NPs are synthesized at high temperatures. Even

though reducing Ag^+ ions to Ag NPs at elevated temperatures produces considerable high monodisperse NPs, in most instances, the NPs produced have broad size distribution with a variety of nanoparticle geometry. In this study, the effect of polyphenolic, flavonoid and polysaccharide laden *Tetrapleura tetraptera* fruit extract mediated the reduction of Ag^+ ions to Ag NPs. Flavonoids and polyphenolic compounds have been established to be effective reducing and stabilizing agents whereas polysaccharides due to their long polymer chains can effectively stabilize the whole body of NPs in solution. At high pH (11.2), enol forms of flavonoids and phenolic compounds are capable of releasing electrons that can interact with Ag^+ ions reducing them to Ag NPs as shown in fig, 5. Basic synthetic medium can result in the activation of the flavonoids and polyphenolic compounds making them better reducing agents. Relative to their neutral or moderately acidic pH media counterparts as shown as depicted in figure 5.

3.6. Antibacterial Analysis

The minimum inhibition concentration (MIC) determined for each bacteria species treated with the prepared Ag NPs at different pH are shown in figure 6. To evaluate the difference in bacterial growth inhibition among the different Ag NPs biosynthesized using different combinations of AgNO3 concentrations and pH, a triplicated minimum inhibition concentration (MIC) of each class of Ag NPs was evaluated versus the three strains of bacteria – Salmonella Typhimurium (fig 6).

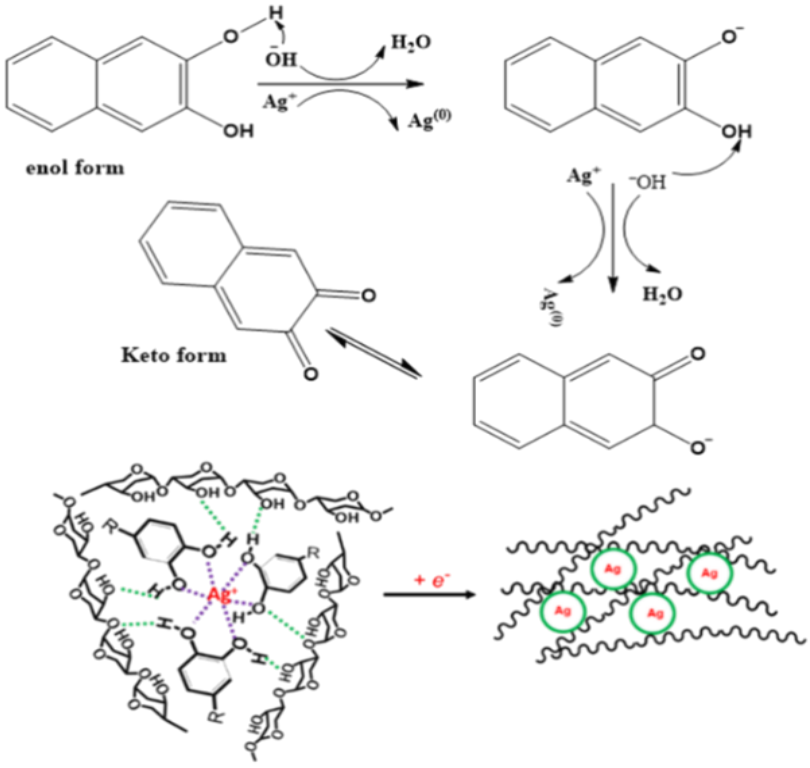

Figure 5. A schematic showing the interaction of Ag ions before and after reduction into colloidal silver nanoparticles with phytochemicals.

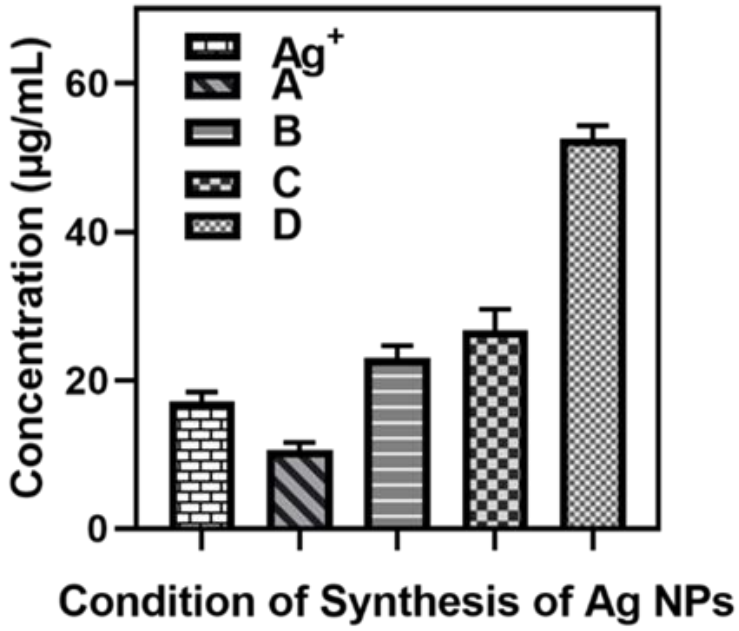

Figure 6. The least concentration (MIC) of Ag NPs needed to inhibit visible growth of *Salmonella typhimurium* with each bacteria treated Ag^+, and Ag NPs synthesized using a combination of the following $AgNO_3$ concentration and pH: A; 25 mM and11.2, B; 100 mM and11.2, C; 25 mM and 7.4, and D: 25 mM and 4.7 respectively

It is evident from this MIC study that *Tetrapleura tetraptera* fruit caped Ag NPs made using $AgNO_3$ with 2.5 mM at a pH of 11.2 (fig. 6 A) exhibited significantly ($P<0.05$) the lowest MIC values compared to the other *Tetrapleura tetraptera* caped Ag NPs at different $AgNO_3$ concentrations and pH combinations (fig. 6 B, C, D and Ag+ or $AgNO_3$). Generally Ag NPs made in neutral and basic media also exhibited significantly ($P<0.05$) lower MIC values compared to NPs made in acidic medium. However, there was an insignificant difference in MIC values for Ag NPs synthesized at a pH of 11.2 with $AgNO_3$ concentration of 100 mM and 7.4 with $AgNO_3$ concentration of 2.5 mM. This clearly showed that a combination of both basic pH and low $AgNO_3$ concentration is necessary for producing Ag NPs with the most active antibacterial properties. It is evident that Ag NPs synthesized at acidic pH (3.6) exhibited the lowest antibacterial activity. Noticeably, the efficacy of the Ag NPs strongly depended on the concentration of the reagent $AgNO_3$ and the reacting pH which is also directly related to

and the reacting pH which is also directly related to the size of the NPs as smaller size Ag NPs exhibited better antibacterial activity compared to bigger size NPs. As shown by the SEM micrographs, Ag NPs synthesized using 100 mM agglomerates forming larger particles thereby losing their size associated large surface area to volume ratio reactivity. The ease of reduction of Ag^+ ions to Ag NPs depends on the degree of dissociation of polyphenols and the resulting release of electrons and stabilization of the Ag NPs by the enolates. Since at basic pH (11), the dissociation of the polyphenols occurs more readily and than at acidic pH (3.6), more Ag NPs will be produced and stabilized per unit volume of colloidal solution for a given $AgNO_3$ concentration in the basic medium than in acidic medium. Mechanistically, Ag NPs inhibit bacteria growth through attachment to the surface of bacteria cells and the resulting penetration of the cell wall or release of ions and reactive oxygen species which are all favoring smaller size NPs compare to larger size ones in this study [41].

4.0 CONCLUSION

In this study, aqueous *Tetrapleura tetraptera* fruit extract has been used for the first time as a green reducing and stabilizing agent in synthesizing eco-friendly Ag NPs. Phytochemical analysis and FT-IR studies showed that the extract contains several polyhydroxy compounds with potential reducingand stabilizing capacity. The formation of the Ag NPs was characterized and confirmed using UV-Visible, XRD, and XPS spectra. The size and effective stabilization of the NPs are dependent on the concentration of the $AgNO_3$ and the pH of the reaction medium. Lower concentration $AgNO_3$ and basic medium produced smaller size, well dispersed and stabilized Ag NPs whereas higher $AgNO_3$ and acidic medium resulted in larger size NPs, varying size and shapes, and agglomerated Ag NPs. The biosynthesized NPs exhibited broad antibacterial properties by inhibiting the growth of both gram-positive gram-negative *Salmonella Typhimurium.* Ag NPs which were synthesized using lower concentration of Ag NPs and in basic medium were the most efficacious as the Ag NPs exhibited better antibacterial properties with the lowest MIC values against gram-negative bacteria. Conceivably, these biosynthesized Ag NPs can be incorporated into packaging systems and biomedical membranes for food and wound healing applications.

DECLARATION OF COMPETING INTEREST

The authors confirm that there are no known conflicts of interest associated with this publication and there has been no significant financial support for this work that could have influenced its outcome.

ACKNOWLEDGEMENT

Authors are grateful to the University of Ghana Building a New Generation of African Academics (BANGA-AFRICA) Project funded by the Carnegie Corporation of New York for financial support. We are grateful to The Electron Microscopy Center at the University of South Carolina for their assistance with our TEM analysis.

DATA AVAILABILITY

The data used to support the findings of this research are included within the article.

REFERENCES

[1] G.G. de Lima, D.W. de Lima, M.J. de Oliveira, A.B. Lugão, M.T. Alcântara, D.M. Devine, M.J. de Sá, ACS Applied Bio Materials 1 (2018) 1842.

[2] Y. Ran, P. Strobbia, V. Cupil-Garcia, T. Vo-Dinh, Sensors and Actuators B: Chemical 287 (2019) 95.

[3] N. Karim, S. Afroj, S. Tan, K.S. Novoselov, S.G. Yeates, Scientific reports 9 (2019) 8035.

[4] M. Park, J. Im, M. Shin, Y. Min, J. Park, H. Cho, S. Park, M.-B. Shim, S. Jeon, D.-Y. Chung, Nature nanotechnology 7 (2012) 803.

[5] A. Martínez-Abad, J.M. Lagaron, M.J. Ocio, Journal of agricultural and food chemistry 60 (2012) 5350.

[6] V. Apalangya, V. Rangari, B. Tiimob, S. Jeelani, T. Samuel, Applied Surface Science 295 (2014) 108.

[7] R. Bryaskova, N. Georgieva, D. Pencheva, Z. Todorova, N. Lazarova, T. Kantardjiev, Colloids and Surfaces A: Physicochemical and Engineering Aspects 444 (2014) 114.

[8] P. Xu, C. Cen, N. Chen, H. Lin, Q. Wang, N. Xu, J. Tang, Z. Teng, Journal of colloid and interface science 526 (2018) 194.

[9] Z. Qiao, Y. Yao, S. Song, M. Yin, J. Luo, Journal of Materials Chemistry B 7 (2019) 830.

[10] w.A. Oddy, M. Bimson, S.L. Niece, Studies in Conservation 28 (1983) 29.

[11] R.E. Leader-Newby, Silver and society in late antiquity: functions and meanings of silver plate in the fourth to seventh centuries. Routledge, 2017.

[12] W. Hill, D. Pillsbury, Baltimore, 1939.

[13] M. Pollini, F. Paladini, M. Catalano, A. Taurino, A. Licciulli, A. Maffezzoli, A. Sannino, Journal of Materials Science: Materials in Medicine 22 (2011) 2005.

[14] A. Roy, O. Bulut, S. Some, A.K. Mandal, M.D. Yilmaz, RSC advances 9 (2019) 2673.

[15] O.V. Mikhailov, Crystallography Reviews 25 (2019) 54.

[16] J.R. Morones, J.L. Elechiguerra, A. Camacho, K. Holt, J.B. Kouri, J.T. Ramírez, M.J. Yacaman, Nanotechnology 16 (2005) 2346.

[17] M. Raza, Z. Kanwal, A. Rauf, A. Sabri, S. Riaz, S. Naseem, Nanomaterials 6 (2016) 74.

[18] S. Iravani, H. Korbekandi, S.V. Mirmohammadi, B. Zolfaghari, Research in pharmaceutical sciences 9 (2014) 385.

[19] Z. Chen, T. Balankura, K.A. Fichthorn, R.M. Rioux, ACS nano 13 (2019) 1849.

[20] J. Xiong, X.-d. Wu, Q.-j. Xue, Colloids and Surfaces A: Physicochemical and Engineering Aspects 423 (2013) 89.

[21] Y. Wang, J.F. Wong, X. Teng, X.Z. Lin, H. Yang, Nano Letters 3 (2003) 1555.

[22] H. Hu, X. Wu, H. Wang, H. Wang, J. Zhou, Carbohydrate Polymers 213 (2019) 419.

[23] G.M. Nazeruddin, N.R. Prasad, S.R. Prasad, Y.I. Shaikh, S.R. Waghmare, P. Adhyapak, Industrial Crops and Products 60 (2014) 212.

[24] R.D. Rivera-Rangel, M.P. González-Muñoz, M. Avila-Rodriguez, T.A. Razo-Lazcano, C. Solans, Colloids and Surfaces A: Physicochemical and Engineering Aspects 536 (2018) 60.

[25] K. Hileuskaya, A. Ladutska, V. Kulikouskaya, A. Kraskouski, G. Novik, I. Kozerozhets, A. Kozlovskiy, V. Agabekov, Colloids and Surfaces A: Physicochemical and Engineering Aspects (2019) 124141.

[26] M.K. Swamy, K. Sudipta, K. Jayanta, S. Balasubramanya, Applied nanoscience 5 (2015) 73.

[27] M.N. Nadagouda, N. Iyanna, J. Lalley, C. Han, D.D. Dionysiou, R.S. Varma, ACS Sustainable Chemistry & Engineering 2 (2014) 1717.

[28] M.F. Zayed, R.A. Mahfoze, S.M. El-kousy, E.A. Al-Ashkar, Colloids and Surfaces A: Physicochemical and Engineering Aspects (2019) 124167.

[29] S.S. Nogueira, A.R. de Araujo-Nobre, A.C. Mafud, M.A. Guimarães, M.M.M. Alves, A. Plácido, F.A.A. Carvalho, D.D.R. Arcanjo, Y. Mascarenhas, F.G. Costa, P. Albuquerque, P. Eaton, J.R. de Souza de Almeida Leite, D.A. da Silva, V.S. Cardoso, International Journal of Biological Macromolecules 135 (2019) 808.

[30] B. Darfour, S. Agbenyegah, D. Ofosu, A. Okyere, I. Asare, Radiation Physics and Chemistry 102 (2014) 153.

[31] D.A. Abugri, G. Pritchett, Journal of herbs, spices & medicinal plants 19 (2013) 391.

[32] J.A. Ojewole, C.O. Adewunmi, Journal of Ethnopharmacology 95 (2004) 177.

[33] L.A.A. Bashair H Al Kinani, Der Pharma Chemica (2017).

[34] Y. Htwe, W. Chow, Y. Suda, M. Mariatti, Materials Today: Proceedings 17 (2019) 568.

[35] D. Paramelle, A. Sadovoy, S. Gorelik, P. Free, J. Hobley, D.G. Fernig, Analyst 139 (2014) 4855.

[36] S.M. Roopan, Rohit, G. Madhumitha, A.A. Rahuman, C. Kamaraj, A. Bharathi, T.V. Surendra, Industrial Crops and Products 43 (2013) 631.

[37] T. Petit, L. Puskar, T. Dolenko, S. Choudhury, E. Ritter, S. Burikov, K. Laptinskiy, Q. Brzustowski, U. Schade, H. Yuzawa, The Journal of Physical Chemistry C 121 (2017) 5185.

[38] S. Ramanathan, S.C.B. Gopinath, P. Anbu, T. Lakshmipriya, F.H. Kasim, C.-G. Lee, Journal of Molecular Structure 1160 (2018) 80.

[39] R. Das, M. Das, International Journal of Plastics Technology (2019) 1.

[40] L. Fontana, M. Bassetti, C. Battocchio, I. Venditti, I. Fratoddi, Colloids and Surfaces A: Physicochemical and Engineering Aspects 532 (2017) 282.

[41] E.T. Hwang, J.H. Lee, Y.J. Chae, Y.S. Kim, B.C. Kim, B.I. Sang, M.B. Gu, Small 4 (2008) 746.

.

Carcass characteristics and meat quality of Japanese quails as influenced by *Canarium schweinfurthii* (Atili)-based diets

Oshibanjo D.O.[1*], Adediran O. A.[2], Adelowo V. O.[3], and Okpara Jude Obi[3]

[1]Department of Animal Production, University of Jos, Plateau State, Nigeria
[2]Department of Animal Science, University of Ibadan, Ibadan Oyo State Nigeria
[3]Department of Animal Production, Federal College of Animal Health and Production Technology, N.V.R.I., Vom, Plateau State

*__Corresponding author:__ dimu4ever@yahoo.com

ABSTRACT

This study evaluated the effect of *Canarium schweinfurthii* (Atili) based diets on carcass characteristics and meat quality of Japanese quails. One hundred and twenty day-old quail chicks were used. Initial weights were taken and quails were randomly allotted to five dietary treatments thus: 0% (T1), 2.5 % (T2) 5% (T3), 7.5% (T4) and 10% (T5) graded-levels of Atili leaf meal (ALM). Each treatment had 30 chicks with 3 replicates of 10 birds. Data obtained was subjected to analysis of variance. The defeathered weight, eviscerated weight and carcass weight were significantly different, with quails fed 5.0% Atili based diet having the highest value (94.46%) and least values obtained in quails fed 2.5% Atili-based diet. The head weight was significantly higher in quails fed 5.0% Atili-based diet (5.23%) with least value in quails fed 2.5% Atili-based diet (3.97%). The neck weight was higher in quails fed 10.0% Atili based diet (5.44%) with least value in quails fed 2.5% Atili-based diet (3.58%). Breast, drumstick and thigh weights were significantly higher in quails fed 5.0% Atili-based diet (25.62%, 6.94% and 9.69% respectively). Quail meat from birds fed 5.0% Atili-based diet had the highest pH, water holding capacity and oxidative rancidity (7.00, 53.33% and 2.27mg/kg respectively). Meat from birds fed 5.0% Atili-based diet had the least values for cooking loss in all the muscle types. In conclusion quails can be fed with Atili leaf meal up to 5.0% due to higher values obtained from both the carcass characteristics and meat quality.

Keywords: Carcass characteristics, Meat quality, Japanese quails and Quail meat

1.0 INTRODUCTION

The poultry industry in the developing countries is facing some challenges, one of which is increase in the cost of feed because of high prices of protein and energy sources (Abbas, 2013). According to Adelowo *et al*. (2019) the rapid growth of human and livestock population creating increased needs for food and feed in the less developed countries, demands that alternative feed resources must be identified and evaluated. In Low-Income Food-

Deficit Countries (LIFDCs), surplus of cereals is generally not available; therefore, it's not advisable to develop a wholly grain-based feeding system. The recommended policy is to identify and use locally available feed resources to formulate diets that are as balanced as possible (Guèye and Branckaert, 2002). Hence, the need, to explore the use of non-conventional feed sources that have the capacity to yield the same output as conventional feeds, and perhaps at cheaper cost. In essence, any similar high protein ingredient which could partially or completely be used as a substitute for soyabean meal or fishmeal is desirable.

There is therefore need to research into the use of non-conventional feed resources. Example of such is *Canarium schweinfurthii,* it belongs to the family *Burseraceae* and the genus *Canarium* (Keay, 1989). *Canarium schweinfurthiii* (Atili) trees are rich in phenolic substances having significant biological properties, the most important of which is oleuropein. Oleuropein is the heterosidic ester of elenolic acid and hydroxytyrosol (Mujić *et al.,* 2011). The most important natural source of this compound is the Atili leaf (Govaris *et al.,* 2010). Studies on *Canarium schweinfurthiii* (Atili) leaf demonstrated that it includes some medical compounds having antihypertensive, antiatherogenic, cardioprotective, hypocholesterolemic, hypoglycemic, antimicrobial, antiviral, antitumor, anti-inflammatory and antioxidant properties (Mujić *et al.,* 2010; Bahsi *et al.,* 2016). *Canarium schweinfurthiii* is a large, evergreen forest tree with its crown reaching to the upper canopy of the forest, it belongs to the family Burseraceae and the genus *Canarium*. From a global perspective, the quest to reduce the use of drugs in animal production is on the increase. Therefore, plant extracts rich in bioactive compounds with anti-microbial, antioxidant, and anti-inflammatory properties are promising alternatives to antibiotics (Lillehoj *et al.,* 2018).

Therefore, this study was designed to evaluate the effects of *Canarium schweinfurthii* (Atili-based) diet on carcass characteristics and meat quality of Japanese quails.

2.0 MATERIALS AND METHODS

2.1 Experiment site

The study was carried out at the Livestock Investigation Department of the National Veterinary Research Institute (N.V.R.I.), Vom, Plateau State. No ethical approval was requested for this study, because it did not include the use of any known toxic substance or the use of any unstandardized procedure.

2.2 Experimental animals

One-hundred-and-twenty-day old quail chicks were obtained from Poultry Division, Livestock Investigation Department of the National Veterinary Research Institute (N.V.R.I.), Vom, Plateau State were used and weighed at the beginning of the experiment to obtain the initial weight and randomly

allotted in a completely randomized design to 5 dietary treatments of 0% (T1), 2.5 % (T2) 5% (T3), 7.5% (T4) and 10% (T5) graded levels of *Canarium schweinfurthii* (Atili) leaf meal (ALM). Each dietary treatment had 30 chicks with 3 replicates of 10 birds.

2.3 Experimental feed

The diets were isonitrogenous and isocaloric to meet the recommended crude protein and Metabolizable energy requirements as stated by NRC (1994). Feed was provided in treatment specific troughs daily and water were given *ad libitum.*

2.4 Parameters measured

2.4.1 pH

The pH value of raw and cooked meat samples were determined by weighing 10 grams of sample into a blender with 90ml of distilled water and homogenised until smooth slurry was formed. The digital pH meter was placed in a buffer solution in order to allow equilibrium for two minutes before placing it into prepared slurry. An average of three readings taken gave the pH value according to method described by AOAC (2000).

2.4.2 Water holding capacity

Water Holding Capacity (WHC) was determined according to Wardlaw, Maccaskill, and Acton (1973). Minced meat (20 g) was placed in a centrifuge tube containing 30 ml of 0.6 M NaCl and was stirred with glass rod for 1 min. The tube was then kept at 4 ± 1 °C for 15 min, stirred again and centrifuged at 3000g (R-24, Remi Instruments, India) for 25 min. The supernatant was measured and WHC was expressed in percentage.

2.4.3 Analysis of oxidative rancidity (Lipid oxidation)

Thiobarbituric acid value (TBA) was estimated by modified methods of Buege and Aust (1978). Three mls each of glacial acid and 1% TBA solution were added to test tubes appropriately labelled blank and tests. 0.6ml of distilled water was added to the blank, while 0.6ml of the homogenised sample was added to each of the tests tubes. These were thoroughly mixed, incubated in a boiling water bath for 15 minutes, then allowed to cool, after which they were centrifuged and their supernatants collected. The supernatant from the blank was used to zero the spectrophotometer (preset at 532nm) before reading the absorbance of the supernatant from the test solutions. The amount of TBARS was expressed as milligrams of malondialdehyde per gram of sample.

$$TBA = \frac{O.D \times V \times 1000}{A \times v \times l \times Y}$$

Where:

O.D = Absorbance of test at 532nm.

V= Total volume of the reaction mixture = 6.6mL

A= Molar extinction coefficient of the product, and according Buege and Aust (1978) is equal to $1.56x10^5$

I= Length of light path =1cm.

Y= mg of tissue in the volume of the sample used.

v= volume of tissue extract used =0.6ml

2.4.4 Cooking loss

The weight of meat was recorded before and after cooking and the loss was expressed as percentage

$$\text{Cooking loss} = \frac{\text{Weight of raw meat} - \text{Weight of cooked meat}}{\text{Weight of raw meat}} \times 100$$

2.4.5 Sensory evaluation

A total of 20 trained individuals aged between 20 and 40 years were used to assess two replicates of the prepared sausage. The samples were evaluated using a 9-point hedonic scale for flavor, colour, juiciness, tenderness, and overall acceptability The scale had a maximum score of 9 while the lowest score of 1 was assigned to the poorest condition (Mahendraker *et al.*, 1988).

2.5 Statistical Analysis

Data obtained from the experiment were analysed using the statistical analysis of variance (ANOVA) procedure of SAS 2010 and significant level of p=0.05 was used. The treatment means were compared using the New Duncan multiple range test of the same software.

3.0 RESULTS

Table 1 shows the effect of Atili-based diet on live weight and carcass characteristics of quails. The defeathered weight, eviscerated weight and carcass weight were significantly different with quails fed 5.0% Atili based diet having the highest value 94.46%, 79.54% and 67.07% respectively with least values obtained in quails fed 2.5% Atili based diet.

Table 1: Effect of Atili-based diet on live weight and carcass characteristics of quails

Parameters (g)	Control	2.50% Atili-based Diet	5.00% Atili-based diet	7.50% Atili-based diet	10.00% Atili-based diet	SEM
Live weight	153.42^{ab}	166.25^{a}	136.73^{b}	144.70^{ab}	158.37^{ab}	4.11
Bled weight	96.21	94.62	95.85	94.1	93.8	0.41
Defeathered weight	91.63^{ab}	92.17^{ab}	94.46^{a}	90.00^{b}	90.97^{ab}	0.55
Eviscerated weight	72.73^{b}	69.33^{b}	79.54^{a}	72.14^{b}	73.29^{ab}	1.11
Carcass weight	62.17^{ab}	58.51^{b}	67.07^{a}	56.02^{b}	61.30^{ab}	1.31

$^{a, b, c}$ *means with different superscripts on the same row differ significantly (P<0.05)*

SEM=Significant Error of Mean.

The effect of Atili-based diet on relative weight of offals of quails is shown in Table 2. The shank, heart, full gizzard and liver weights shows no significant differences. The head weight was significantly higher in quails fed 5.0% Atili based diet (5.23%) with least value in quails fed 2.5% Atili based diet (3.97%). The neck weight was higher in quails fed 10.0% Atili based diet (5.44%) with least value in quails fed 2.5% Atili based diet (3.58%). The intestinal weight was higher in quails fed 2.5% Atili based diet (7.10%) with least value in quails fed 5.0% Atili based diet (3.48%). Table 3 presents the effect of Atili-based diet on relative weight of primal cuts of quails. Breast, broomstick and thigh weights were significantly higher in quails fed 5.0% Atili based diet (25.62%, 6.94% and 9.69% respectively) with least values in quails fed 2.5% Atili based diet (21.38%, 5.13% and 7.59% respectively). The back and wings showed no significant difference.

Table 2: Effect of Atili-based diet on relative weight of quail offals

Parameters (g)	Control	2.5% Atili-based diet	5.0% Atili-based diet	7.5% Atili-based diet	10.0% Atili-based diet	SEM
Head weight	4.38^{b}	3.97^{b}	5.23^{a}	4.22^{b}	4.24^{b}	0.13
Neck weight	3.99^{bc}	3.58^{c}	5.18^{ab}	5.25^{ab}	5.44^{a}	0.22
Shank weight	1.64	1.49	1.84	1.68	1.73	0.05
Heart weight	0.99	0.87	1.11	0.89	0.88	0.04
Full gizzard weight	3.13	3.46	2.77	2.85	2.96	0.11
Liver weight	2.41	3.03	2.28	2.17	2.33	0.14
Intestinal weight	4.88^{ab}	7.10^{a}	3.48^{b}	5.23^{ab}	5.57^{ab}	0.38

$^{a, b, c}$ *means with different superscripts on the same row differ significantly (P<0.05)*

SEM=Significant Error of Mean.

Table 3: Effect of Atili-based diet on relative weight of primal cuts of quails

Parameters (g)	Control	2.5% Atili-based diet	5.0% Atili-based diet	7.5% Atili-based diet	10.0% Atili-based diet	SEM
Breast weight	24.23^{ab}	21.38^{c}	25.62^{a}	22.55^{bc}	24.42^{ab}	0.46
Back weight	19.84	17.71	18.68	16.09	17.95	0.54
Drumstick weight	6.22^{ab}	5.13^{c}	6.94^{a}	5.73^{bc}	5.95^{bc}	0.17
Thigh weight	8.45^{ab}	7.59^{b}	9.69^{a}	9.04^{ab}	8.76^{ab}	0.25
Wings weight	5.34	4.90	6.00	5.56	4.85	0.18

$^{a, b, c}$ *means with different superscripts on the same row differ significantly (P<0.05)*

SEM=Significant Error of Mean.

Table 4 shows the effect of Atili-based diet on meat quality of quails. Significant differences were observed for pH, water holding capacity and oxidative rancidity. Quail meat from birds fed 5.0% Atili based diet had the highest pH, water holding capacity and oxidative rancidity (7.00, 53.33% and 2.27mg/kg respectively). The cooking loss from breast, drumstick and thigh muscles showed no significant difference but quail meat from birds fed 5.0% Atili based diet had the least values for cooking loss in all the muscle types.

Table 4: Effect of Atili-based diet on quail meat quality

Parameters	Control	2.5% Atili-based diet	5.0% Atili-based diet	7.5% Atili-based diet	10.0% Atili-based diet	SEM
pH	6.87^{b}	6.90^{b}	7.00^{a}	7.00^{a}	6.90^{b}	0.02
Water holding capacity (%)	41.67^{c}	43.33^{bc}	53.33^{a}	46.67^{b}	20.00^{d}	3.04
Oxidative rancidity (mg/kg)	1.47^{b}	1.21^{b}	2.27^{a}	1.11^{b}	1.15^{b}	0.12
Breast cooking loss (%)	27.00	25.30	22.41	26.54	23.42	2.32
Drumstick cooking loss (%)	13.43	15.82	9.59	18.16	13.99	1.22
Thigh cooking loss (%)	14.50	15.28	12.37	12.67	13.06	1.63

$^{a, b, c}$ *means with different superscripts on the same row differ significantly (P<0.05)*

SEM=Significant Error of Mean.

4.0 DISCUSSION

Similar observations were seen in Table 2 for Head weight, Shank and Heart weights respectively on relative live weight of quail offals. However, relative weight of primal cuts of quails, Drumstick weight, thigh weight, breast weight and wings weight was higher in quails fed diet T3 at (5.0%) graded level of inclusion. This suggests that inclusion of Atili-based diet at 5.0% level could bridge the existing gap between the conventional feeding stuff thereby reducing the cost of over -depending on the said feeding stuff, this will result in minimizing cost of feed production and maximizing production of poultry birds as required to meet the demand of poultry meat consumption in Nigeria and other countries of the world.

The absence of variation observed in relative weight of quail carcass characteristics in Bled weight and offals (the shank, heart, full gizzard weight and liver weight), primal cuts of quails (Back weight and wings weight) could be attributed to the nutrient availability of the Atili-based diets which produced uniform sizes of the birds (P>0.05). However, significant effect (P<0.05) recorded on some parameters evaluated at different level of inclusion across the treatment may probably because the inclusion levels of the test ingredients did not reach the threshold level that could have affected the weight of the various visceral organs and cuts parts (Alu *et al.,* 2018).

There was significant variation in pH values, water holding capacity and oxidative rancidity across treatment levels. A pH of 6.87 was observed and falls within the same range value of 6.17 and 6.00 reported by some authors (Genchev *et al*.,2008). This can be attributed to equal sanitary measures during slaughter which might increase the microbial load leading to a higher pH. Cooking loss of meat from breast, drumstick and thigh muscle revealed no significant difference (P>0.05). Control diet had the highest cooking loss for breast while meat obtained from 5.0% Atili-based diet had the lower cooking loss of (22.41%). This may be seen as pH reduced the water holding capacity. Atili-based diet at 5.0% level of inclusion recorded highest water holding capacity WHC than the control diet which is in consonant with the report of Naveena and Mendiratta (2001). The water holding capacity as presented in Table 4, showed significant difference ($p < 0.05$) across the treatments. This result contradicts the finding of Samson et. al., 2019 on meat quality of Japaneses quail feed graded levels fermented mango kernel meal. Which shows that water holding capacity remain constant and indicated that quail meat has high water holding capacity. With this result, variance in nutrient composition of mango kernel meal, processing method and microbial activities could be responsible for the differences in the result of this present findings.

5.0 CONCLUSION

The carcass evaluation and meat quality of Japanese quails fed (Atili-based) diet in this experiment shows that the birds assigned 5.0% based diet recorded highest values and produced reasonable meat quality which is associated with De-feathered weight, eviscerated weight and carcass weight.

Conceptualization, Oshibanjo D.O.; methodology, Oshibanjo D.O.; investigation, Oshibanjo D.O., Adelowo V. O., Okpara Jude Obi, Adediran O. A.; data curation, Oshibanjo D.O; writing—original draft preparation, Oshibanjo D.O; writing—review and editing, Adediran O. A.; project administration, Oshibanjo D.O.. All authors have read and agreed to the published version of the manuscript.

CONFLICT OF INTEREST

The authors declare that there are no conflicts of interests.

REFERENCES

Abbas, T.E. (2013). The use of Moringa oleifera in poultry diets. *Turkish Journal of Veterinary and Animal Science*. 37: 492-496

Adelowo, O. V., Oshibanjo, D. O., Olaiya, O. D., Banjo, A. A., & Machen, M. J. 2019. Effects of Feeding Roasted Canarium schweinfurthii Seed Meal on Performance and Carcass Characteristics of Broiler Chicken. Asian Journal of Research in Animal and Veterinary Sciences,4(2), 1-6. Retrieved from http://www.journalajravs.com/index.php/AJRAVS/article/view/30060

AOAC 2000. Association of Official Analytical Chemistry Official Methods of Analysis of AOAC international (17th ed.). MD, USA.

Bahşi, M., Çiftci, M., Simsek, Ü.G., Azman, M.A., Özdemir, G., Yilmaz, Ö. & Dalkilic, B., 2016. Effects of olive leaf extract (oleuropein) on performance, fatty acid levels of breast muscle and some blood parameters in Japanese quail(Coturnix coturnix Japonica) reared in different stocking densities. Vet. J. of Ankara Univ. 63, 61-68. http://vetjournal.ankara.edu.tr/tr/download/article-file/657231

Buege, J.A., and Aust, S.D. 1978. Microsomal lipid, Peroxidation. In: Flesicher, S., Packer, L. (Eds.), Methods in Enzymology. Vol. 52. Academic Press, New-York, pp. 302–310

Genchev A. Mihaylov R. Ribarski S. Pavlov A. and Kabakchiev M. 2008. Slaughter analysis protocol in experiments using Japanese quails (Coturnix japonica). *Trakia Journal of Science* 6:66–71.

Govaris, A., Solomakos, N., Pexara, A. and Chatzopoulou, P. S. 2010. The antimicrobial effect of oregano essential oil, nisin and their combination against Salmonella enteritidis in minced sheep meat during refrigerated storage. Int. J. Food Microbiol. 137, 175-80.

Gueye, E.F. and Branckaert, R.D.S. 2002. FAO's programme for support to family poultry Production. Proceedings of a workshop on poultry as a tool in poverty eradication and promotion of gender equality,Animal production and Health Division, FAO, Rome, Italy.

Keay, R.W.J., 1989. Trees of Nigeria. Oxford Science Publication, New York, ISBN: 0-19-854560-6, Pages: 476

Lillehoj, H. Liu, Y.. Calsamiglia, S Fernandez-Miyakawa, M.E. Chi, F.. Cravens R.L, Oh, S. and Gay C.G. 2010. Phytochemicals as antibiotic alternatives to promote growth and enhance host health Vet. Res., 49 (2018), p. 76

Mahendrakar, N.S., Khabade, U.S and Dam, N.P (1988). Studies on the effect of fatting on carcass characteristics and quality of meat from Bannur lambs. *J. Food Sci. Tech.25: 225-231.*

Mujić A., Grdović N., Mujić I., Mihailović M., Živković J., and Poznanović G. 2011. Antioxidative effects of phenolic extracts from chestnut leaves, catkins and spiny burs in streptozotocin-treated rat pancreatic β-cells. *Food Chem.* 125 841–849. 10.1016/j.foodchem.2010.08.068

Mujić I., Zeković Z., Lepojević Ž, Vidović S., and Živković J. 2010. Antioxidant properties of selected edible mushroom species. Journal of Central European Agriculture, 11/4: 387–39.

National Research Council. Nutrient Requirements for Poultry. 9 rev. edn. National Academy Press, Washington DC. 1994.

Naveena B.M. and Mendiratta, S.K. 2001. Tenderization of spent hen meat using ginger extract *Br. Poult. Sci.,* 42 (2001), pp. 344-349.

NRC, 1994. Nutrient requirements of poultry. 9th edition. National Academy Press. Washington DC, USA.

Samson, Kyakma S., Idu Gibson and Wilson M. 2019, Meat Quality of Japanese Quail (Coutonix CoutonixJapanica) Fed Graded Levels of Fermented Mango Kernel Meal. *International Journal of Environment, Agriculture and Biotechnology* (IJEAB) Vol-4, Issue-3, Page | 602. http://dx.doi.org/10.22161/ijeab/4.3.3

Wardlaw, F.B., Maccaskill, L.H. and Acton, J.C. 1973. Effect of postmortem muscle changes in poultry meat loaf properties. Journal of Food Science, 38, 421–424.

Detection, Identification and Management of Seed-borne fungal Pathogens on farmer saved Soybean (*Glycine max* (L.) Merrill) seeds in Ghana

Ansah, A. F.[1, 3], Ofoe, R.[1, 2], Osabutey, S.[1], Darkwa, E.[1], Tongoona, B. P.[1], and Eleblu, J. S. Y[1, 2*]

[1]West Africa Centre for Crop Improvement, University of Ghana, Legon, Ghana.
[2]Biotechnology Centre, University of Ghana, Legon.
[3]Savanna Agricultural Research Institute, Council for Scientific and Industrial Research, Tolon Rd, Nyankpala.

***Corresponding author:** jeleblu@wacci.ug.edu.gh

ABSTRACT

Soybean is infected by a wide range of diseases, many of which are seed-borne. Infection by seed-borne pathogens leads to seed rot, low seed germination, low seedling vigour and reduced plant growth as well as marketability. This study investigates seed-borne fungal pathogens that are associated with farmer saved soybean seeds and identify best seed treatment for controlling them to enhance seed quality. Seed-borne fungal pathogens on farmer-saved seeds of soybeans was investigated by examining a total of eleven (11) seed samples from two districts (Saboba and Yendi) in the Northern region and one from CSIR-Savanna Agricultural Research Institute (CSIR-SARI). A total of nine fungi genera were identified to be associate with the soybean seeds including pathogenic *Cercospora spp., Alternaria spp., Fusarium spp., Macrophomina phaseolina* and saprophytic *Aspergillus flavus, Aspergillus niger, Penicillium spp., Curvularia spp.* and *Rhizopus stolonifer. Rhizopus stolonifer* (21.5%) and *Aspergillus niger* (7.0%) revealed the highest and lowest prevalence respectively. Treatment of soybean seeds with Monceren GT 390 FS, Insector T 45, Garlic extract and Neem seed extract over a period of 90 days resulted in a decrease in fungal prevalence as well as improved seed germination and seedling vigour. Pot experiment conducted to determine pathogenicity of *Microphomina phaseolina, Cercospora spp., Aternaria spp.* and *Fusarium spp.* proved to be pathogenic. These findings indicate that farmers saved soybean seeds in Ghana is fungal infected and seed treatment alleviates the destructive effect of these microbes, thus enhancing seed quality and promoting food security in Ghana.

Keywords: Pathogens, Seed-borne, pathogenicity

1.0 INTRODUCTION

Soybean (Glycine max (L.) Merrill) is an important legume crop, cultivated in the tropical, subtropical and temperate climates (Shurtleff and Aoyagi 2007; IITA, 2009). The world production is 318.95

million metric tonnes with 89% from Argentina, Brazil, United States and China (FAO, 2014). In Africa, South Africa is the leading producer of 948,000 MT followed by, Nigeria (679,000), Zambia (214,179), Malawi (120,903) and Zimbabwe (74,951) (FAO, 2014). Moreover, soybean production in Ghana is mainly in the Northern, Upper West, Upper East, Central and Volta regions where Northern region is the major production area (Lawson et al., 2008) which contributes to about 77% of the national production (SRID, 2012). Soybean is an excellent source of major nutrients, about 40% protein, 30% carbohydrate, 20% oil and varying levels of vitamins and minerals, including calcium, folic acid, and iron (Sauvant et al., 2004; Lakshmeesha et al., 2013).

Locally, it can be processed into many food products such as wean mix, soy 'khebab', 'apapransa', soymilk, 'koose', stew, and 'tubani' (Mbanya, 2011). However, like other grain legumes, its production is significantly constrained by abiotic and biotic stresses. Among these stresses, diseases are the major limiting factor against the vast global production of which many are seed-borne (Lakshmeesha et al., 2013). More than 100 pathogens including over thirty fungi and six bacteria are known to be seed-borne pathogens of soybean (Kulik and Sinclair, 1999a; Roy et al., 2000). Infection by seed-borne pathogens results in seed rots, poor germination, reduction in seedling vigour, plant growth and crop productivity (Kubiak and Korbas, 1999; Dawson and Bateman, 2001; Akranuchat et al., 2007). Several studies have reported species of seed-borne pathogens that are associated with soybean in different ecological zones and different approaches have been employed globally to mitigate the destructive effect of these pathogens and ensure quality yield (Ramannuj et al., 2014; Oladimeji et al., 2016). Efforts made include breeding for disease resistant varieties, use of biological agents, crop management, and the use of seed treatment. Moreover, in Ghana, not much studies have been reported on seed-borne fungal pathogens that are associated with soybean. In view of this, investigating and providing information on seed-borne fungal pathogens that are associated with farmer saved soybean seeds and identifying the best seed treatment in controlling them will enhance seed quality, thus promoting global food security. This study aims to detect and identify seed-borne fungal pathogens associated with farmer saved soybean seeds and asses the effect of different seed treatments on fungal growth, seed germination and seedling vigour.

2.0 MATERIALS AND METHODS

2.1 Experiment site and Seed Collection

The research was conducted at the Seed Laboratory of Ghana Seed Inspection Directorate, Pokuasi, Plant Pathology Laboratory and the Research field of Department of Crop Science, University of Ghana, Legon.

Soybean seeds were randomly sampled from farmers within ten communities in two districts in the Northern region of Ghana. These communities include Nalog Tindando, Gbadagbam, Garimata Yankazia, Zang, Kanisheigu, Zangban, Gumbaliga and Sunsong-Gbung. A check sample was obtained from the CSIR-Savanna Agricultural Research Institute. Seeds were kept in plastic bags and stored in a cold room at a temperature of 4°C prior to seed health test and treatment application.

2.2 Isolation and detection of Fungal Pathogens

Isolation of seed-borne fungal pathogens was performed using the blotter and agar plate methods described by ISTA (2007) and Mathur and Kongsdal, (2003) respectively with slight modification. For the blotter method, three sets of blotter papers were moistened with a sterilized distilled water and lined in 90 mm diameter petri plates. Seeds were surface sterilized with 1% sodium hypochlorite for 1 minute and rinsed three times with sterilized distilled water. A Completely Randomized Design (CRD) was used with four replications. 200 seeds from each sample were used with 50 seeds per replicate. Ten seeds were plated per petri plate using a pair of forceps and incubated at 24 ± 2°C for 7 days. Fungi isolates that associates with the seeds were culture onto a Potato Dextrose Agar (PDA) medium and incubated 24 ± 2°C for 7 days depending on the sporulation nature of the fungi. Fungi isolates were sub-culture thrice to obtained pure culture for easy identification. Culture morphologies such as the colour, shape and growth rate were also used in the identification. Each isolate was prepared on a slide, examined under a compound microscope and identity confirm with the aid of a mycological literature.

2.3 Pathogenicity test

Pathogenicity test was conducted for four fungal isolates to confirm their identity following Koch's postulate. Spore suspension of Cercospora spp., Alternaria spp., Fusarium spp., and Macrophomina phaseolina were prepared from two weeks old sporulated culture and inoculated onto a four weeks old soybean plants. Control plants were sprayed with distilled water and disease development was observed after 2 weeks.

2.4 Seed Treatment

Highly fungi infected seed samples were treated with Monceren GT 390 FS, Insector T 45, Neem seed (Azadirachta indica) extract and Garlic (Allium sativum) extract (Table 1). Neem seed extract was prepared following modification of method described by Adjei (2011). Garlic extract was prepared by blending gloves to form a paste. Fifty percent (50%) concentration of both garlic and neem extracts were prepared by adding fifty grams of the

the paste to 100 ml of distilled water and filtered with four layers of clean cheese cloth into a conical flask.

Table 1: Treatments composition and application rate

Treatments	Active ingredient	Rate of application
Insector T 45	Imidacloprid 350g/kg + Thiram 100g/kg	5g/kg
Moncern GT 390 FS	20% Imidacloprid and 20% Pencycuron	2.5 ml/kg
Neem seed extract	Azadirachtin	100 ml/kg
Garlic extract	Allicin	100 ml/kg
Untreated control	N/A	N/A

2.5 Treatment application

Seed treatment with garlic and neem seed extracts were performed by applying 10 mL extract to 100 g seeds in a zip lock bag, shaken vigorously for evenly distribution and incubated for 20 minutes. The seeds were dried under shade on a surface transparent plastic bag for 30 minutes. A 2.5 mL of Monceren GT 390 FS was used for seed treatment at a rate of 1 kg of the seed weight, and 5 g of Insector T 45 was used to treat 1 kg of seeds. Both treated and untreated seeds were kept in a zip lock bags and stored in a cold room at 4°C over a period of three months. Seeds were assessed monthly for a three months period. The prevalence of fungal pathogens were calculated using the formula below:

$$\text{Percentage prevalence of individual fungal} = \frac{\text{Number of infected seeds by individual fungi}}{\text{Total number of seeds planted}} \times 100\%$$

2.6 Seed germination and seedling vigour Assessment

Germination and seedling vigour test were conducted before and after seed treatments. Germination test was performed following the sand method (ISTA, 2007) by sowing 400 seeds in seed trays with 100 seeds per replicates and grown in a growth room with temperature of 22°C. Germination count, dead seeds as well as normal and abnormal seedlings were evaluated on the 8th day and germination percentage determined using the formula below.

Germination count, dead seeds as well as normal and abnormal seedlings were evaluated on the 8th day and germination percentage determined using the formula below.

$$\text{Germination percentage (\%)} = \frac{\text{Number of germinated seeds}}{\text{Total number of seeds planted}} \times 100\%$$

For vigour test, 10 seedlings were randomly selected from each treatment and their lengths measured. Seedling vigour index was calculated using the formula below described by (Oshone et al., 2014; Khan et al., 2015). Seedling vigour index = Mean seedling length (cm) × Germination percentage (%).

2.7 Statistical analysis

Data obtained including incidence of seed-borne fungi, germination percentage and seedling vigour were subjected to analysis of variance (ANOVA) using GenStat (12th Edition) and the differences between means were separated using the Least Significance Difference (LSD) at 5% level of probability. Data on fungi prevalence were Arcsine transformed to stabilize the variance before analysis.

3.0 RESULTS

3.1 Detection and identification of Seed-borne Fungal Pathogens on Soybean Seed Samples obtained from CSIR-SARI, Saboba and Yendi District of Ghana

In order to identify the fungal isolates that associates with saved-soybean seeds, sample seeds were plated on a moist blotter paper and PDA. A total of nine seed-borne fungal pathogens were isolated from the soybean seed samples obtained from the different locations (Table 2; Table 3, Figure S1). Among these nine fungi isolated, four are pathogenic fungi species (*Cercospora* spp., *Alternaria* spp., *Fusarium* spp., *Macrophomina phaseolina)* and five are saprophytic species (*Aspergillus flavus, Aspergillus niger*, *Penicillium* spp., *Curvularia* spp. and *Rhizopus stolonifera)* (Figure S1) suggesting that both class of fungi are associated with the soybean seed samples. Moreover, In Saboba district, three (*Rhizopus stolonifer*, *Fusarium* spp. and *Aspergillus niger*) were isolated from all five seed samples obtained in all the communities (Table 2). However, Penicillium spp., Cercospora spp. and Macrophomina phaseolina were isolated from seed samples from four seed samples and Alternaria spp. Curvularia spp. and Aspergillus flavus were isolated from three seed samples. Furthermore, seed health test conducted on seed samples obtained from Yendi district revealed that 6 fungal pathogens including Rhizopus stolonifer, Fusarium spp., Aspergillus flavus, Aspergillus niger, Macrophomina phaseolina, and Curvularia spp. were associated with all the seed samples (Table 3).

Table 2: Prevalence of Fungal Pathogens on Seed Samples obtained from Saboba District and CSIR-SARI

Fungal Pathogens (%)	Communities					
	Nalong	Tindando	Gbadagbam	Garimata	Yankazia	CSIR-SARI
Alternaria spp.	10.7	9.0	12.2	-	-	11.7
Aspergillus flavus	9.0	-	10.5	9.8	-	11.5
Aspergillus niger	10.5	12.6	12.0	7.8	9.8	9.6
Cercospora spp.	9.0	10.5	-	9.3	11.9	9.8
Curvularia spp.	9.8	9.0	-	12.6	-	-
Fusarium spp.	14.1	12.8	13.2	14.6	15.2	9.8
Macrophomina phaseolina	-	13.4	12.0	8.5	12.2	9.0
Penicillium spp.	12.0	7.0	9.0	-	9.9	-
Rhizopus stolonifer	17.4	17.9	18.4	17.8	21.5	16.9
LSD ($p<0.05$)	2.9	3.9	3.2	5.7	4.3	3.0

Moreover, In Saboba district, three (Rhizopus stolonifer, Fusarium spp. and Aspergillus niger) were isolated from all five seed samples obtained in all the communities (Table 2). However, Penicillium spp., Cercospora spp. and Macrophomina phaseolina were isolated from seed samples from four seed samples and Alternaria spp. Curvularia spp. and Aspergillus flavus were isolated from three seed samples. Furthermore, seed health test conducted on seed samples obtained from Yendi district revealed that 6 fungal pathogens including Rhizopus stolonifer, Fusarium spp., Aspergillus flavus, Aspergillus niger, Macrophomina phaseolina, and Curvularia spp. were associated with all the seed samples (Table 3). Besides, Cercospora spp. was isolated from three seed samples, while Penicillium spp. was isolated from two seed samples (Table 3) and seed samples obtained from CSIR-SARI were found to be associated with seven fungi pathogens (Table 2). Also, there were significant ($p<0.05$) difference among fungal prevalence which suggest that fungi prevalence is community specific. However, there were no differences among prevalence of *Cercospero spp., Alternaria spp., Fusarium spp., Macrophomina phaseolina, Aspergillus flavus, Aspergillus niger.*

The highest fungal prevalence was revealed on *Rhizopus stolonifer* (16.9%), Alternaria spp. (11.7%), *Aspergillus flavus* (11.5%). *Fusarium spp.* and *Cercospora spp*. also with prevalence of 9.8% each, while Aspergillus niger, and *Macrophomina phaseolina*, had 9.6% and 9.0% respectively. However, *Penicillium spp.* and Curvularia spp. fungal pathogens were not associated with the seed sample.

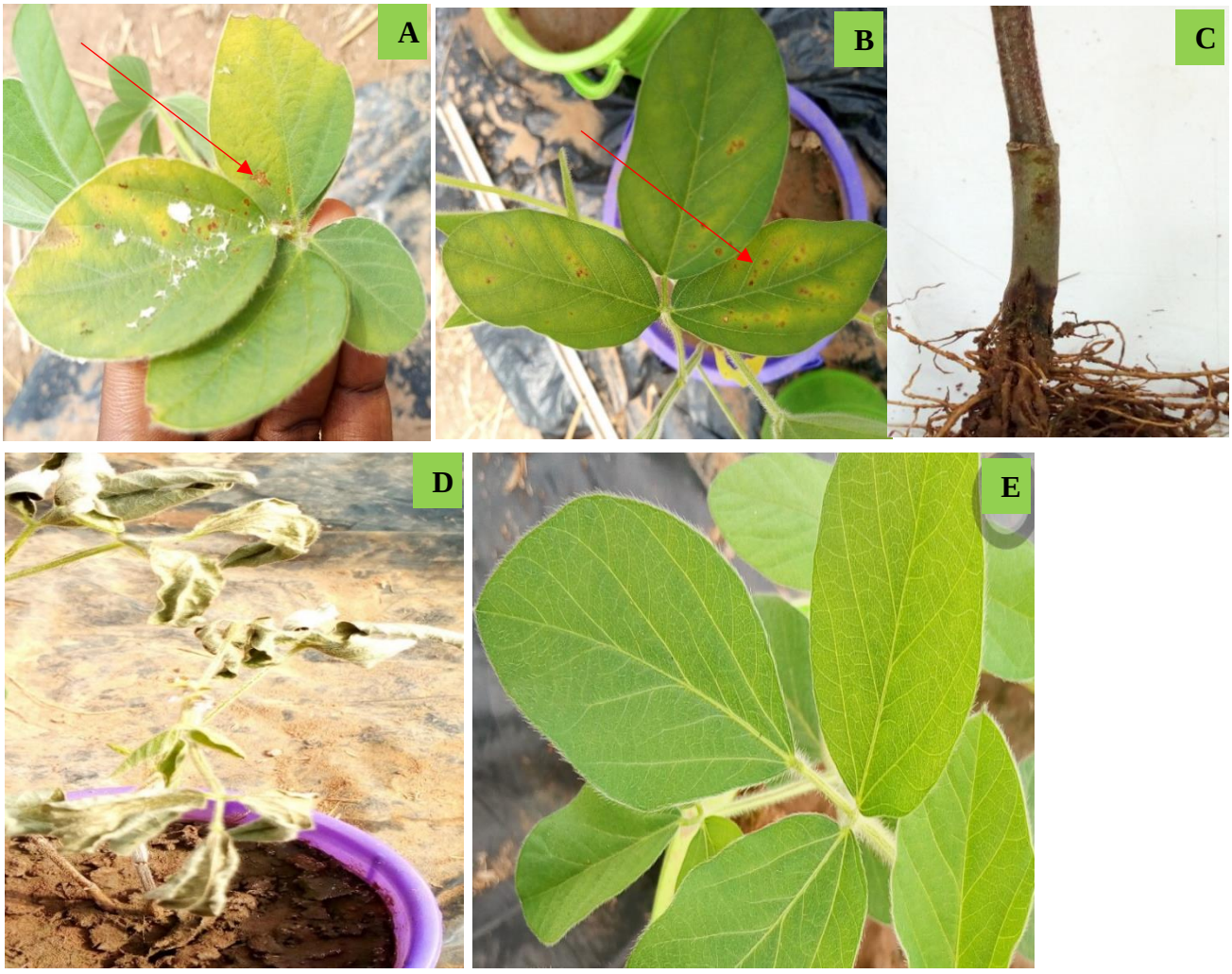

Figure 1: Soybean seedlings showing infection of the various pathogenic fungi: (A) Leaf spot (*Cercospora* spp.), (B) Leaf spot (*Alternaria* spp.), (C) rot (*Macrophomina phaseolina)*, (D) Post-emergence death (*Fusarium* spp.), (E) Negative control. The red arrows indicate symptoms of the various isolates.

3.2 Pathogenicity Test of Four Fungal Isolates on Soybean Plants

To confirm whether the isolated pathogens infect soybean plants, a 4-week-old soybean plants were inoculated with four different fungal isolates. The pathogenicity test revealed that all inoculated plant developed disease symptoms a week after inoculation compared with the control (Figure 1). Re-isolation tests revealed that, inoculated fungal isolates were the causal organism of the observed disease symptoms on the plants as all plants samples had a degree of chlorosis, lesions (spot) and wilt.

Table 3: Prevalence of Fungal Pathogens on Seed Samples obtained from Yendi District

	Communities				
Fungal Pathogens (%)	Zang	Kanisheigu	Zangban	Gumbaliga	Sunsong-Gbung
Alternaria spp.	14.2	13.2	8.5	-	10.5
Aspergillus flavus	12.9	12.2	9.9	9.8	11.5
Aspergillus niger	13.5	8.5	10.7	7.0	12.0
Cercospora spp.	11.4	8.1	-	10.5	-
Curvularia spp.	9.8	12.6	10.7	13.2	9.3
Fusarium spp.	11.4	12.0	11.9	12.6	15.2
Macrophomina phaseolina	12.0	10.5	7.8	12.9	13.2
Penicillium spp.	14.1	10.5	-	-	-
Rhizopus stolonifer	18.8	17.9	18.4	19.7	17.8
LSD ($p<0.05$)	3.0	5.7	5.6	4.0	4.5

3.2 Effect of Seed Treatments on Seed-borne Fungal Pathogen

To further evaluate the effect of various treatments on the identified seed-borne fungal pathogens, seeds were subjected to different treatments. Seed treatments were able to reduce fungal prevalence in the seed sample when treated and stored over a period of 90 days. There was a significant ($p<0.05$) differences among fungi prevalence when seeds were treated with Monceren GT 390 FS and stored over a period of 90 days (Table 4). Moreover, the prevalence of *Alternaria spp., Aspergillus flavus, Aspergillus niger, Cercospora spp. Curvularia spp., Macrophomina phaseolina* and *Penicillium spp.* did not show any significant difference and

Table 4: Prevalence of Fungal Pathogens after Treatment and Storage for 90 days

	Seed Treatments				
Fungal Isolates (%)	Monceren GT 390 FS	Insector T 45	Neem Seed Extract	Garlic Extract	Untreated Seeds
Alternaria spp.	4.1	5.3	5.3	9.1	19.4
Aspergillus flavus	4.1	4.1	5.3	7.8	16.9
Aspergillus niger	4.1	4.1	4.1	6.6	16.4
Cercospora spp.	4.1	5.3	5.3	6.6	16.4
Curvularia spp.	4.1	4.1	4.1	7.4	17.4
Fusarium spp.	5.3	4.1	6.6	7.8	16.3
Macrophomina phaseolina	4.1	4.1	6.6	5.3	18.4
Penicillium spp.	4.1	5.3	4.1	5.3	16.9
Rhizopus stolonifer	10.7	9.1	7.8	11.5	21.5
LSD ($p<0.05$)	1.5	2.1	3.1	3.8	2.4

their prevalence were reduced to 4.1% each compared with untreated seeds (Table 4). *Fusarium* spp. and *Rhizopus stolonifer* also revealed a prevalence of 5.3% and 10.7% respectively, while the untreated had 16.3% and 21.5% respectively (Table 4). Furthermore, seed treated with Insector T 45 over a period of 90 days recorded a significant ($p<0.05$) reduction on fungal prevalence. The prevalence of *Aspergillus flavus, Aspergillus niger, Curvularia* spp., *Fusarium* spp. and *Macrophomina phaseolina* were reduced to 4.1% each compared with the untreated seeds (Table 4), while prevalence of *Rhizopus stolonifera* was reduced from 21.5% in untreated seed to 9.1%. Although, there was no significant ($p>0.05$) difference among fungal prevalence when seeds were treated with neem seed extract for a period of 90 days, the prevalence of *Aspergillus niger*, *Penicillium* spp. and *Curvularia* spp. were reduced to 4.1% each compared with the untreated seeds which observed an increase prevalence of 16.4%, 16.9% and 15.4% respectively (Table 4). Similarly, *Alternaria* spp., *Aspergillus flavus* and *Cercospora* spp. revealed a prevalence of 4.1% each, while *Fusarium* spp. and *Macrophomina phaseolina* both observed a prevalence of 6.6% (Table 4). Seeds treated with garlic extract and stored

for a period of 90 days revealed no significant ($p>0.05$) difference among fungi prevalence (Table 4). Both *Macrophomina phaseolina* and *Penicillium* spp. revealed the least (5.3%) prevalence, while the untreated seeds revealed 18.4% and 16.9% respectively.

3.3 Effect of Seed Treatments on Germination and Seedling Vigour of Soybean Seeds

To determine the efficacy of seed treatment on the seed health, germination and seedling vigour test were perform prior to treatment and after 30, 60 and 90 days of seed treatment and storage. Results obtained showed a significant ($p<0.05$) difference on germination percentage and seedling vigour among the seed samples. In the Saboba district, germination percentage of seed samples obtained from Nalong, Tindando and Yankazia did not show any differences (Table 5). The highest germination was revealed on seed samples obtained from Garimata (79.8%) while Nalong and Yankazia revealed the least with 76.8% each (Table 5). Similarly, there were differences among seed samples obtained from the Yendi district (Table 5). Seed sample obtained from Zangban observed the highest germination (78%), while the lowest was observed on seed sample obtained from Zang with 71.3%. With respect to seedling vigour, seed samples obtained from Tindando (1114.3) and Yankazia (1034.2) in the Saboba district recorded the highest and lowest seedling vigour respectively. However, Zangbang (1092.0) and Zang (892.6) in the Yendi district recorded the highest and lowest seedling vigour respectively.

Table 5: Germination Percentage and Seedling Vigour on Seed Samples obtained from CSIR-SARI, Saboba and Yendi Districts

Locations	Communities (Samples)	Germination Percentage (%)	Seedling Vigour Index
	Nalong	76.8	1047.7
	Tindando	77.3	1114.3
Soboba	Gbadagbam	78.0	1092.1
	Garimata	79.8	1098.6
	Yankazia	76.8	1034.2
	Zang	71.3	892.6
	Kanisheigu	75.0	1020.0
Yendi	Zangban	78.0	1092.0
	Gumbaliga	73.3	1062.2
	Sunsong-Gbung	74.3	1007.9
CSIR-SARI	CSIR-SARI	78.8	1145.8
LSD ($p<0.05$)		1.4	45.7

The various seed treatment showed an increased in seed germination and seedling vigour for the period 30, 60 and 90 days of treatment and storage (Figure 2, Figure 3). However, there was a significant ($p<0.05$) increase in germination and seedling vigour when treated and stored over a period of 90 days. Monceren GT 390 FS seed treatment increased seed germination from 60.8% in untreated seed to 85% (Figure 2), while seedling vigour increased to 1360.1 (Figure 3). Furthermore, Insector T 45 seed treatment was able to increase seedling vigour from 732.2 in untreated seeds to 1360.1. Neem seed extract revealed an increase in germination and seedling vigour. Germination was increased to 75% after 90 days of seed treatment and storage. Meanwhile, seedling vigour was increased to 1107.5 (Figure 3). It was observed that seed treated with garlic extract and stored for a period of 90 days obtained a high germination of 75.5% (Figure 2) and seedling vigour of 1070.2 (Figure 3).

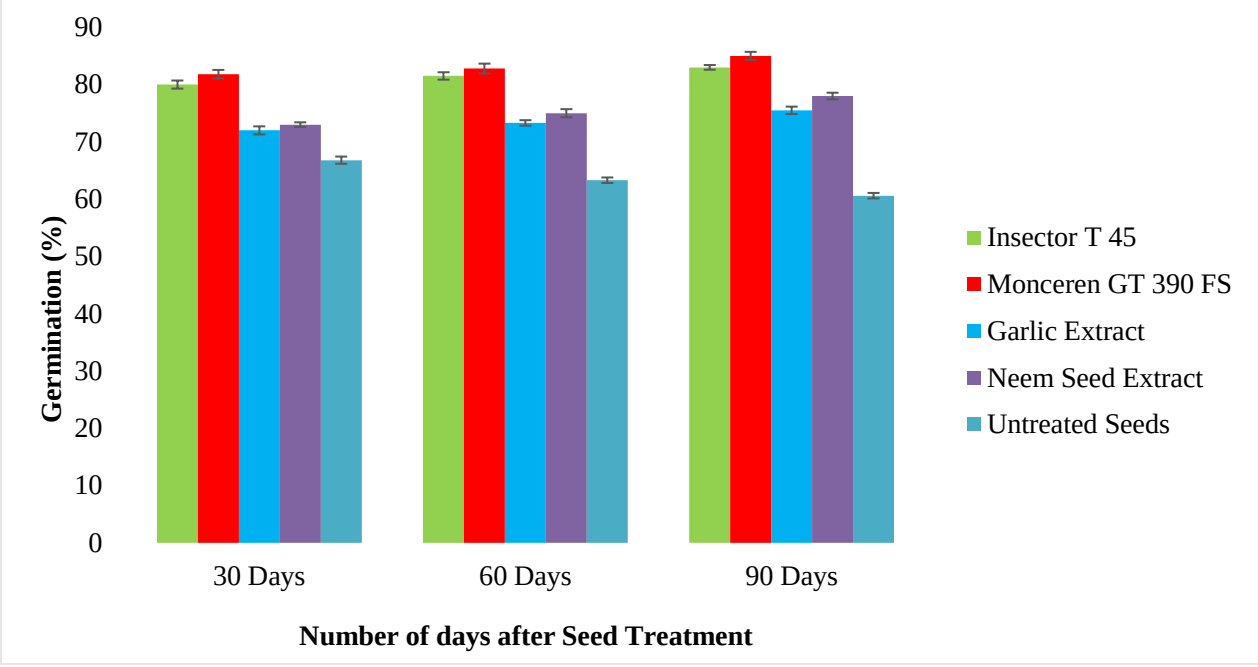

Figure 2. Effect of seed treatments on germination after storage for 90 days period

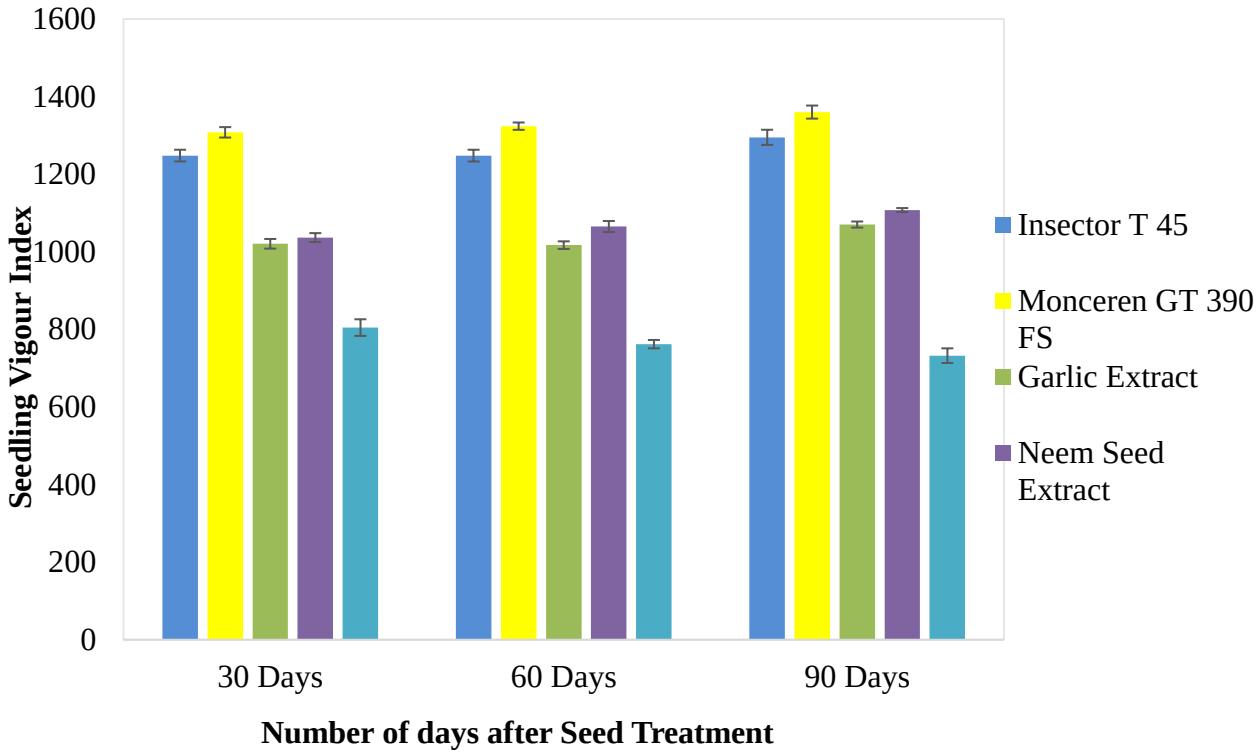

Figure 3. Effect of seed treatments on seedling vigour after storage for 90 days period

4.0 DISCUSSION

Soybean production is significantly constrained by diseases of which seed-borne pathogens are a threat to the attainment of food security in sub Saharan Africa (Lakshmeesha *et al.*, 2013; Gao *et al*., 2014). Seed quality and health examination indicates that all eleven seed samples were found to be associated with eight fungal genera, comprising of four pathogenic; *Cercospora* spp., *Alternaria* spp., *Fusarium* spp., *Macrophomina phaseolina*, and five saprophytic *Curvularia* spp., *Aspergillus niger*, *Aspergillus flavus*, *Rhizopus stolonifer* and *Penicillium* spp. *Rhizopus stolonifera*. Moreover, prevalence of fungal pathogen varied across location except for *Fusarium* spp. and *Aspergillus niger* which were found on all seed samples obtained from the different locations suggesting that the prevalence of fungi pathogen is location specific and that trade and/or transport of infected seeds could enhance the prevalence pathogens in new areas (Anderson *et al*, 2004). This variation could be as a result of the different farming practices which contributes to increase in pathogens (Pickett and Pruitt, 1989).

The prevalence of Rhizopus stolonifer, Penicillium spp., Aspergillus flavus, Aspergillus niger and Curvularia spp. could be attributed to poor storage and environmental conditions (Gupta et al., 1993, and Anwar et al., 1995). The fungal pathogens that were isolated from the seed samples have been reported to be associated with soybean seeds by several authors (Moss and Smith, 2006; Shovan et al., 2008; Ramesh et al., 2013; Ibrahim, 2015; Venugopal et al., 2015). Furthermore, all seed treatments suppress the prevalence of the pathogens that were associated with soybean seeds. Reduction in fungal prevalence by the individual seed treatment could be attributed to the effect of the active ingredients in reducing the primary source of disease inoculum in the seeds (Amare et al., 2014).

Seed treated with fungicide revealed a reduction in pathogen severity (Scherm et al., 2012). This show the effectiveness of the various treatments because each treatment was able to reduce the fungal population which suggest that these chemicals can prolong the storability of soybean seeds. Interestingly, seed samples treated with Monceren GT 390 for a 90-day period was very effective in reducing Alternaria spp., Aspergillus flavus, Aspergillus niger, Cercospora spp. Curvularia spp., Macrophomina phaseolina and Penicillium spp. to a lower prevalence due to the active ingredient (Imidacloprid and Pencycuron) inhibiting fungal inoculum (Table 4). All fungal pathogens were reduced to a lower prevalence when seeds were treated with Insector T 45 (Table 4) which could be due to the effect of the active ingredient (Imidacloprid and Thiram) in reducing fungal inoculum. Thiram has been reported to be effective in suppressing pre- and post–emergence of damping-off where cultivars were artificially inoculated with Fusarium graminearum Group 1 (Lamprecht et al., 1990). Similarly, Solanke et al., (1997) detected that pre- and post-emergence mortality caused by Aspergillus spp., F. moniliforme, Curvularia lunata, A. alternate and Penicillium spp. were controlled using thiram. Interestingly, combination of thiram and procloraz application suppresses mycelial growth of some Fusarium species (Song et al., 2004) and that of thiram and carboxim effectively reduced Gaeumannomyces zeae (Southwell et al. 2003). In this study, neem seed extract was effective in managing the fungal pathogens that were isolated (Howlader, 2003).

The reduction of these pathogens could probable be the azadirachtin property in the neem seed extract proven to inhibit the incidence of Fusarium moniliforme and other seed-borne fungal infections in sorghum (Masum et al., 2009). Similarly, Macrophomina phaseolina associated with seeds were controlled with neem extract (Dubey *et al*., 2009; Javaid and Saddique, 2011). Mondall *et al*., (2009) also reported that seed treatment with garlic extract, neem, gagra, vatpata, Bishkatali leaf extracts reduced seed-borne prevalence and increased germination percentage of wheat seeds.

Germination and seedling vigour analysis that

Germination and seedling vigour analysis revealed that all seed treatment improved seed germination and seedling vigour compared with untreated seed (Figure 2, Figure 3) due to the effectiveness of the active ingredients in the treatments (Mancini and Romanazzi, 2014). Higher germination recorded could be an indication that the treatments protected the seedling against phytopathogens (Taye et al., 2013). Increased in seed vigour index in treated seeds of tomato, rice, castor and chickpea seeds has been reported (Jamadar and Chandrashekar, 2015; Patil et al., 2015). Germination percentage and seedling vigour of seeds treated with Monceren GT 390 FS increased compared with the untreated at the end of the 90 days. This increment observed could be attributed to the reduction in fungal prevalence by the seed treatment. Similarly, Patil et al. (2015) and Sivparsad et al. (2014) reported that seed treatment of sesame and chickpea seeds increased germination percentage similar to that observed in this current study. Seeds infected with pathogens may result in poor seed germination and seedling vigour as untreated seeds are mostly infected with pathogens resulting in poor seed germination and seedling vigour. Besides, seed-borne pathogens such as Curvualria lunata and Fusarium spp. have been reported to cause reduction in seed germination in pearl millet cultivar (Ijaz et al., 2001). Seed treated with Insector T 45 resulted in significant increase in germination and seedling vigour compared to untreated seeds. Seed treated with thiram has proved to be effective in improving maize viability and emergence (Pinto, 1997) and increased germination and emergence of pea seeds by 33% and 29% respectively (Xue, 2003). High germination percentage and emergence were recorded on maize seeds treated with combined thiram and carboxim (Southwell et al., 2003). Seed treatment with garlic extract enhanced effective control seed-borne fungal pathogens and improved germination from 60.65% in untreated to 75.5% in treated seeds as well as seedling vigour. Garlic contains an active ingredient called allicin, which serves as a precursor for biosynthesis of sulphur compounds including ajoene, allyl sulfides, and vinyldithiins (Koscielny et al., 1999). Scientifically, garlic has been confirmed as a natural antibiotic, antiviral and antifungal agent (Michelle, 2003). Allicin in garlic extract suppress rice seed-borne pathogens (Mansur et al., 2013) and application of garlic extract reduced Bipolaris sorokiniana and Drechslera tritici-repentis infection on two wheat cultivars (Perelló et al., 2013). Mansur et al. (2013) reported an increase germination of rice seeds treated with garlic extract from 67.68% in untreated to 91.67% in treated seeds. However, low germination percentage recorded on untreated seeds could be as a result of the high fungal infection (Islam and Monjil, 2016a). The pathogenicity test revealed that four fungal isolates inoculated onto the plants proved to be pathogenic as all inoculated plants developed

disease symptoms of the individual fungal isolate. Re-isolation of fungal pathogens from diseased plants confirmed that these fungi were the causal organism of the observed symptoms. Soybean plants inoculated with Macrophomina phaseolina developed symptoms such as leaf spots, wilting and defoliation. Lower stems of infected plants also showed brown lesions, with black strips when cut open. Similar results have been reported, when pathogenicity test was conducted on adzuki bean with isolate of Macrophomina phaseolina (Gupta and Chauhan, 2005; Sun et al., 2015; Mishra, 2017). The adzuki bean showed symptoms of leaf chlorosis, wilting, stunted growth, withering, dried leaves as well as dark microsclerotia on the stem. Also, plants inoculated with isolate of Alternaria spp. exhibited symptoms of chlorosis, dark brown lesions on the leaves and ultimately infected leaves withered and dropped. Similar result was reported by Carla (2013), who observed brown spot and small brown lesion on the basal leaves of potato plants when inoculated with Alternaria alternate resulting in premature leave drop. Nayyar et al., (2017), also observed similar result on sesamum indicum. A. solani has been reported to cause premature defoliation when the entire leaf lamina became necrotic, even in the absence of petiole lesions (Vloutoglou and Kalogerakis, 2000). A. macrospora has been reported to cause premature defoliation which affected yield (Spross-Blickle et al., 1989). Furthermore, plants inoculated with inoculum of Cercospora spp. showed symptoms of leaf chlorosis and lesions on the leave surfaces resulting in wilting and defoliation. This study agrees with reports by Poornima (2010), who observed symptoms of brown to dark brown spots on the upper leaves of Betavulgaris during a pathogenicity test conducted using isolates of Cercospora beticola. In the same way, Lartey et al. (2005) reported similar symptoms on safflower. Plants inoculated with Fusarium spp. showed high incidence which resulted in complete wilting by the end of the study period. Besides, inoculated plants exhibited foliar symptoms including chlorosis, wrinkling and defoliation as well as infected roots had rot resulting in complete wilting and drying up of the plants. These results suggest that these pathogens are indeed associated with soybean seeds although further studies in required to elucidate how these pathogens infect the seed.

5.0 CONCLUSION

All eleven seed samples were found to be associated with eight fungal genera, comprising of four pathogenic; Cercospora spp, Alternaria spp., Fusarium spp., Macrophomina phaseolina, and five saprophytic; Curvularia spp., Aspergillus niger, Aspergillus flavus, Rhizopus stolonifer and Penicillium spp Rhizopus stolonifera and their prevalence vary from location to location. Treatment of seed with chemicals and botanicals significantly reduced the fungal prevalence as well as enhanced germination and seedling vigour of treated seeds samples, thus enhancing seed quality and promoting

the attainment of food security in Ghana.

ACKNOWLEDGEMENT

We are grateful to the German Academic Exchange Services (DAAD) and the West Africa Centre for Crop Improvement for funding this study.

REFERENCES

Adjei, J. (2011). Investigation into fungal seedborne pathogens of farmer-saved seed maize (Zea mays L.) collected from three ecological zones of Ghana and efficacyof plant extracts in controlling the pathogens (Doctoral dissertation).

Akranuchat, P., Noimanee, P., Krittigamas, N., Horsten D.V. and Vearasilp. S. (2007). Control of seed borne fungi by radio frequency heat treatment as alternative seed treatment in barely (*Hordeum vulgare*). *Conference on International Agricultural Research for Development.* October 9-11. University of Gottingen, Germany.

Anderson, P. K., Cunningham, A. A., Patel, N. G., Morales, F. J., Epstein, P. R., & Daszak, P. (2004). Emerging infectious diseases of plants: pathogen pollution, climate change and agrotechnology drivers. *Trends in ecology & evolution*, *19*(10), 535-544.

Anwar, S. A., Abbas, S. F., Gill, M. M., Rauf, C. A., Mahmood, S., and Bhutta, A. R. (1995). Seed borne fungi of soybean and their effect on seed germination. *Pakistan Journal of Phytopathology (Pakistan)*.

Carla Marias (2013). Effect of Inoculum Source, Alternaria Host and Cultivar on Development of Brown Spot and Black pit of Potatoes in South Africa. Thesis Submitted to University of Pretoria.

Dawson, W. A. J. M., and Bateman, G. L. (2001). Fungal communities on roots of wheat and barley and effects of seed treatments containing fluquinconazole applied to control take-all. *Plant Pathology*, *50*(1), 75-82.

Dubey, R.C., Kumar, H.and Pandey, P.R. (2009). Fungi toxic effect of neem extracts on growth and sclerotial survival of *Macrophomina phaseolina in vitro*. *Journal of Animal Science*, 5: 17-24.

Food and Agriculture Organization of the United Nations (2014). FAOStat. Retrieved from http://faostat.fao.org/default.aspx?lang=en.

Gao, X., Wu, M., Xu, R., Wang, X., Pan, R., Kim, H. J., & Liao, H. (2014). Root interactions in a maize/soybean intercropping system control soybean soil-borne disease, red crown rot. *PLoS One*, *9*(5), e95031.

Gupta, G. K., and Chauhan, G. S. (2005). Symptoms, identification and management of soybean diseases. National Research Centre for Soybean, Indian Council of Agricultural Research.

Gupta, I.S., Schmittener, A.F. and Mc. Donald, M.B. (1993). Effect of storage fungi on seed vigour of soybean. Seed Sci. and Tech. 21: 581-589.

Howlader, A. N. (2003). Effect of seed selection and seed treatment on the development of phomopsis blight and fruit rot of eggplant. An M.S. Thesis submitted to the Dept. of Plant Pathology, BAU, Mymensingh. pp. 40-68.

Ibrahim, E. A. M. (2015). Effect of some treatments on seed health and viability of soybean. Plant Pathology Journal, 14(4), 158.

Ijaz, A., Anwar, S. A., Riaz, A., and Khan, M. S. A. (2001). Seed borne pathogens associated with wheat seed and their role in poor germination. Pakistan Journal of Phytopathology, 13(2), 102-106.

International Institute of Tropical Agriculture, (2009). Soybean Overview. Summary. 5pp.

Islam, M. M., and Monjil, M. S. (2016). Effect of aqueous extracts of some indigenous medicinal plants on sheath blight of rice. Journal of the Bangladesh Agricultural University, 14(1), 7-12.

Jamadar, M. I., and Chandrashekhar, S. (2015). Effect of chemical and biological seed treatments on germination performance of GCH-7 hybrid castor (Ricinus communis L.). The Bioscan, 10(1), 37-41.

Javaid, A., and Saddique, A. (2011). Management of Macrophomina root rot of mungbean using dry leaves manure of Datura metel as soil amendment. Spanish Journal of Agricultural Research, 9(3), 901-905.

Khan, M. J., Iqbal, T. M. T., Kabir, M. A., Muhammad, N. and Islam, M. R., (2015). Quality assessment of yard long bean (Vigna unguiculata) seeds through the controlled deterioration technique. International Journal of Agronomy and Agricultural Research, 7 (4): 117-127.

Koscielny, J., Klüssendorf, D., Latza, R., Schmitt, R., Radtke, H., Siegel, G., and Kiesewetter, H. (1999). The antiatherosclerotic effect of Allium sativum. Atherosclerosis, 144(1), 237-249.

Kubiak, K., and Korbas, M. (1999). Occurrence of fungal diseases on selected winter wheat cultivars. Postepy Ochronie Roslin, 39(2), 801-804.

Kulik, M. M., and Schoen, J. F. (1981). Effect of seedborne Diaporthe phaseolorum var. sojae on germination, emergence, and vigor of soybean seedlings. Phytopathology, 71(5), 544-547.

Lakshmeesha, T.R., Sateesh, M.K. Vadashree, S. and Mohammad, S.S. (2013). Antifungal activity of some medicinal plants on soybean seed-borne Macrophomina phaseolina. Journal of Applied Pharmaceutical Science 3(02): 084-087.

Lawson, I. Y. D., Mensah, E. A., and Yeboah, E. N. (2009). Improving the establishment and yield of soybean through planting depth and land preparation methods in northern Ghana. West African Journal of Applied Ecology, 14(1).

Mancini, V., and Romanazzi, G. (2014). Seed treatments to control seedborne fungal pathogens of vegetable crops. Pest management science, 70(6), 860-868.

Mansur A., Mehbub H., Kamrul H. and Chandra K. D. (2013). Efficacy of Different Plant Extract on Reducing Seed Borne Infection and Increasing Germination of Collected Rice Seed Sample. Universal Journal of Plant Science 1(3): 66-73.

Lamprecht, S. C., Marasas, W. F. O., Knox-Davies, P. S., and Calitz, F. J. (1990). Seed treatment and cultivar reaction of annual Medicago species and wheat to Fusarium avenaceum and Fusarium graminearum Gr. 1. Phytophylactica, 22(2), 201-208.

Lartey, R. T., Caesar-TonThat, T. C., Caesar, A. J., Shelver, W. L., Sol, N. I., and Bergman, J. W. (2005). Safflower: a new host of Cercospora beticola. Plant Disease, 89(8), 797-801.

Masum, M. M. I., Islam, S. M. M., and Fakir, M. G. A. (2009). Effect of seed treatment practices in controlling of seed-borne fungi in sorghum. Scientific Research and Essays, 4(1), 022-027.

Mathur, S. B., and Kongsdal, O. (2003). Common laboratory seed health testing methods for detecting fungi.

Mbanya, W. (2011). Assessment of the constraints in soybean production: A case of Northern Region, Ghana. Journal of Developments in Sustainable Agriculture, 6(2), 199-214.

Michelle, M. (2003). Garlic extract and two diallyl sulphides inhibit methicillin-resistant Staphylococcus aurens infection in mice. Journal of Antimicrobial Chemotherapy, 52: 974-980.

Mondall, N. K., Mojumdar, A. S. K., Chatterje, A., Banerjee, J. K. and Gupta, S. (2009). Antifungal activities and chemical characterization of neem leaf extracts on the growth of some selected fungal species in vitro culture medium. Journal of Applied Sciences and Environmental Management 13(1):49-53.

Moss, M.O. and Smith, J.E. (2006). Mycotoxins: Formulation, Analysis and Significance. John Willey and Sons. Chichester, Britain, 143.

Nayyar, B. G., Woodward, S., Mur, L. A., Akram, A., Arshad, M., Naqvi, S. S., and Akhund, S. (2017). The incidence of Alternaria species associated with infected Sesamum indicum L. seeds from fields of the Punjab, Pakistan. The plant pathology journal, 33(6), 543.

Oladimeji, A., Olusegun, S. B, Oluyemisi, B. F., Oluwatoyin, A. F., Aliyu, T. H. and Kassoum, O. K. (2016). Seed-Borne Fungi of Soybeans (Glycine Max [L.] Merr) in the Guinea Savannah Agroecology of Nigeria. Journal of Agricultural Sciences. Vol. 61, No. 1. Pages 57-68.

Oshone, K., Gebeyehu, S., and Tesfaye, K. (2014). Assessment of common bean (Phaseolus vulgaris l.) Seed quality produced under different cropping systems by smallholder farmers in eastern Ethiopia. African Journal of Food, Agriculture, Nutrition and Development, 14(1), 8566-8584.

Patil, V. B., Gawade, D. B., Surywanshi, A. P., and Zagade, S. N. (2015). Biological and Fungicidal Management of Chickpea Wilt caused by Fusarium oxysporum f. sp. ciceri. The Bioscan, 10(2), 685-690.

Perelló, A., Gruhlke, M., and Slusarenko, A. J. (2013). Effect of garlic extract on seed germination, seedling health, and vigour of pathogen-infested wheat. Journal of plant protection research, 53(4), 317-323.

Pickett, L. S. and Pruitt, J. D. (1989). Non-Chemical Methods for Controlling Diseases in the Home Landscape and Garden. Oklahoma Cooperative Extension Fact Sheets available on website: http://osufacts.okstate.edu.

Pinto, N.F.J. DE A. (1997). Efficiency of fungicides in the treatment of maize seeds to control Fusarium moniliforme and Pythium sp. Pesquisa Agropecuria Brasileira 32: 797-801.

Poornima (2010). Studies on Cercospora beticola Sacc. Causing Leaf Spot of Palak (Beta vulgaris var. bengalensis Hort.). Thesis submitted to the University of Agricultural Sciences, Dharwad

Ramannuj, P., Patel, D. R., and Pandey, A. K. (2014). Study on seed borne mycoflora of soybean, sorghum and groundnut of different zones of Madhya Pradesh. International Journal of Plant Protection, 7(1), 9-14.

Ramesh, B. V., Hiremath, S. V., Naik, M. K., Amaresh, Y. S., Lokesh, B. K., and Vasudevan, S. N. (2013). Study of seed mycoflora of soybean from north eastern Karnataka. Karnataka Journal of Agricultural Sciences, 26(1).

Roy, K.W., Baird, R.E. and Abney, T.S. (2000). A review of soybean (Glycine max) seed, pod, and flower mycofloras in North America, with methods and a key for identification of selected fungi. Mycopathologia. 150:15-27.

Sauvant, D., Perez, J., andTran, G. (2004). Tables of composition and nutritional value of feed materials. Second revised and corrected edition ed.

Shovan, L. R., Bhuiyan, M. K. A., Sultana, N., Begum, J. A., and Pervez, Z. (2008). Prevalence of fungi associated with soybean seeds and pathogenicity tests of the major seed-borne pathogens. International Journal of Sustainable Crop Production, 3(4), 24-33.

Shurtleff, W., and Aoyagi, A. (2007). The soybean plant: Botany, nomenclature, taxonomy, domestication and dissemination. Soy info Center, California, 40pp.

Sivparsad, B. J., Chiuraise, N., Laing, M. D. and Morris, M. J., (2014). Negative effect of three commonly used seed treatment chemicals on biocontrol fungus Trichoderma harzianum. African Journal of Agricultural Research, 9 (33): 2588-2592.

Solanke, R. B., Kore, S. S., and Sudewad, S. M. (1997). Detection of soybean seed borne pathogens and effect of fungicides. Journal of Maharashtra Agricultural Universities, 22(2), 168-170.

Song, W., Zhou, L., Yang, C., Cao, X., Zhang, L., and Liu, X. (2004). Tomato Fusarium wilt and its chemical control strategies in a hydroponic system. Crop protection, 23(3), 243-247.

Southwell, R.J., Moore, K.J., Manning, W., and Haymna, P.T. (2003). An outbreak of Fusarium head blight of durum wheat on the Liverpool plain in Liverpool plain in Northern New South Wales in 1999. Australian Plant Pathology 32: 465-471.

Spross-Blickle, B., Rotem, J., Perl, M., and Kranz, J. (1989). The relationship between infections of the cotyledons of Gossypium barbadense and G. hirsutum with Alternaria macrospora and cotyledon abscission. Physiological and molecular plant pathology, 35(4), 293-299.

Statistics, Research and Information Directorate, SRID of Ministry of Food and Agriculture. (2012). Production Estimates. Accra, Ghana.

Sun, S., Wang, X., Zhu, Z., Wang, B. and Wang, M. (2015). Occurrence of Charcoal Rot Caused by Macrophomina phaseolina, an Emerging Disease of Adzuki Bean in ChinaJournal of Phytopathology. Pp (1-5).

Taye, W., Laekemariam, F., and Gidago, G. (2013). Seed germination, emmergence and seedlings vigor of maize as influenced by pre-sowing fungicides seed treatment. J Agric Res Dev, 3(3), 35-41

Venugopal Rao T., Rajeswari, B., Keshavulu, K., and Sandeep Varma V. (2015). Studies on Seed borne Fungi of Soybean. SSRG International Journal of Agriculture & Environmental Science (SSRG-IJAES), 2(1), 16-24.

Vloutoglou, I., and Kalogerakis, S. N. (2000). Effects of inoculum concentration, wetness duration and plant age on development of early blight (Alternaria solani) and on shedding of leaves in tomato plants. Plant pathology, 49(3), 339-345.

Xue, A. G. (2003). Biological control of pathogens causing root rot complex in field pea using Clonostachys rosea strain ACM941. Phytopathology, 93(3), 329-335.

PHYSICAL & ENGINEERING SCIENCES

BIOLOGICAL & AGRICULTURAL SCIENCES

CBAS
College of Basic and Applied Sciences
University of Ghana

ISSN 2550-3421
9 772550 342008